UNIVERSITÀ
DI PAVIA

PhD in Biomedical Sciences

Department of Brain and Behavioral Sciences

Unit of Neurophysiology

Investigation of cerebellar nuclei neuronal plasticity and physiological connectivity *in vivo*

PhD Tutor: Prof. Egidio D'Angelo

PhD Tutor: Dr. Lisa Mapelli

PhD dissertation of

Ileana Montagna

Academic year 2018-2019

Table of contents

Chapter 1

Introduction

The cerebellum is the structure of the central nervous system that is commonly known to be involved in sensory-motor integration and learning. Sensory inputs deriving from the spinal cord, brain stem and other parts of the central nervous system are finally integrated and elaborated by the cerebellar network in order to allow a fine-control of motor activity.

The mechanisms of synaptic plasticity play a critical role in cerebellar motor learning processes. Indeed, several studies report that plastic changes in the cerebellar circuitry are necessary to regulate motor performance and motor learning in regions receiving cerebellar outputs, such as striatal and motor cortex, both representing key nodes in the motor pathway.

Interestingly, recent findings also report that the cerebellum may play an important role in cognition *(Gowen and Miall 2007; Kansal et al. 2017).* Supporting this hypothesis, evidence of anatomical and functional interconnection between the cerebellum and prefrontal areas involved in cognitive functions have been described *(Palesi et al. 2015; Watson et al. 2014; Watson et al. 2009)*. Moreover, several clinical studies report that cerebellar abnormalities, such as the cerebellar cognitive affective syndrome (CCAS) are related to cognitive dysfunctions *(Schmahmann and Sherman 1998)*. Impaired cerebello-cortical connections have also been related to various brain pathologies, ranging from sensori-motor ataxia to autism spectrum disorders (ASD) and Alzheimer's disease *(D'Angelo and Casali 2012; Giza et al. 2010; Konarski et al. 2005)*. Therefore, alterations in cerebellar activity and impkonaaired connectivity within and across the cerebello-cerebral network might finally lead to motor and cognitive dysfunction.

Following these observations, the functional role of the cerebellum in cognitive and motor cortical pathways prompts further investigations.

1.1 The cerebellum

In humans, the cerebellum is located in the posterior cranial fossa, above the brain stem, and it is separated from the overlying occipital lobe of the cerebral cortex by the *tentorium cerebelli*. At the level of gross anatomy, the cerebellum consists of two hemispheres and a median zone called *vermis* (Fig.1.1A).

The surface of the cerebellum is composed by a layer of gray matter characterized by a large number of convolutions forming the cerebellar laminae, each one named *folium*, and is crossed mediolaterally by two deep transverse fissures that divide the cerebellum into three lobes: anterior, posterior and flocculo-nodular. Each lobe is divided in smaller areas called lobules (Fig 1.1A).

In midsagittal sections the white matter of the cerebellum is arranged in a way that remembers the branches of a tree (Fig 1.1B). For this reason, cerebellar white matter is also named *arbor vitae*. All outputs from the cerebellum originate from four symmetrical pairs of nuclei lying deep within the white matter. From medial to lateral, deep cerebellar nuclei (DCN) are: the fastigial nucleus; globose and emboliform nuclei (which in non-primate mammals, such as rodents, form a single nucleus called interposed nucleus) and the dentate nucleus (Fig. 1.1B).

All cerebellar connections travel through the brain stem, whose dorsal part is connected to the cerebellum by three pairs of cerebellar peduncles. The superior peduncle (or *brachium conjunctivum*) is formed almost entirely from efferent fibers from DCN directed to red nucleus, thalamus and reticular formation, giving rise to the cerebellorubral, the cerebellothalamic and the fastigioreticular tract, respectively; the afferent fibers include the anterior spinocerebellar and tectocerebellar tracts. The middle peduncle (or *brachium pontis*) connects the cerebellum to the pons, conveying afferent fibers from the contralateral pontine nuclei; which axons are connected to cerebral cortex and superior colliculus. The inferior peduncle contains both afferent fibers from the medulla (posterior spinocerebellar, cuneocerebellar, trigeminocerebellar tracts, olivocerebellar and vestibulocerebellar fibers) and efferent fibers to the vestibular nuclei arising from vestibulocerebellum (Rand S. and Swenson 2006; Swenson et al. 1984).

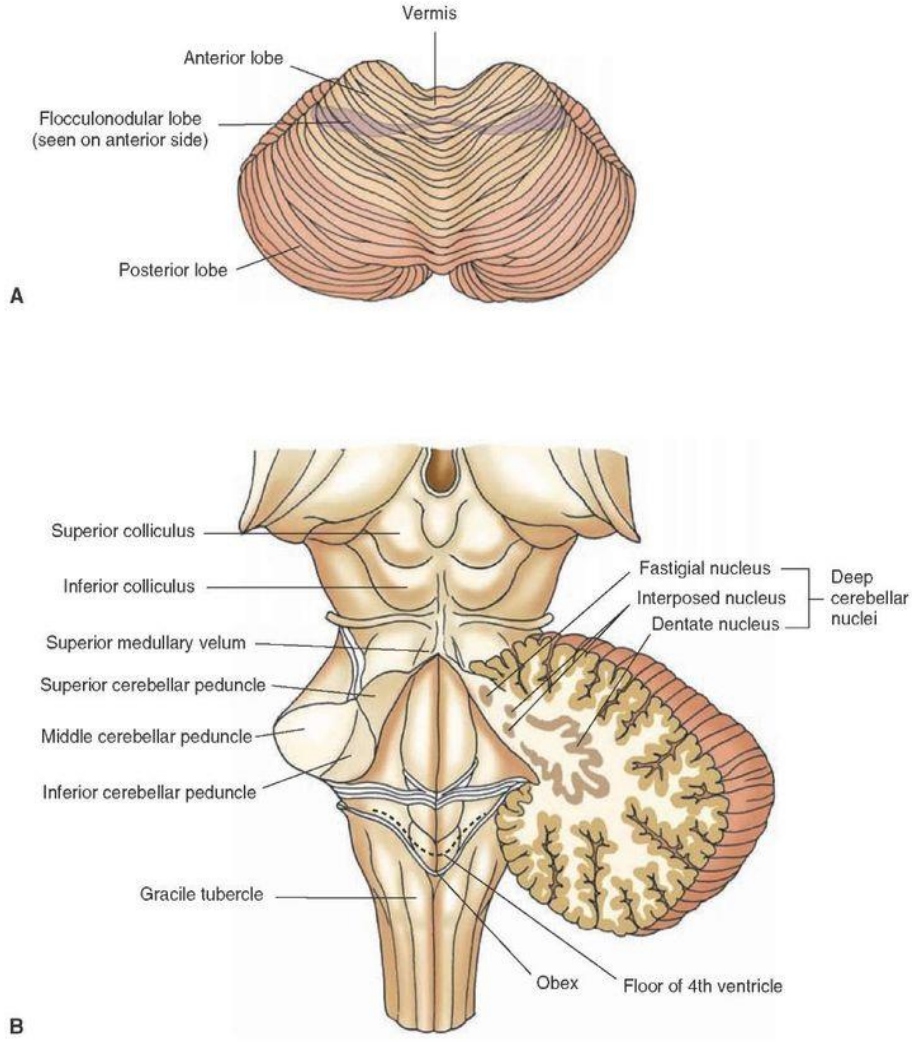

Figure 1.1| Cerebellar anatomy. *(A) Dorsal view of the cerebellum. (B) Midsagittal cut through the cerebellum and brain stem showing white matter entering the vermal lobules. View of the lower part of the brain stem after removal of the cerebellum.*

Anatomy and cytoarchitecture of the cerebellum are quite conserved between humans and other mammals (Apps and Hawkes, 2009; fig 1.2). According to phylogenetic and functional criteria it is also possible to divide the cerebellum into three subdivisions, each of which forms connections with a specific part of the brain. The vestibulocerebellum (*archicerebellum*), phylogenetically the oldest, is located in the flocculo-nodular lobe, regulates balance and eye movements and is characterized by a bidirectional communication with vestibular nuclei in the

medulla oblongata. The vermis and intermediate zone, as well as interposed and fastigial nuclei, form the spinocerebellum (*paleocerebellum*), that receives sensitive inputs from the spinocerebellar tract and regulates body and limb movements and it is involved in the regulation of sensory input with motor commands to adapt motor coordination. The cerebrocerebellum (*neocerebellum, pontocerebellum*) includes lateral parts of the hemispheres and dentate nuclei. It receives projections exclusively from the nuclei located in the pons that relay the informations coming from cerebral cortex. It is involved in planning and timing of movements, as well as in cognitive functions of the cerebellum (Rand S. and Swenson 2006).

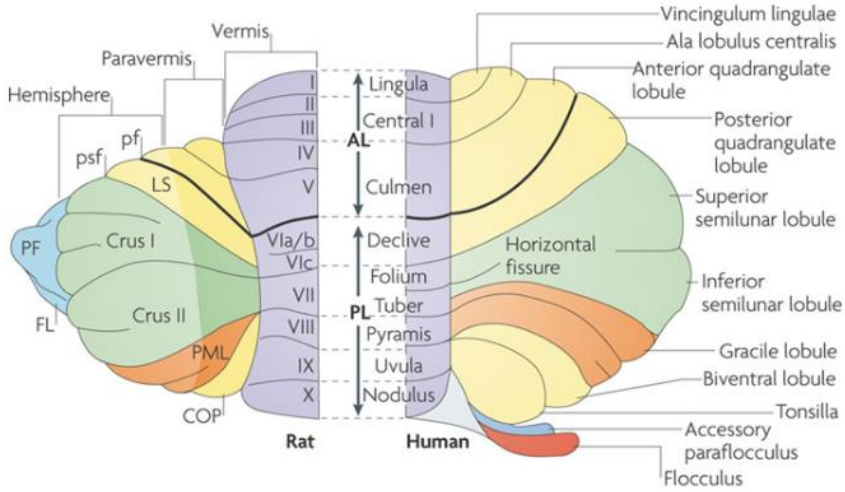

Figure 1.2| Comparative anatomy and nomenclature of the main cerebellar subdivisions. *Simplified illustration of rat (on the left) and human (on the right) dorsal view of the cerebellum. Equivalent regions in rat and human cerebellum are indicated with the same color (Apps and Hawkes 2009). In rodents, the fastigial nucleus is located in the cerebellar vermis, the interposed nucleus (globose and emboliform nuclei in human) lies in the intermediate zone of the cerebellar hemisphere (paravermis) and the dentate nucleus is embedded in the lateral zone of the hemisphere. The cerebellar hemispheres are more extended laterally in humans, due to a greater length and number of folia and also the amount of corticopontocerebellar projections coming from higher brain areas is larger, whereas the parafloccular lobule is larger in rodents. Abbreviations:* ***Pf****, primary fissure;* ***AL****, anterior lobe;* ***COP****, copula pyramidis;* ***Crus I*** *and* ***Crus II****, ansiform lobule;* ***FL****, flocculus;* ***LS****, lobulus simplex;* ***PF****, paraflocculus;* ***PL****, posterior lobe;* ***PML****, paramedian lobule;* ***psf****, posterior superior fissure.*

1.2 Cerebellar circuit

The cerebellar cortex can be divided into three layers organized in a highly regular arrangement that is characterized by the repetition of the same circuit scheme (Fig 1.3). Considering its organized and relatively simple structure containing fundamental neural circuits, the cerebellum represents an extraordinary ideal model to study the complexity of mechanisms that regulate brain functions.

The outer layer is the molecular layer, containing molecular layer interneurons (MLIs), such as stellate and basket cells (SCs and BCs, respectively), the dendritic tree of Purkinje cells (PCs) and the parallel fibers (PFs) originating from the branching of ascending glutamatergic axons of the granule cells (GrCs). PCs dendrites receive excitatory synaptic contacts from PFs and inhibitory contacts from MLIs at the level of the initial segment of their axon. In addition, each PC is reached by a single climbing fiber (CF) originating from the inferior olive (IO). The PCs layer, underneath the molecular layer, contains the somata of PCs. The PCs axons represent the sole output from the cerebellar cortex, making inhibitory synapses with DCN neurons lying in the white matter. Recent studies report that PCs send recurrent collaterals to other PCs and MLIs *(Witter et al. 2016)*. The granular layer is the innermost layer, made of tightly packed GrCs and Golgi cells (GoCs). GoCs are inhibitory interneurons making GABAergic synapses with GrCs. Other types of interneurons observed in the granular layer are unipolar brush cells (UBCs), Lugaro cells, synarmotic neurons, candelabrum neurons and the perivascular neurons, although their function is still under debate *(Ambrosi et al. 2007).* GrCs receive glutamatergic excitatory inputs from mossy fibers (MFs) coming from different precerebellar area. The sole cerebellar output projecting to other parts of the CNS is provided by the DCN (the only exception being PCs of the vestibulocerebellum sending direct projections to the vestibular nuclei). DCN neurons receive excitatory synapses from collaterals of MFs and CFs and inhibitory synapses from PCs. Further studies highlighted the presence of projections from the DCN exerting either inhibitory or excitatory effects over their final targets.

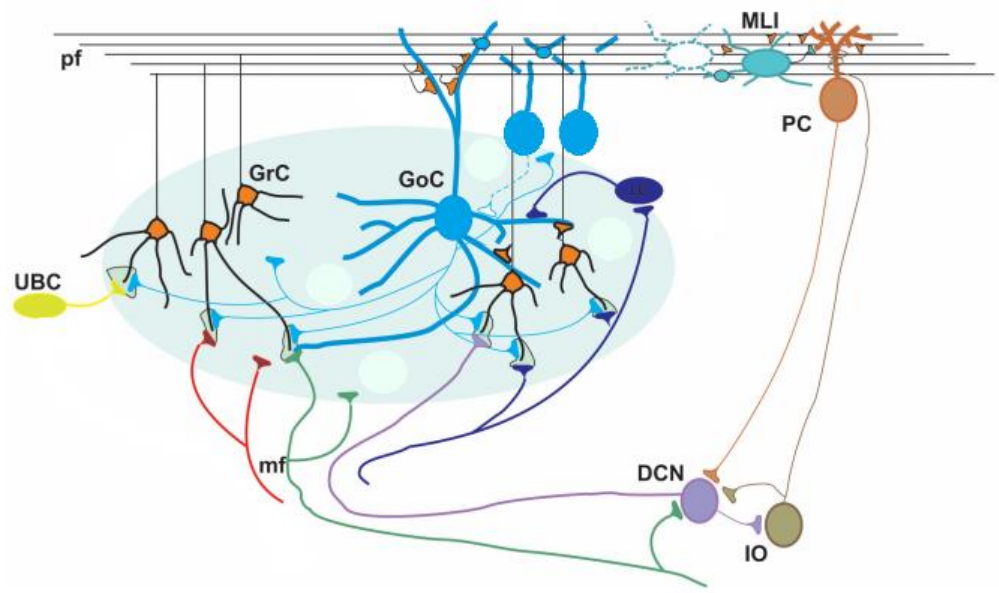

Figure 1.3| Schematic representation of the cerebellar circuit. *The cerebellum receives two main afferents: MFs and CFs. MFs coming from precerebellar structures form synaptic contacts with GrCs and DCN neurons. CFs coming from the IO contact both DCN neurons and PCs. DCN neurons integrate excitatory synaptic inputs coming from MFs and CFs and inhibitory inputs coming from GrC-PC pathway regulating the cerebellar output. Abbreviations:* ***Pf****: parallel fiber;* ***MLI****: molecular layer interneuron;* ***PC****: Purkinje cell;* ***GrC****: granule cell;* ***GoC****: Golgi cell;* ***UBC****: unipolar brush cell;* ***NTc****: non-traditional cell;* ***mf****: mossy fiber;* ***DCN****: deep cerebellar nuclei;* ***IO****: inferior olive. Figure modified from (D'Angelo et al. 2016b).*

DCN GABAergic projecting neurons reach the IO, thus forming loop connections with the cerebellar cortex that endow cerebellum of complex processing properties (Uusisaari and De Schutter 2011; Houck and Person 2014). DCN glutamatergic projections reach the spinal cord and several nuclei in the brainstem related to motor control but also the thalamus, which finally relay signals to motor and associative areas in the cerebral cortex. These last anatomical connections indicate that the cerebellum might be involved not only in precise motor control but also in cognitive functions. The existence of feedback projections from the cerebral cortex to the cerebellum through the pontine nuclei forming a closed-loop network strengthens this hypothesis.

1.3 Cerebello-prefrontal cortex interactions

The evidence of cerebellar involvement in cognitive functions is supported by numerous studies reporting the existence of connections between the cerebellum and cerebral associative areas of the brain, such as the prefrontal cortex (PFC). The nature of cerebello-cerebral connections in humans was made clearer by anatomical studies as well as integral tractographic reconstruction of cerebellar projections passing through the superior cerebellar peduncle (Palesi et al. 2015). The superior cerebellar peduncle carries cerebellar outputs from the DCN that are directed to motor nuclei of the thalamus [the ventro-anterior (VA) and ventro-lateral (VL)] projecting to motor cortices, but also to intralaminar nuclei and the medial dorsal (MD) thalamic nucleus, which projections ultimately reach the PFC (Schmahmann, 1996). Interestingly, tractography revealed that the majority of cerebellar connections are directed to cerebral cortex areas involved in cognitive functions, rather than involved in sensori-motor control (around 80% vs. 20%) (Palesi et al. 2015, fig. 1.4). A study in non human-primates using trans-synaptic viral tracers allowed to determine the regions of the cerebellar cortex that receive projections from the primary motor cortex and prefrontal area 46 (Kelly and Strick, 2003). The results showed that the primary motor cortex mainly projects to cerebellar lobules which roles in skilled motor control are well established, whilst afferents from the prefrontal area reached regions in cerebellar hemispheres that are not connected with the primary motor cortex. These observations sustain the involvement of the cerebellum in functions that extend beyond the motor domain, with each region of the cerebellar cortex responding to specific inputs originating from other areas of the brain.

The combination of tracing studies and lesion-symptom mapping, allowed to estabilish a functional coherence between prelimbic subdivision (PrL) of the medial prefrontal cortex (mPFC) in rodents and PFC in humans and non-humans primates (Uylings et al., 2003, Seamans et al., 2008}.

Indeed, the existence of cerebello-prefrontal interconnection was supported by *in vivo* electrophysiological experiments in rodents which reported that stimulation of PrL of the mPFC was able to elicit local field potentials (LFP) response in PCs.

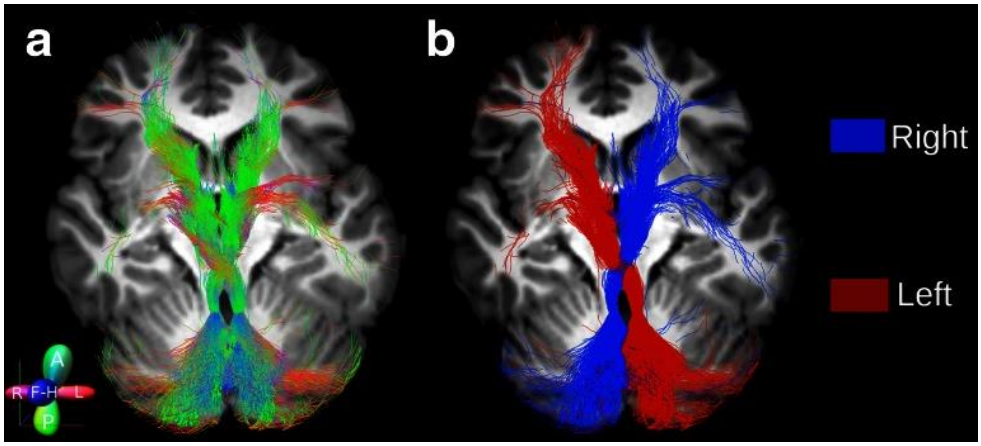

Figure 1.4| 2D rendering of cerebello-thalamo-cortical pathways of a representative subject. (***a)*** *The tracts are* color*-coded by direction to represent their anatomy (**b)** A single* solid colour *has been used for each tract to distinguish the streamlines from the left (*red*) and right (*blue*) pathways (Palesi et al. 2015).*

LFPs were more pronounced in the lobule VII of contralateral vermis, a well-known cerebellar region involved in the control of eye movements, through projections originating from the fastigial nucleus (FN) (Watson et al. 2009, fig 1.5). These observations led to suppose that the eye movement depending on cerebello-cerebral connection is more related to goal-directed behaviour instead of purely cortical information processing (Watson et al. 2009).

Nevertheless, a consistent amount of studies reports a relationship between cerebellar abnormalities with cognitive disorders (Konarski et al. 2005; Pierce and Courchesne 2001; Schmahmann and Sherman 1998). A further investigation *in vivo* reported that DCN stimulation was able to elicit heterogeneous response patterns in mPFC neurons of rats, thus providing evidence of the reciprocal influence between the cerebellum and the cerebral prefrontal area (Watson et al. 2014, fig 1.6).

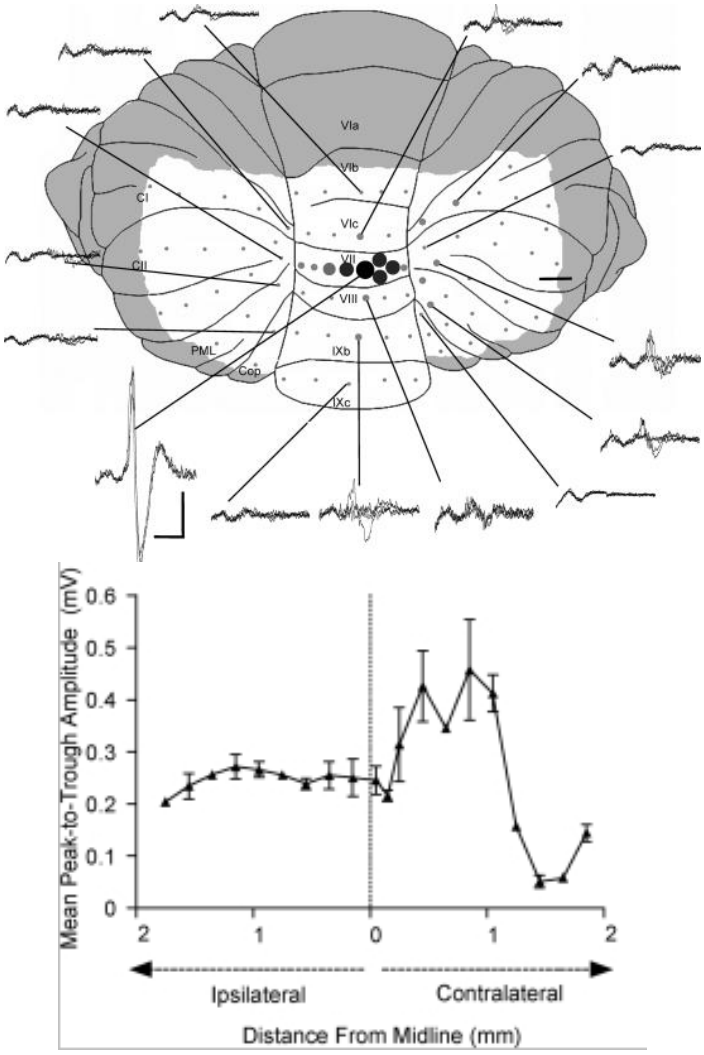

Figure 1.5| Prefrontal cortex projections to the contralateral cerebellar cortex of rat. *On top, a schematic representation of the dorsal view of the cerebellum reporting the distribution of LFP responses evoked by the stimulation of the mPFC. The amplitude of the LFP responses are represented by example waveforms recorded within each cerebellar region and the size of circles. On bottom, the field potential amplitude change is shown as a function of the medio-lateral position along the vermal lobule VII. Data points are reported as mean of four responses ± SEM (Watson et al. 2009).*

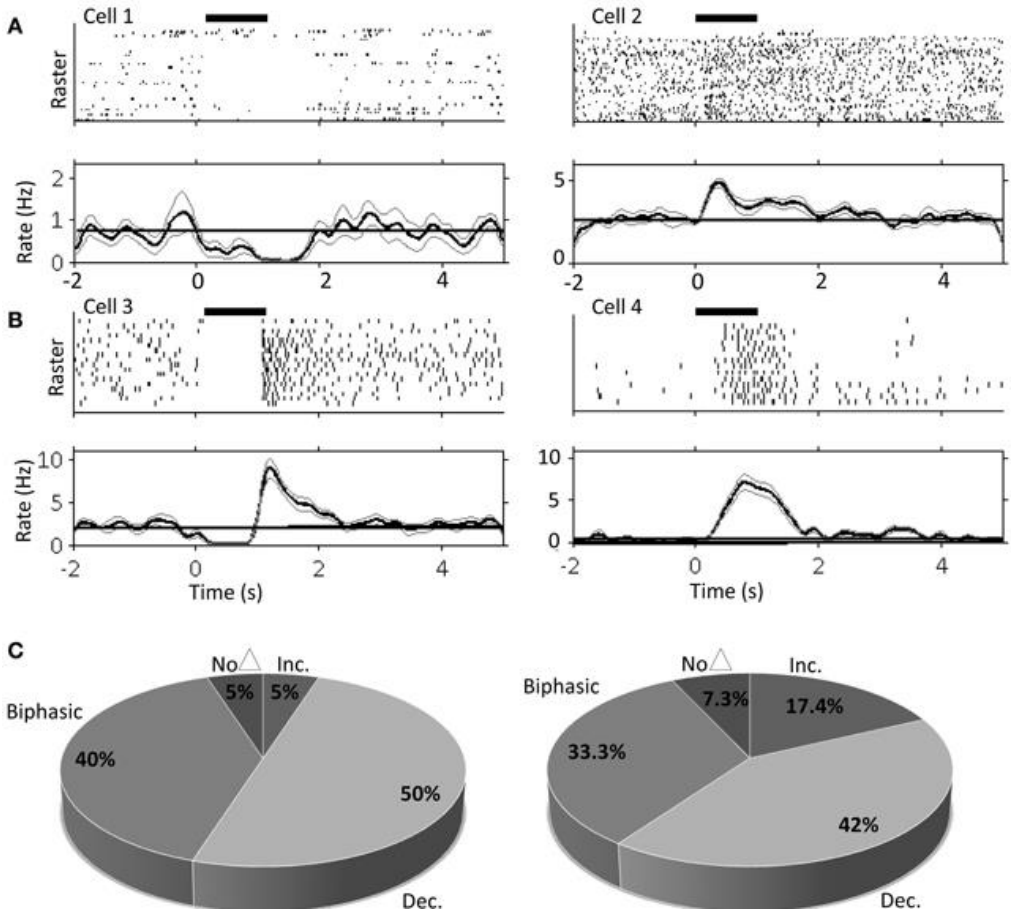

Figure 1.6| PrL neurons response patterns to the electrical stimulation of the contralateral FN. *Raster plots and peri-stimulus time histograms of typical responsive neurons in the PrL of awake* ***(A)*** *and urethane-anesthetized rat* ***(B)****. High frequency FN stimulation (100 Hz, 100 stimuli, 1s duration, 100 μA) evokes 3 typical response patterns in both awake and anesthetized animals: decrease of firing rate compared to baseline activity (****cell 1*** *in Figure A); increase of spike discharge (****cell 2*** *in Figure A;* ***cell 4*** *in Figure B); biphasic response consisting in a decrease of firing rate followed by a rebound increase (****cell 3*** *in Figure B). In* ***(C)*** *are reported the response patterns percentages following FN stimulation in awake (n=20) and anesthetized (n=69) rats (Watson et al. 2014).*

The stimulation of the dentate nucleus (DN) is reported to induce dopamine (DA) release in the mPFC which in turn might modulate cortical neurons responses to cerebellar stimulation (Mittleman et al. 2008). The release of DA in mPFC driven by cerebellar output might be induced through different pathways, through the ventral tegmental area (VTA) or thalamus (Kehr et al. 1976; Snider and Maiti 1976; Snider et al. 1976; Watson et al. 2014), but also via substantia nigra or basal ganglia (Nieoullon et al. 1978). The heterogeneous pattern of responses evoked in the mPFC might be caused by the expression of different DA receptors in mPFC neurons. DA receptors expressed in mPFC neurons belong to the family of D1-like and D2-like receptors. In rodents, a higher expression of D1-like receptors has been reported in the PFC, compared to that of D2-like receptors (Gaspar et al. 1995). The activation of D1-like receptors on pyramidal neurons engages NMDA receptor and GABA receptor-mediated synaptic responses thus eliciting both excitatory and inhibitory effects, whilst the recruitment of D2-like receptors reduces the excitability of pyramidal cells and their GABAergic transmission (Floresco and Magyar 2006; Floresco et al. 2006). Therefore, DA release in mPFC generates a complex variety of effects on cortical pyramidal cells and local interneurons, which reciprocal connections complicate the interpretation of responses evoked in mPFC by cerebellar activation (Dembrow and Johnston 2014, fig. 1.7).

Recent studies using optogenetics in freely moving mice revealed that dopaminergic release in mPFC induced by cerebello-VTA pathway activation is not sufficient for remarkable behavioural changes (Carta et al.,2019).
This observation makes reasonable to assume that the sole contribution of the cerebello-VTA pathway over mPFC functioning is not sufficient to fully explain the involvement of cerebellum in cognition.

Considering this scenario, the investigation of the measure in which other cerebellar pathways reaching mPFC contribute to cortical activity appears unavoidable.

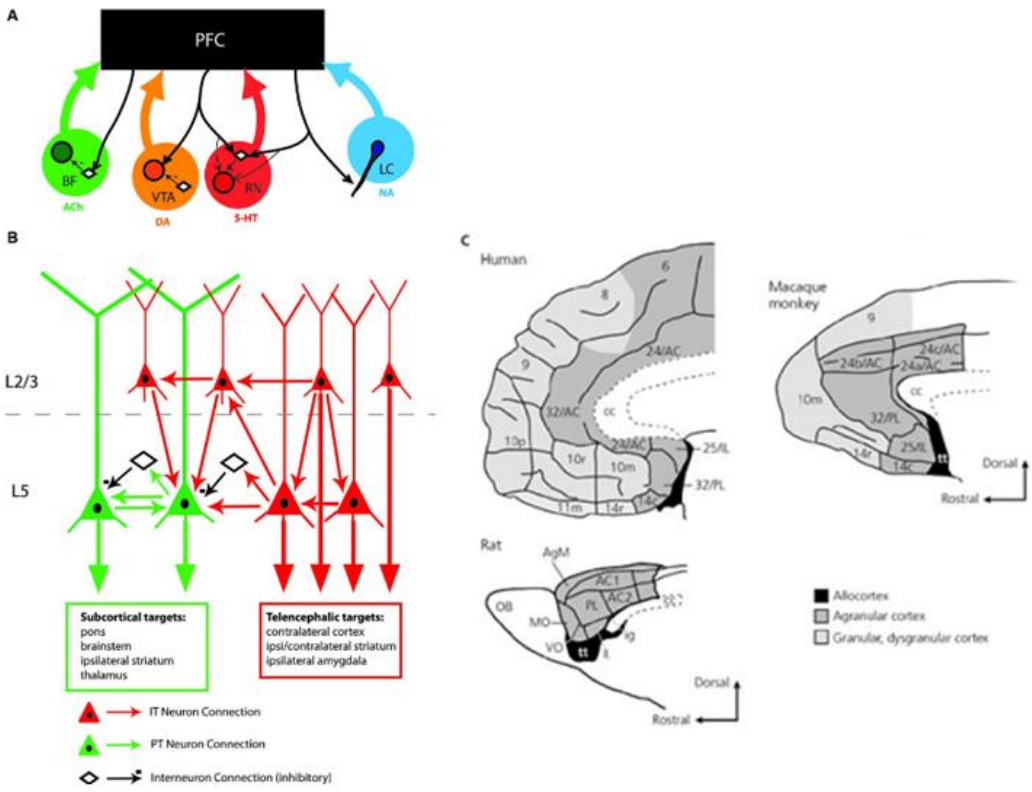

Figure 1.7| Schematic representation of anatomy and network connectivity within and across the rodent mPFC. *(A) Schematic representation of projections to and from the PFC. Noradrenaline (NA) is released from the locus coeruleus (LC) terminals; Acetylcholine (ACh) from the basal forebrain (BF); Serotonin (5-HT) from the raphe nuclei (RN); Dopamine (DA) from the ventral tegmental area (VTA) and substantia nigra (SN). PFC neurons project to the neuromodulatory centers, contacting back the neuromodulator-synthesizing neurons (shaded circles), inhibitory interneurons (open diamonds), or both.* ***(B)*** *Schematic representation of the connections within the mPFC. The pyramidal tract (PT, green) neurons are located in the layers 5/6 (L5/6); intratelencephalic (IT, red) neurons throughout L2-6. PT neurons receive input from other PT neurons, IT and inhibitory interneurons. IT neurons receive inputs only from other IT neurons (Dembrow and Johnston 2014).* ***(C)*** *Homologies among prefrontal areas: medial view of human, macaque monkey and rats PFC. The cytoarchitecture of human and primate PFC is relatively similar to rodents PCF, except for the presence of the granular layer IV. Indeed, in rodents the PFC is agranular and it contains two different classes of neurons: pyramidal neurons projecting subcortically to ipsilateral striatum, thalamus and/or brainstem and interneurons which project mainly within the cortex (Dembrow and Johnston 2014; Murray et al. 2017).*

In particular, the thalamus represents a well-known target of cerebellar output that is crucial for overall brain activity, due to its involvement in many processes as sensation, perception, and consciousness (John, 2002; Alitto and Usrey, 2003). Hence, thalamic glutamatergic projections reaching the mPFC gain attention in the analysis of cerebello-prefrontal cortex functional interaction. The thalamic regions receiving cerebellar axons are involved either in sensory-motor control (VA and VL nuclei) or in cognitive processes (intralaminar and MD nuclei) (Schmahmann, 1996). Interestingly, several findings report that the mPFC receives prominent innervations from the MD region of the thalamus, which seems to play a crucial role in multiple cognitive processes, such as working memory, cognitive flexibility and social interaction (Parnaudeau et al., 2018, Ferguson and Gao, 2018). Moreover, the stimulation of the cerebellar dentate nucleus *in vivo* is reported to exert some dopamine-mediated neuromodulatory effect on mPFC through the activation of the glutamatergic ventral or MD thalamic nuclei (Hoover and Vertes 2007). Despite these observations, further investigation is required to fully explain the neuronal processes involved in modulation of mPFC activity driven by the cerebellar output.

1.4 Medial prefrontal cortex organization

Four defined areas compose the mPFC, from dorsal to ventral axis: the medial precentral area (PrCm), the anterior cingulate cortex (ACC), the prelimbic area (PrL) and the infralimbic cortex (ILC) (Heidbreder and Groenewegen, 2003). The neuronal population in the mPFC is represented for 80-90% by excitatory pyramidal cells, whilst the remaining 10–20% consists of inhibitory GABAergic interneurons, although it is possible to further distinguish cortical neurons on the basis of morphological, physiological and molecular features (Ascoli et al. 2008; DeFelipe et al. 2013). Three main subpopulations of cortical GABAergic interneurons have been identified based on the expression of speficic proteins: perisomatic targeting fast spiking parvalbumin (PV) interneuron, dendritic targeting somatostatin (SST) interneurons, and vasoactive intestinal polypeptide (VIP) interneurons expressing ionotropic serotonin receptor 5HT3a (Rudy et al,

2011). Another subtype of cortical interneuron is represented by NPY-expressing-neurons, which activation in IL directly inhibits pyramidal neurons in ipsilateral PrL modulating the activation of its downstream targets (Saffari et al. 2016; Kuljis and Rakic, 1989). GABAergic interneurons are widely distributed throughout the cortex, although their arrangement is notably different within the PFC (Saffari et al. 2016, fig 1.8).

Cortical interneurons have a great impact over local circuitry, as they are able to synchronize the firing of pyramidal cells originating neuronal oscillations (Kvitsiani et al., 2013). Optogenetic approaches demonstrated the pivotal role of GABAergic interneurons acivity to gamma oscillations and emotional behavior (Vertes, 2006; Cruikshank et al., 2012; Yizhar, 2012; Little and Carter, 2013). Optogenetic approach allowing selective photostimulation of PV interneurons demonstrated that increase in PV neurons activity manifested as fast, powerful and uniform inhibition on pyramidal cell firing, thus influencing their outputs (Kvitsiani et al., 2013). In constrast, SST neurons appeared to modulate input signals reaching principal pyramidal neurons, as their photostimulation resulted in a weak, more variable and prolonged inhibitory effect on pyramidal cells firing (Kvitsiani et al., 2013).

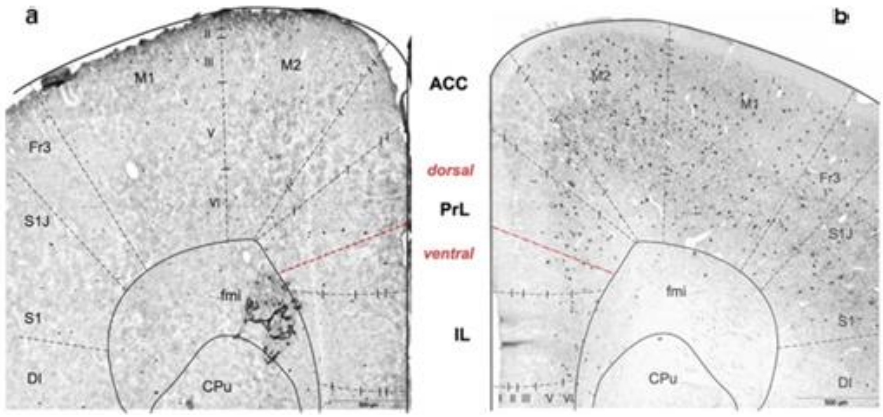

Figure 1.8| The distribution of GABAergic neurons is different in ACC, PrL and ILC. *(A) NPY+ −stained coronal sections of PFC in higher magnification and schematic drawing of different areas.* ***(B)*** *Overview of PV-stained coronal sections of PFC and quantification of the overall density of PV+-GABAergic neurons in M2, ACC, PrL and ILC. (Adapted from Saffari et al, 2016).*

Pyramidal neurons in layer V (see below) of the mPFC can be classified either as thick-tufted, subcortically projecting cells or thin-tufted, long-range projecting cells (Dembrow and Johnston, 2014). Photostimulation of long-range projecting cells showed that they interconnect to both interneurons subtypes, although PV interneurons preferentially exert their inhibitory effect on subcortically projecting pyramidal neurons (Lee et al., 2014a). Pyramidal cell subtypes can also be distinguished based on expression of the dopamine D1 or dopamine D2 receptor (D1-like and D2-like), both involved in reward circuitry (Floresco et al., 2006).

1.4.1 Layers and connectivity of the mPFC

Neurons in mPFC are organized in functional microcolumns, each processing different information in a supramodal manner (Opris et al., 2013; Swadlow et al., 2002).The organization of mPFC in rodents is slightly different from that of other cortical areas, due to the lacking of the classical input layer IV (Uylings et al., 2003). Deep layers V and VI give rise to the efferent projections to subcortical areas, whilst neurons in the superficial layers II and III are mainly responsible for cortico-cortico connections (Douglas and Martin, 2004). The laminar organization has relevant consequences over inputs integration in the mPFC. Projections from the contralateral mPFC, MD thalamus, basolateral amygdala (BLA), and ventral hippocampus (HPC) reach layer II PrL pyramidal neurons at different dendritic locations, showing preference for specific categories of spines with a defined volume (Little and Carter, 2012). The observation that intensity of excitatory postsynaptic currents (EPSCs) is correlated with spine volume (Humeau et al., 2005) allows to speculate that this finely tuned anatomical and functional connectivity of the mPFC allows the integration of inputs from preferential afferent origin.

Thalamo-cortical interactions play a crucial role for processes of sensation, perception, and consciousness (John, 2002; Alitto and Usrey, 2003).
Axons projected from midline and paralaminar thalamic nuclei preferentially reach and excite late-spiking interneurons in layer I, rather than pyramidal cells (Cruikshank et al., 2012). Cortical interneurons are crucial for the regulation of

pyramidal cells firing through feed forward inhibition and gain control activity (Cruikshank et al., 2012; Ferguson and Gao, 2018). Interestingly, repetitive photostimulation of thalamo-cortical projections elicited strong, sustained synaptic responses of mPFC interneurons, suggesting that their prolonged activation is necessary for working memory function (Cruikshank et al., 2012).

Several studies also report that multiple subcortical regions, including VTA and MD talamic nuclei, send their long-range projections to pyramidal neurons in the mPFC at the level of layer III (Hoover and Vertes,2007; Kuroda et al., 1996). Layer III pyramidal neurons then relay information not only in horizontal manner, but also onto downstream onto pyramidal neurons in layer V (Thomson and Bannister, 2003). On the other hand, pyramidal neurons in layer V also receive long-range inputs from the same subcortical regions, as well as from the MD region of the thalamus (Kuroda et al., 1993; Kuroda et al., 1996), eventually integrating that information with the inputs deriving from layer III. The pivotal role of cortical GABAergic interneurons in cognitive functions was enlighted by in vivo experiments using pharmacological tools (Sawaguchi et al.,1989; Paine et al., 2011) and electrophysiological recordings (Rao et al., 2000). Indeed, it has been reported that the majority of projections from the MD nuclei reach PV interneurons in layer III, which in turn contact pyramidal neurons in layer V (Rotaru et al., 2005). Moreover, it has been assumed that activation of PV interneurons is mainly due to the recruitment of excitatory inputs, such as those from MD (Povysheva et al., 2006; Floresco and Grace., 2003). Following these observations it is reasonable to hypothesize that MD glutamatergic projections to mPFC provide strong excitation of PV interneurons, that finally exert their inhibitory effect onto pyramidal neurons in layer V (Ferguson and Gao, 2018; fig 1.9).

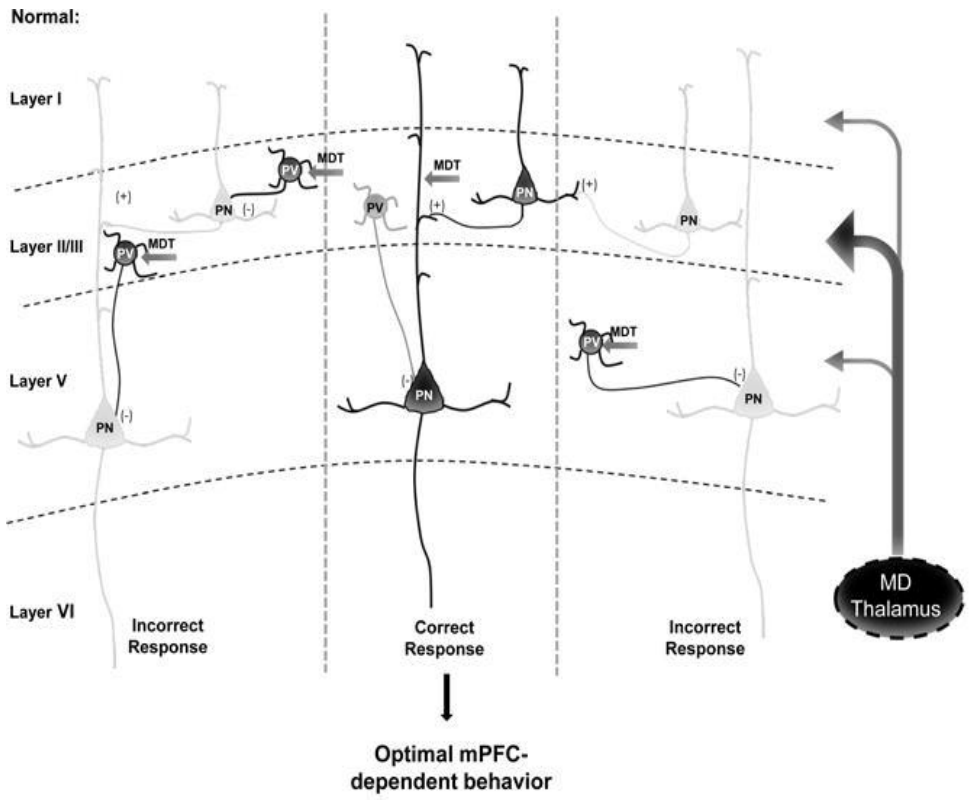

Figure 1.9| MD thalamus regulates mPFC E/I balance to impact cognition. *Under normal conditions, the MD thalamus provides a stronger drive to layer II/III PV interneurons vs pyramidal neurons in the mPFC to maintain a high level of inhibition relative to excitation in layer V pyramidal neurons. Potentially this allows for lateral inhibition of functional microcolumnar units representing distracting information, such that only relevant information is fed forward to optimize behaviors such as cognitive flexibility and social interaction. Dark grey and black represent high levels of activity, vs the light grey that indicates reduced or lower activity. (Adpated from Ferguson and Gao, 2018)*

This circuit organization leads to a fine regulation of excitation/inhibition balance with evident consequences on mPFC-dependent cognitive behavior. Further evidence has been provided by the observation that the dysfunction of thalamic connection to mPFC causes disruption of excitation/inhibition balance resulting in cognitive impairment (Ferguson and Gao, 2018; Fig 1.10).

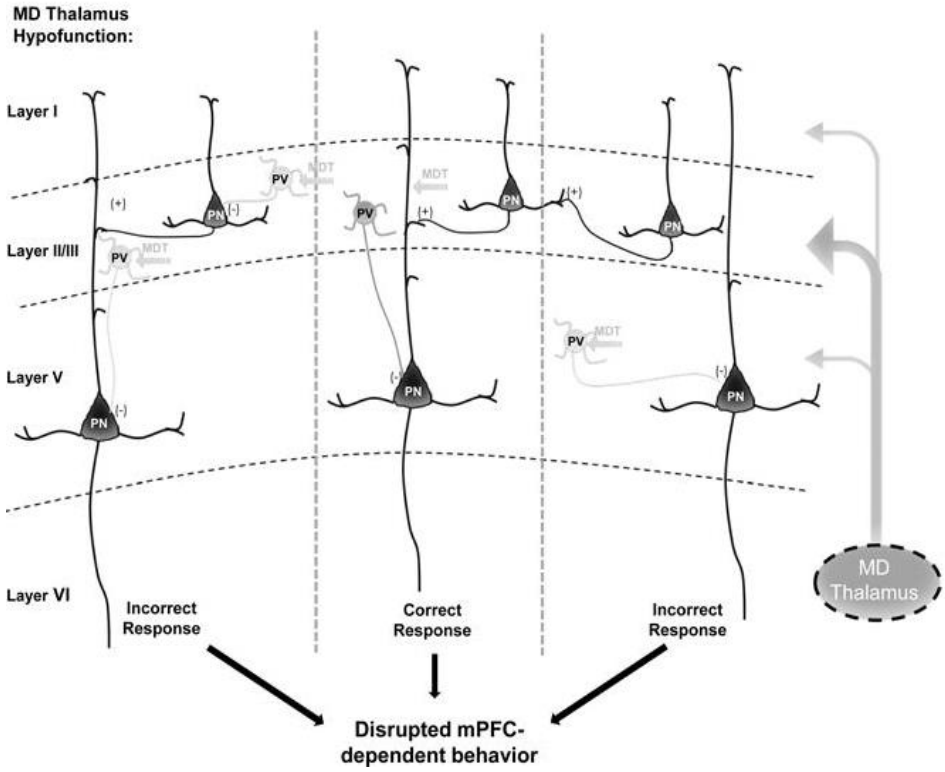

Figure 1.10| MD thalamus regulates mPFC E/I balance to impact cognition. *When MD activity is decreased, activation of PV interneurons by MD afferents is removed, leading to dishinibition of neurons in microcolumns representing distracting or irrelevant information, and disrupting behavior. Dark grey and black represent high levels of activity, vs the light grey that indicates reduced or lower activity. (Adpated from Ferguson and Gao, 2018)*

The role played by mPFC in visceral, automatic, limbic and cognitive functions is related to its long-range projections to other cortical and subcortical brain areas (Miller and Cohen, 2001; Hoover and Vertes, 2007). Optogenetic approach allowed to identify glutamatergic (Britt et al., 2012; Suska et al., 2013) and GABAergic (Lee et al., 2014c) projections of the mPFC to the nucleus accumbens. This observation demonstrates that not all GABAergic neurons in the mPFC are local interneurons. In addition, glutamatergic PrL projections to the BLA are supposed to be involved in integration of higher cognitive processes linked to innate emotional responses (Yizhar, 2012). Two distinct pyramidal cell populations in PFC layer II either project to the contralateral mPFC or to the BLA (Little and Carter, 2013).

PrL-BLA projections also contact GABAergic interneurons in the BLA, which in turn exert feed-forward inhibition of GABAergic transmission *(Hübner et al., 2014*). This peculiar interconnectivity between the PrL and other brain regions is crucial for highly efficient bi-directional communication, and for top-down control over responding to emotional stimuli. The role of cerebellum in regulating mPFC activity may then have important consequences over the integration of stimuli at the cortical level and over high cognitive function processing. This may lead to a new perspective on cerebellar functions and paves the way for new investigations that have never been considered before.

1.5 Mouse peri-oral tactile sensory input transmission and cerebellar receptive fields

The two major excitatory inputs to the cerebellar cortex, MFs and CFs, originate from different pre-cerebellar pathways. CFs arise from IO and send direct projections to PCs while MFs excite PCs via cerebellar cortex GrC-PF and MLI pathway. Different gene expression patterns allow the identification of different cerebellar cortex regions named "transverse zones", each corresponding to specific lobules *(Apps and Hawkes 2009)*. In mouse, the anterior zone corresponds to lobules I-V; the central zone is related to lobules VI and VII; the posterior zone comprehends lobules VIII-IX while ventral lobule IX and lobule X form the nodular zone. It is possible to further divide each transverse zone into stripes, characterized by the expression of specific molecular markers.

The most representative molecular marker is Zebrin II, particularly expressed by a subset of PCs also known as Zebrin II+. PCs in which this marker is not expressed are defined as Zebrin II-. The heterogeneous pattern of expression of Zebrin II in PCs causes an alternate distribution of Zebrin II+/- stripes within the transverse zones (Apps and Hawkes 2009; fig 1.11). During the embryological development, the first neurons of the cerebellar cortex to differentiate are the PCs.

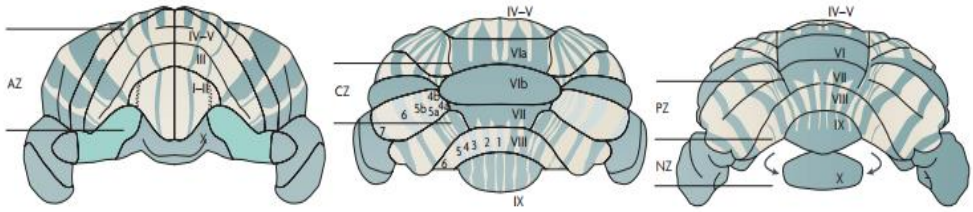

Figure 1.11| Anterior, dorsal and posterior views of transverse zones and stripes. *The distribution of zebrin II+ PCs (green in the figure) reveals the presence of transverse zones. Each transverse zone can be further subdivided in stripes running along the rostrocaudal axis and defined by the expression of zebrin II molecular marker. Zebrin II- stripes are beige in the figure.* Abbreviations: **AZ**, anterior zone; **CZ**, central zone; **PZ**, posterior zone; **NZ**, nodular zone *(Apps and Hawkes 2009).*

Consequently, the Zebrin II+/- stripes start to distribute already at this stage (Apps and Hawkes 2009; Larouche et al. 2006). Nevertheless, the topographic organization of afferents is reported to be secondary to the PCs formation, with MFs terminals forming transient connections with embryonic PCs before establishing mature connections with GrCs (Apps and Hawkes 2009; Grishkat and Eisenman 1995; Mason and Gregory 1984; Takeda and Maekawa 1989). During the following developmental stages the longitudinal zones extend perpendicularly to the axis of the lobules, so that it is possible to identify the topographical organization of CFs inputs and PCs output in the cerebellar cortex (Apps and Hawkes 2009). CFs arising from a particular subnucleus of the IO reach selectively a restricted number of zones (usually one or two), whilst MFs with a specific origin end dividing in multiple longitudinal zones.

The topographic organization of cerebellar afferents was obtained by the electrophysiological mapping of PCs and GrCs responses to sensory tactile stimulation of different parts of the body. Responses to tactile stimulation of a specific body area displayed a "fractured somatotopy", in which receptive fields are represented multiple times, in non-contiguous areas of the cerebellar cortex (Apps and Hawkes 2009, fig 1.12). This observations lead to the assumption that a very localized tactile stimulus is able to activate multiple patches of cerebellar granular and PCs layers (Bower and Woolston 1983).

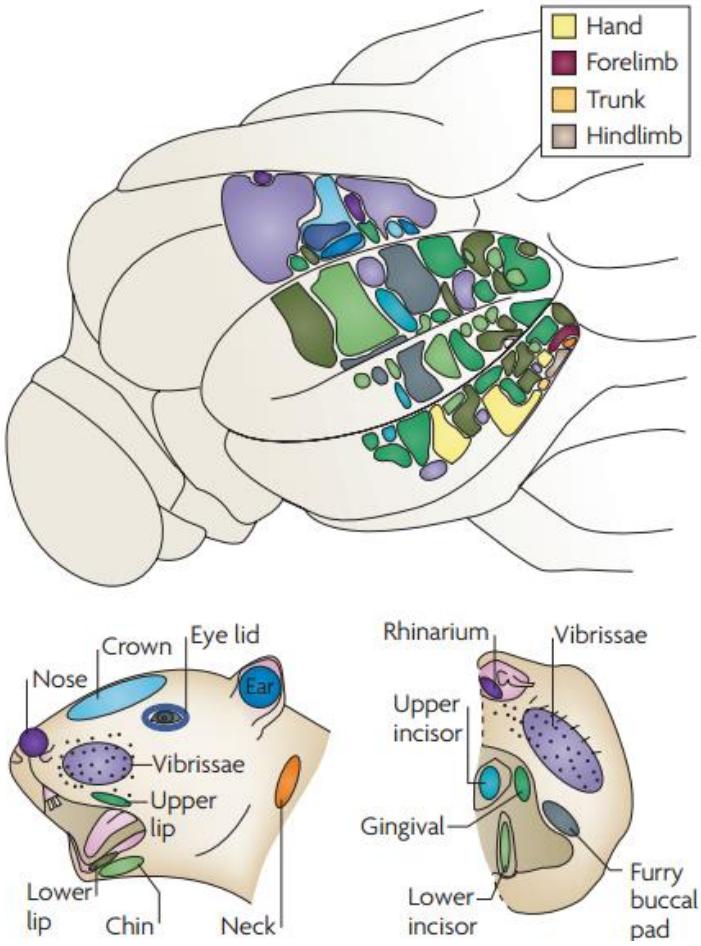

Figure 1.12| Spatial distribution of receptive fields in the granular layer of the rat cerebellum. *The granular layer shows a "fractured somatotopy" in which the same part of the body is represented several times, in discontinuous patches along the layer. The image shows the somatotopic representation of the body regions in the cerebellar granular layer. The colors of the body regions subjected to tactile stimulation match with the colors of the corresponding cerebellar areas activated by the stimulation (Apps and Hawkes 2009).*

Interestingly, body surface tactile stimulation elicited in DCN neurons constant response patterns (Rowland and Jaeger 2005). Somatotopic representation of different body parts was bilateral and similar in all the DCN including ipsilateral and contralateral facial regions and forepaws (Rowland and Jaeger 2005, fig 1.13). Different pathways relay sensory tactile inputs from the mouse peri-oral region to the cerebellum: trigeminal nuclei, inferior olive and thalamo-cortical-pontine loop (Bosman et al. 2010, fig 1.14). GrCs in the cerebellar cortex and DCN neurons receive excitatory synapses from MFs, while CFs from the IO reach both PCs and DCN neurons. The convergence of signals from MF-GrC and CF pathways to PCs has two distinct effects on their firing activity: PFs arising from the granular layer modulate PCs simple-spike firing whilst CFs generate complex spikes (Bosman et al. 2010). PCs represent the sole output of the cerebellar cortex projecting to DCN neurons, together with MFs and CFs. The patterns of response generated by DCN neurons following sensory tactile stimulation of the peri-oral region reflect the different combination of excitatory and inhibitory inputs that they receive. Sensory-evoked responses are characterized by three main components: short-latency inhibition, excitation and long-latency rebound excitation (Rowland and Jaeger 2005; 2008).

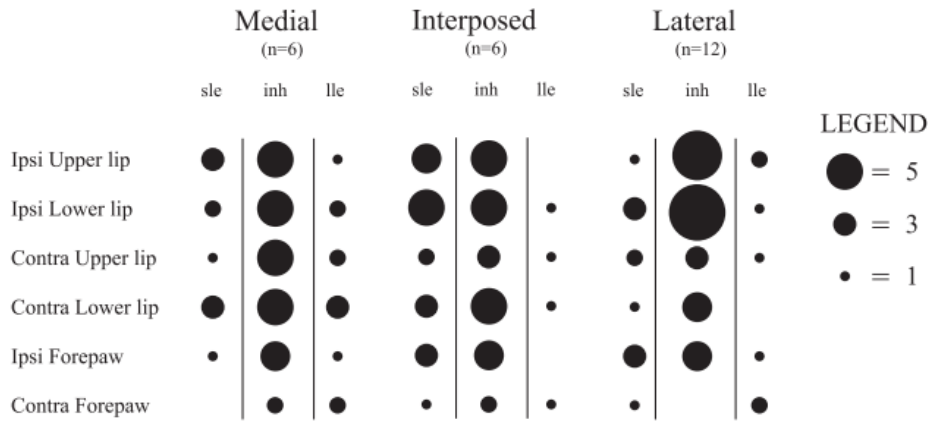

Figure 1.13| DCN neurons response patterns following the stimulation of different part of the body. *The amount of neurons showing a particular response pattern following the stimulation of a given body area is represented by a proportioned size dot (Rowland and Jaeger 2005).*

The short-latency inhibition presumably reflects the activation of the GrC-PC pathway, whilst the short-latency excitation pattern is supposed to originate from the activation of the trigeminal pathway. The long-latency rebound excitation following an inhibitory response could be explained considering that a pause in PCs discharge provokes the disinhibition of DCN neurons activity, thus generating a rebound excitation in nuclear neurons firing (Dykstra et al. 2016).

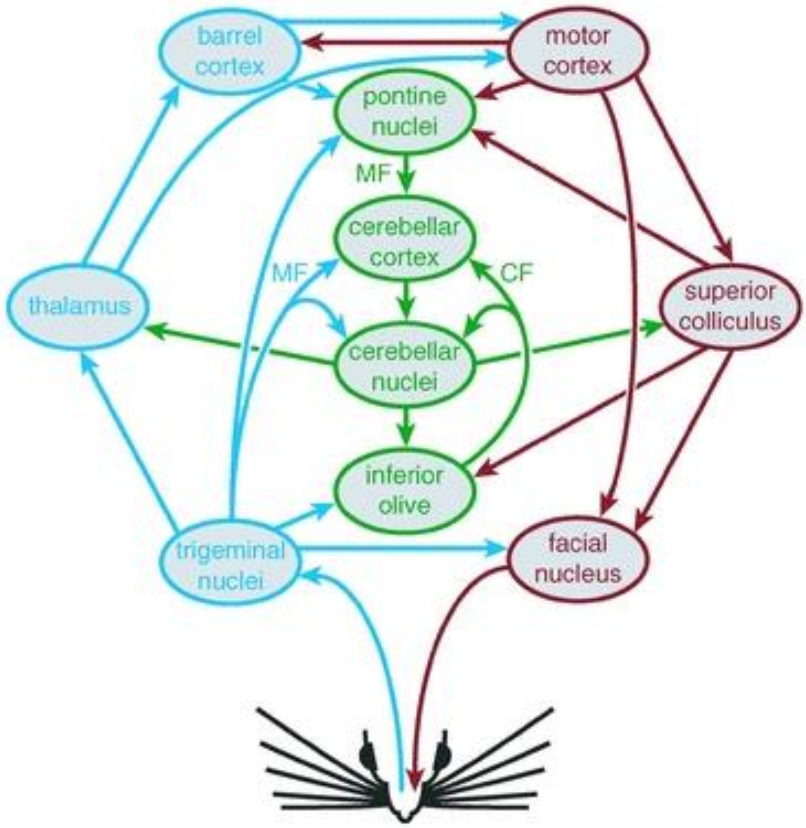

Figure 1.14| Pathways involved in the transmission of the sensory inputs from the mouse peri-oral region. *Cerebellar neurons display typical response patterns resulting from the sensory activation of synaptic pathways converging on these neurons (Bosman et al. 2010).*

1.6 Plasticity in the cerebellar circuit

Sinaptic plasticity represents the biological basis for neuronal learning as is generally used to indicate the capability of neurons to enhance or decrease the efficiency of their synaptic transmission in response to changes in their own activity. Over the years the cerebellum has been object of many investigations on different forms of synaptic plasticity and their mechanisms of induction, given their fundamental contribution to cerebellar inputs integration.

Long-lasting modifications of synaptic strength are known as potentiation (LTP) or depression (LTD). The existence of forms of LTP and LTD occurring at the PF-PC synapse, under the control of CFs teaching signal, led to the formulation of the Motor Learning Theory, which considered these synapses as the major responsible of motor activity control (Albus 1971b; Marr 1969). Nevertheless, further investigations revealed the existence of multiple forms of long-term plasticity at synapses in the molecular layer, granular layer and DCN, thus demonstrating that the properties of cerebellar learning emerge from all these forms of synaptic plasticity distributed at different connections (D'Angelo et al. 2016b). Both *in vitro* and *in vivo* studies report the existence of various forms of synaptic and non-synaptic plasticity in the cerebellar cortex (Antonietti et al. 2016a; D'Angelo 2014; Gao et al. 2012; Hansel et al. 2001a; Mapelli et al. 2015a; fig 1.15). Nevertheless, it has to be considered that a fundamental region displaying synaptic plasticity phaenomena is represented by the DCN, receiving both inhibitory inputs from PCs and excitatory inputs from MFs and CFs. (Bagnall and du Lac, 2006; Pugh and Raman, 2006). It is then reasonable to assume that cerebellar plasticity is highly related to fast and precise transmission and conversion of inhibitory-excitatory signals from the cerebellar cortex into a stabilized form in the DCN (Shadmehr et al., 2010). In line with experimental data, computational approaches including the contribution of DCN in cerebellar learning showed more rapid and stable learning capabilities when compared to preceding models considering only plasticity at the cortical level, thus providing a more realistic reproduction of human-like behavior during cerebellar learning of

associative tasks (Antonietti et al. 2016a) and giving new awareness of the role of DCN plasticity in cerebellar functioning.

DCN modulate cerebellar output upon receiving and elaborating excitatory and inhibitory synaptic inputs coming from different pathways. In cerebellar slices, the existence of both LTP and LTD has been reported in inhibitory synapses from PCs to DCN neurons and in the excitatory synapses between MFs and DCN (Medina and Mauk 1999; Morishita and Sastry 1996; Ouardouz and Sastry 2000; Pugh and Raman 2009; Zhang and Linden 2006). *In vivo* studies report that DCN neurons display persistent changes of the intrinsic excitability during cerebellar learning of an associative task, as eyelid conditioning (Zhang et al. 2004).

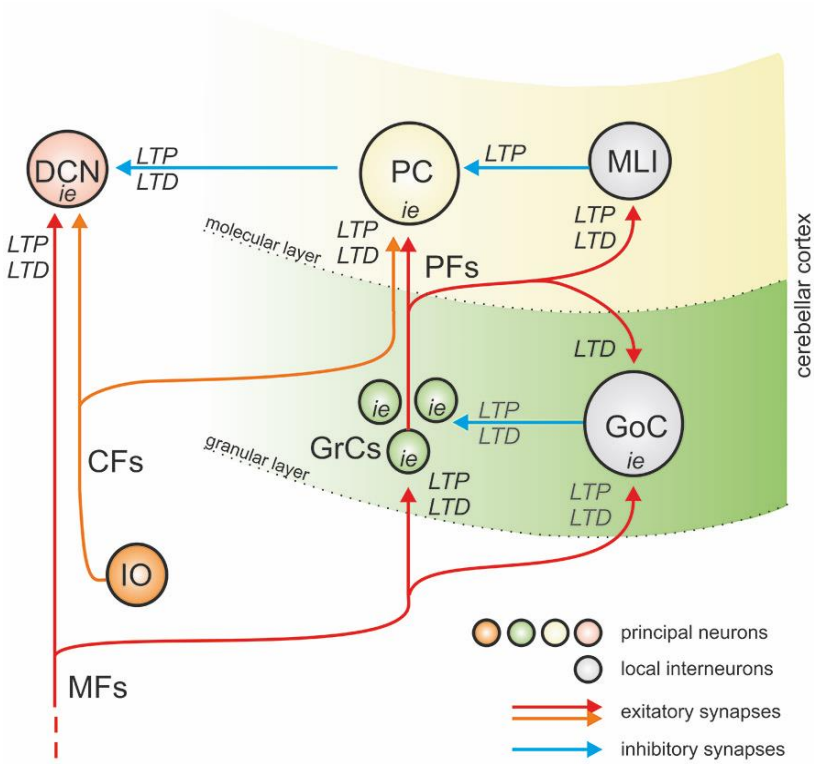

Figure 1.15| Sites of synaptic plasticity in the cerebellar circuit. *The scheme shows that the cerebellum is characterized by three main sub-circuits, including the granular layer, molecular layer and deep cerebellar nuclear. Sites of LTP, LTD and plasticity of intrinsic excitability (i.e.) observed experimentally (in black) or predicted by computational models (in gray) are shown. Adapted from Mapelli et al., 2015.*

The conditioned stimulus (CS, like a tone), is transmitted by MFs while CFs convey the unconditioned stimulus (US, like air puff or periorbital electrical stimulation). Consequently to MFs activation, simple spike frequency in PCs increases while the activation of CFs generates unaffected or facilitated complex spikes (Rasmussen et al. 2008). When the CS and US are paired and repeated, the stimulus-evoked complex spike in PCs generates a brief pause in simple spike firing, which is followed by a post-inhibitory rebound increase in the DCN neurons activity that causes rapid closing of the eyelid (Jirenhed et al. 2007). Moreover, it has been suggested that DCN might have a role in the consolidation of learned movements since responses to CS persist after cerebellar cortex lesion (Ohyama et al. 2003).

1.6.1 Plasticity induced *in vivo* by theta-patterned stimulation

Several studies *in vitro* demonstrated that theta-burst stimulation (TBS; 10 x 100 Hz bursts at 4 Hz) of MF projections is able to induce long-term plasticity in cerebellar cortex neurons (Armano et al. 2000; Gall et al. 2005; Mapelli and D'Angelo 2007). Notably, *in vivo* studies on urethane anesthetized rodents report that TBS, delivered in form of theta-patterned tactile stimulation (TSS), was able to elicit the same pattern of activity in MF, resulting in long-term plastic changes in cerebellar cortex neurons. In particular, TSS delivery induced long-term plastic changes in the granular layer (LTD) (Roggeri et al. 2008), Purkinje cells layer (LTP) and molecular layer interneurons (LTD) (Ramakrishnan et al. 2016; Roggeri et al. 2008). Although plasticity in the cerebellar circuitry has been exstensively investigated, information about plasticity in DCN neurons is still lacking. Several *in vitro* studies report plasticity in cerebellar nuclear neurons (Morishita and Sastry 1996; Ouardouz and Sastry 2000; Pugh and Raman 2008; 2009; 2006; Zhang and Linden 2006; Zheng and Raman 2010), but the impact of patterned sensory stimulation, such as the TSS, on DCN firing activity has never been investigated.

1.6.2 Signal processing in the DCN

The extremely regular organization of neuronal components in the cerebellar cortex and the repetition of the same neuronal scheme allows to subdivide the cerebellum in microzones that can be furtherly divided in microcomplexes (Apps and Garwicz, 2005). Each microcomplex elaborates inputs that are conveyed to PCs in the cerebellar cortex by MFs, or CFs originating from the IO. The afferent signals from MFs and CFs are encoded by PCs as sequence of simple and complex spikes, respectively, (Jacobson et al. 2008) and conveyed through their GABAergic axons to the DCN for further computation. The arrangement of the cerebellar cortex in microcomplexes permits a precise topographic cortico-nuclear connection that targets specific subpopulations of DCN neurons that are connected to specific cortical areas (Uusisaari and De Schutter 2011). So far, six different classes of neurons have been described in the DCN according to neurotransmitters phenotypes (glutamate, GABA and glycine), electrophysiological, and morphological properties (Uusisaari and Knöpfel 2012).

DCN neurons can be either local or projecting, receiving afferents from either PCs and from collaterals of MFs and CFs. They can also send GABAergic projections to the IO. Hence, in the complex mechanisms of encoding and elaboration of cerebellar output, it is important to consider the role of both cortico-nuclear projections and the olivo-cortico-nucleo-olivary loop circuit, but also intrinsic connections between DCN neurons subtypes (Uusisaari and De Schutter 2011). The majority of DCN neurons show spontaneous activity both *in vitro* (Uusisaari and Knopfel, 2010) and *in vivo* [Thach, 1968 (monkey); Le Doux et al. 1998 (rat)] at frequencies ranging from 20 to 90 Hz (Hoebeek et al., 2010; Uusisaari and De Schutter, 2011). Spontaneous firing in DCN neurons is regulated by the cortical output from PCs.

Concerning the projections from PCs to DCN, it is worth noting that they can show various degrees of convergence and divergence. Indeed, the cortical activity pattern can be elaborated by DCN neurons in different ways, depending

on the ratio of direct PC-DCN connection but also on the heterogeneity of PC synapses with different subtypes of DCN neurons (fig 1.16 A,B).

Together with cortico-nuclear projections, signal processing in the DCN also depends on the intrinsic connections formed either by local interneurons and by collaterals of the projection neurons. It is possible that the high convergence of inhibitory inputs from constantly active PCs to DCN neurons minimizes the influence of local synaptic inhibitory network in control of neuronal excitability and synaptic plasticity, but also on synchronization of oscillatory activity (Uusisaari and De Schutter, 2011).

As mentioned above, inhibitory nucleo-olivary projections also play a key role in DCN physiology. IO neurons fire spontaneously at 1–10 Hz and can exhibit rhythmic oscillatory activity around 10 Hz (Llinás 2009). DCN GABAergic neurons are also spontaneously active and their axons contact the IO at the level of glomeruli where also the gap junctions, fundamental for IO oscillations, are located (De Zeeuw et al. 1998; Devor and Yarom, 2002). Inhibitory signals conveyed by DCN to IO cause the de-synchronization of the IO network oscillating-activity (Kistler and De Zeeuw, 2005; Jacobson et al. 2008), with prominent consequences on the frequency of complex spikes in the cerebellar cortex and on PCs firing pattern that, in turns, affects related DCN neurons activity. Complex spikes evoked in PCs are critical for cerebellar learning as they engage mechanisms of synaptic plasticity in the cerebellar cortex that depress the simple spike response of PCs to MFs thus causing the adaptive correction of a motor behaviour.

Therefore, oscillatory activity is crucial for overall cerebellar functioning and might also play a role in mechanisms of synaptic plasticity involved in cerebellar learning. Considering the complex scenario and the multiple stages of cerebellar processing, the lack of available information on the mechanisms by which DCN network integrates and elaborates cerebellar inputs prompts a deeper investigation of the DCN anatomy and physiology in order to better understand the impact of the cerebellum in animal behaviour.

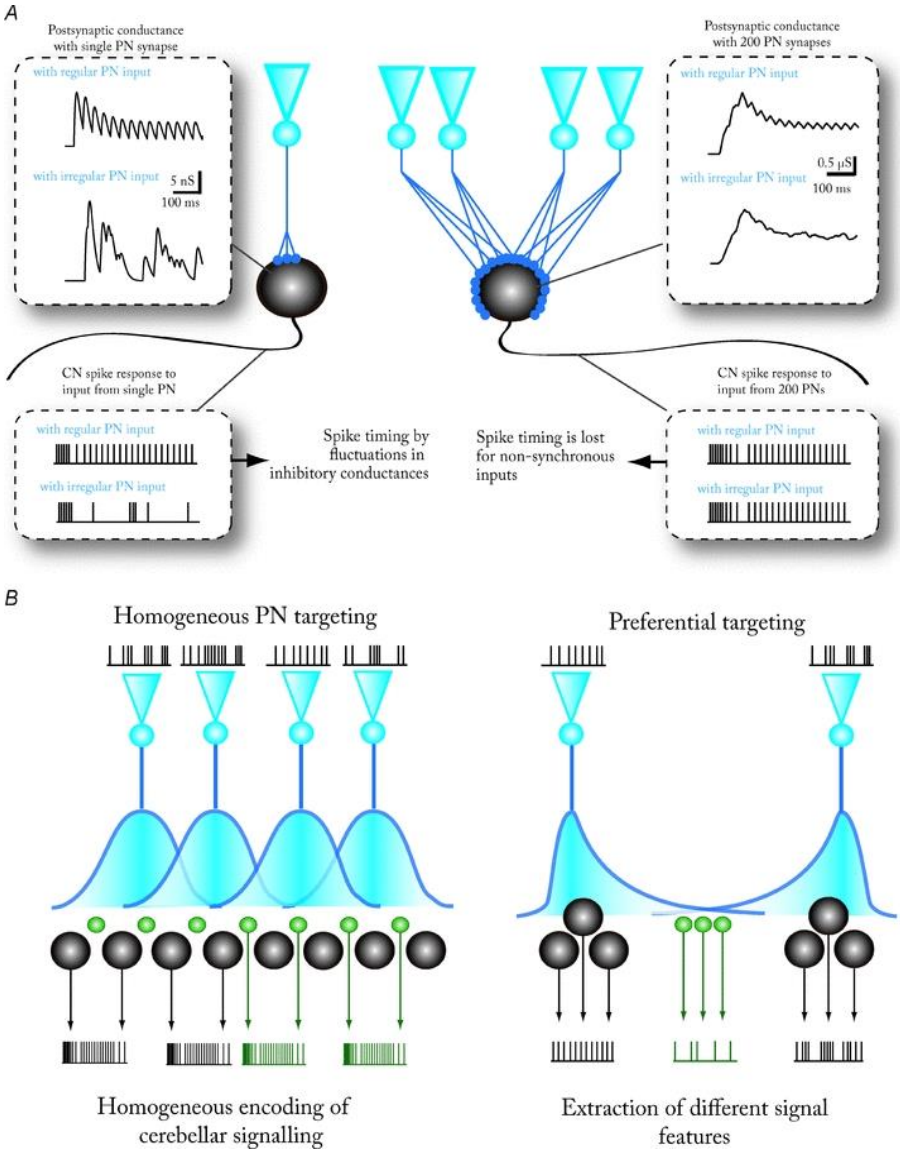

Figure 1.16| Cortico-nuclear convergence and divergence. A) conceptual drawing showing the effect of two extreme cases of PC to DCN convergence Left:: 1 to 1 connection between PCs and DCN neuron results in large inhibitory current fluctuations that can precisely time DCN spikes. Right: at higher (200 to 1) convergence ratios, the individual spikes cannot be resolved in postsynaptic current fluctuations, and the DCN neuron only responds to changes in the average firing rate of the pool of presynaptic PCs. Notably, the DCN output is quasi-identical whether the presynaptic PCs fire regularly or not. **B**) Heterogeneity of PC-DCN divergence determines the diversity of the spiking responses of DCN neurons to a cortical activity pattern. Left: homogeneous divergence and convergence of PCs over all DCN neurons leads to the DCN acting as a homogeneous feature

extractor. All DCN neurons in a given cortical target zone will encode and transmit a single property of the cerebellar computation. If all DCN neurons are equally innervated by a large number of converging PCs, and each PC contacts DCN cells of all neuronal subtypes, the extracted feature is the average firing rate of PCs. Right: in the opposite case, PCs target preferably certain DCN neuron populations (black) that are nearly exclusively contacted by many terminals from single PCs (or a small group of PCs with similar firing patterns). Other DCN populations (green) receive synaptic input from overlapping groups of PCs via fewer synaptic terminals. In this case, the 'black' DCN neurons are able to convey information about individual PC spike timing, whereas the 'green' DCN neurons will encode average cerebellar spike rates in their own output. Note that reliable transmission of either feature to the extracerebellar targets requires that a group of DCN neurons receives exactly the same cortical signal. (In the figure: PN stands for PC, CN stands for DCN; adapted from Uusisaari and De Schutter, 2011)

1.7 Neural oscillations and up-down cortical dynamics

Rhythmic or repetitive patterns of neuronal activity in the brain are generally referred to as neural oscillations. Oscillatory activity is reported at different levels of organization in the CNS, comprehending single-neuron activity, activity of a local group of neurons, as well as activity of interconnected brain regions (Buzsaki, 2006). The impact of neural oscillations on overall brain functioning is extended to a wide-range of situations. Processes of sensation, movement control and cognition have been linked to neural oscillations and synchronization of specific brain areas at specific frequency bands. Oscillatory patterns have been widely studied in large population of neurons and measured by techniques such as electroencephalography (EEG) that revealed the existence of different frequency bands of neural activity related to specific brain states. The first band to be discovered was the alpha activity (8-12 Hz) detected from the occipital lobe during relaxed wakefulness with increase in its frequency when the eyes are closed. Other frequencies bands are: delta (1-4 Hz), theta (4-8 Hz), beta (13-30 Hz), low gamma (30-70 Hz) and high gamma (70-150 Hz), with higher rhytms detected during cognitive processing (Buszaki 2006).

Oscillations have been detected also using more invasive recording techniques such as single-unit recordings, in which rhythmic patterns of firing that are

generated by single neurons are detected. The rhythmicity of neuronal firing is fundamental for information coding in the brain. Moreover, if multiple neighboring neurons fire in synchrony, they can give rise to oscillations that are recorded in form of LFPs.

Further components involved in brain oscillatory networks are neurotransmitters, such as GABA, and certain neuromodulators, such as norepinephrine, dopamine and serotonin whose concentration levels are known to regulate oscillatory activity and have a prominent effect on amplitude of different brain waves (Buzsaki 2006).

In the cerebellum, oscillatory phaenomena have been detected as belonging to various frequencies. The IO, DCN and GrC layer are characterized by low-frequency oscillations in the 4–25 Hz range, whilst both slower frequencies (<1 Hz oscillations), and faster activity (>150 Hz) have been reported in PC layer (D'Angelo et al. 2009; Courtemanche et al. 2013; Cheron et al. 2016). Those oscillatory patterns could have a crucial impact on temporal processing of information in the cerebellum, as demonstrated for the IO-PC-DCN pathway (Jacobson et al. 2008, Llinás 2009), but also on the induction of synaptic plasticity during cerebellar learning, similarly to hippocampal and cortical synapses (Buzsaki 2006; Roy et al. 2014). Moreover, oscillations in the cerebellum have a role for the synchronization of cerebellar activity with other brain areas in both sensorimotor and cognitive contexts (D'Angelo et al. 2009; Courtemanche et al. 2013). Synchronization of neuronal activity within brain networks is possible through long-range connections that allow fast and direct coordination of neuronal firing of spatially separated units that respond to the same stimulus. Reciprocal connections and the creation of feed-back loops between the same areas also support oscillatory activity during specific tasks. Several studies report a coherence between the theta/beta-range oscillations (4–25 Hz) observed in cerebellar cortex and cerebral cortex activities (Courtemanche et al., 2013). The cerebellum and the PFC are anatomically and functionally interconnected (Palesi et al. 2015, Watson et al. 2009; Watson et al. 2014; Kelly and Strick 2003), and theta band

synchronization of both regions is associated with adaptive performance of associative learning behaviour (Chen et al. 2016).

During synchronized brain states, a peculiar pattern of neuronal activity has been observed in the cerebral cortex consisting of the alternation between "up" states, characterized by neuronal tonic firing, and "down" states in which neurons were quiescent (Timofeev et al., 2011). Cortical up-down transitions were initially associated to brain activity during sleep (Steriade et al, 1993) or during induced anesthesia (Steriade et al, 1993), but recent studies observed the existence of up-down cortical dynamics also in awake rodents (Luczack et al., 2007), and in different animal models performing noncognitive tasks (Sachidhanandam et al., 2003; Vyazovskiy et al., 2011; Engel et al., 2016). It has been hypothesized that during up periods network excitability decreases due to physiological mechanisms that are no longer able to sustain tonic excitation, thus causing an automatic transition of the network to a down period characterized by low or absent firing (Contreras et al., 1996; Sanchez-Vives and McCormick, 2000). Then, when the circuit becomes again excitable it autonomously switches into an up state (Cunningham et al., 2006; Sanchez-Vives and McCormick, 2000).

The presence of up-down dynamics in neocortical circuits has been associated with activity in subcortical areas, the most representative being the thalamus. It is known that the spontaneous oscillating activity of thalamocortical neurons at low frequencies is able to either induce or modulate the up-down cortical dynamics (Rigas and Castro-Alamancos, 2007; David et al., 2013; Lemieux et al 2014).

Nevertheless, up-down states also depend on stochastic events from external inputs that trigger up-down transitions (Jercog et al, 2017).

In the interpretation of cerebello-cortical interaction it might be then reasonable to hypothesize a role for both cerebello-thalamic pathway, as well as cerebello-VTA dopaminergic pathway, not only in synchronization of cortical activity during certain behavioural processes, but also in modulation of cortical up-down states.

Indeed, alterations in oscillatory activity in both cerebellum and PFC result in neurological disorders, such as autism (Cornew et al. 2012), schizophrenia (Parker

2016) or Parkinson's disease in which cotical up-down states and low-frequency oscillations are altered by dysfunctional frontal dopamine signaling (Parker 2016).

1.8 Cerebellar role in cognitive processes

In the past decades, a consistent amount of studies focused on the cerebellar role in movement through the investigation of motor pathways organization from the motor cortex to the cerebellum and their role in motor learning. However, the existence of anatomical and functional neuronal pathways between the cerebellum and the PFC in both directions (Palesi et al. 2015; Kelly and Strick, 2003; Watson et al. 2009; Watson et al. 2014) suggest that the cerebellum is involved in functions beyond the motor domain. Indeed, the PFC is a brain region mainly involved in higher cognitive function rather than in motor control. An interesting theory proposes that the brain is able to select and perform motor commands through anticipatory control loops and internal (forward and inverse) models (Ito 2008, fig. 1.17). The extension of this theory to cognition might explain how the brain internalizes information that is ultimately converted into thoughts.

The forward model computes the inputs into a system using only the comparison of current state and the system output, so it is unable to correct errors since it does not use feedback inputs. Conversely, in inverse models some of the output of the system return into the system's input, and the system is then able to adapt or compensate for errors in its desired output. The capability of the brain to create internal models allows to predict movement and the on-line control of dynamic properties of body parts without the need of sensory feedback, just as the movement is repeated (Ito 2008). The role of the cerebellum in anticipatory control loops is fundamental for the coordination, dynamics and smoothness of movements, all reflecting learning of adaptive mechanisms that rely on sensory prediction errors and are responsible for internal modeling of the body state (D'Angelo et al. 2012; Shadmehr and Krakauer 2008).

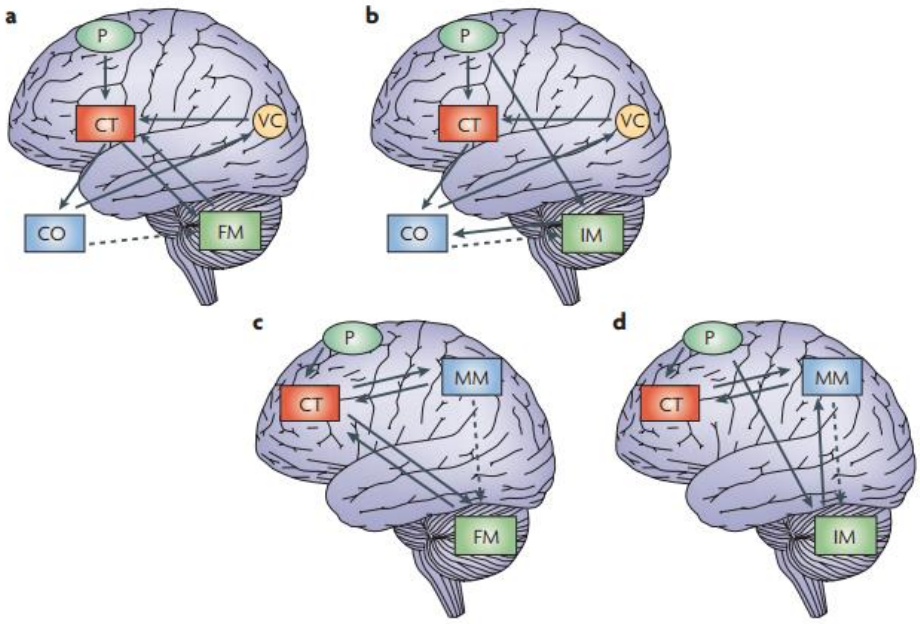

Figure 1.17| Internal-model control systems for voluntary movement and mental activity. a,b | *'Forward' (**a**) and 'inverse' (**b**) model control systems for movement. According to the instruction given by the instructor (P) in the premotor cortex, the controller (CT) in the motor cortex sends command signals to the controlled object (CO; a body part or a lower motor center). The visual cortex (VC) mediates feedback from the body part to the motor cortex. The dashed arrow indicates that the body part is copied into an internal model in the cerebellum (either a forward model (FM) or an inverse model (IM)). In the forward-model control system, control of the CO by the CT can be precisely performed by referring to the internal feedback from the forward model. In the inverse-model control system, feedback control by the CT is replaced by the inverse model itself. **c,d** | Forward- and inverse model control systems for mental activities. In response to an instructor, the controller in the prefrontal cortex initially controls a mental model (MM) that is expressed in the temporo–parietal cortex. The dashed arrow shows that the mental model is copied to a forward model or an inverse model in the cerebellum. (Adapted from Ito, 2008)*

The existence of anticipatory control loops allows not only the on-line control of action, but also the prediction of abstract consequences of actions, and even the imagination and evaluation of novel ones. The similar organization of neuronal pathways involved in motor preparation and imagery supports the idea that existing internal models, together with the acquisition of novel models, are involved in both motor control and cognitive processing during behavior.

The division of the cerebellar cortex in microcomplexes allows the constitution of closed-loop circuits that are fundamental for cerebellar interconnections with the neocortex (Middleton and Strick, 2000; Kelly and Strick, 2003; Apps and Hawkes, 2009). Cerebellar microcomplexes represents the functional learning unit that is ultimately connected to the same group of neurons in DCN and IO (Apps and Hawkes, 2009). In each microcomplex, inputs from MFs to GrCs are relayed to PCs that receive also error signals conveyed by CFs arising from IO, that drive LTD - based learning process at PFs-PC synapses. The capability of the cerebellum to form and adapt internal models finds its fundamentals in this error learning, so that each microcomplex is able to form an internal model for a specific function. The internal model hypothesis speculates on the possibility that during repetitive trials of a thought for which a particular mental model is used, a corresponding internal model (either forward or inverse) is formed in the cerebellum (Ito, 2008). Hence, internal models created in the cerebellum for anticipatory control loops might be employed not only for the recurrence and timing of action but are also executed to sustain cognitive processing and thought. This assumption could also explain the fact that cerebellar deficits have consequences in both motor and cognitive domains (Schmahmann 2004).

A further consideration to make is that neural substrates for abstract or symbolic cognition are not separated. It might be then correct to consider thought as an implicit form of action that reuses and re-enacts the same anticipatory control loops that support on-line action control and adaptive behavior. The creation of abstract internal models and action prediction depends on the combination of inhibition processes, working memory, event representation and learning (Pezzulo 2012).

The PFC is the region of the neocortex that is related to conscious control of thought and action, which comprehends cognitive functions such as abstract reasoning and problem solving (Miller and Cohen, 2001). Neurons in the PFC hold informations about goals and the means to achieve them through the working memory system for which specific patterns of activity of pyramidal cells are

maintained for a protracted time (Miller and Cohen. 2001). The working memory system depends on lateral inhibition from GABAergic interneurons (Rao et al., 2000) and operates together with the novelty system involving hippocampal CA1 area and dopaminergic neurons in the VTA in order to regulate the attention level and develop the opportune mental model during the elaboration of thought (Lisman and Grace, 2005). Interestingly, one of the subcortical structures reached by cerebellar output is indeed the VTA whose dopaminergic projections modulate neuronal activity in PFC (Mittleman et al, 2008; Rogers et al., 2011; Dembrow and Johnston 2014). Moreover, recent studies in mice demonstrated anatomical and functional interaction between the cerebellum and the hippocampus, thus allowing to speculate that the cerebellum may also influence hippocampal neuronal activity and related functions in associative learning (Bohne et al. 2019; Watson et al. 2019). When a new problem shows, there is a mismatch between existing mental models and the novel issue so that the brain needs to elaborate new strategies to solve it (new mental models). In this case the novelty triggers the attentional system which increases magnitude and duration of working memory (Schmajuk et al. 1996), which in turn sends command signals that allow the adaptation of mental models to the novel situation.

Beside the attentional system, the thalamus represents another subcortical structure that plays a key role in regulating cortical neurons activity that is also connected to the cerebellum. The thalamus mediates cerebello-cortical intercommunication as it relays cerebellar outputs to both motor and prefrontal areas of the brain (Schmahmann, 1996; Hoover and Vertes 2007). The thalamus is involved in motor, cognitive and sensation processes (John, 2002; Alitto and Usrey, 2003) and operates a rapid on-line and feedback processing that allows the synchronization of sequences of thought and action (Koziol et al., 2014). In general, alterations in cerebello-cortical pathways that contribute to the regulation of firing activity in PFC neurons is known to be involved in several cognitive diseases such as autism and schizophrenia (Rogers et al. 2011; D'Angelo and Casali 2012; Andreasen et al. 1998).

In conclusion, considering both physiological and computational aspects of neural substrates of motor and cognitive processes, it might be reasonable that thought and action performance represent implicit forms of behavior that use anticipatory control loops originally formed for explicit actions. This means that during learning, neural networks in PFC shift their resources from external (sensation) to internal (memory) processing (Brincat and Miller, 2016). Hence, cognitive processing remains strictly dependent on sensorimotor anticipation. The existing gap between sensorimotor and cognitive control domains could be filled by the cerebellum and other subcortical structures that play the same role in the planning, execution and coordination of action, cognition, and thought.

Chapter 2

Materials and methods

Electrophysiological recordings were performed on 30-40 days old C57BL/6 mice of either sexes. Electrophysiological recordings coupled with optogenetics were performed on 50-60 days old C57BL/6 mice of either sexes, after 3-4 weeks from viral injection. Mice were located in cages and kept with a12 hours day-night cycle (12 hours light from 06.00 am - 06.00 pm, 12 hours dark from 06.00 pm - 06.00 am). Water and food were provided *ad libitum*. All experimental procedures were performed on head-fixed, urethane- anesthetized animals. The comparison of neuronal activity and responsivity between males and females did not show any statistical difference (data not shown). Hence, the stage of the oestrous cycle in female mice unlikely affected the data reported in this thesis.

2.1. Animal preparation

Single-unit recordings were obtained from the fastigial nucleus (FN) or neurons in PrL region of mPFC in two different series of experiments, both performed applying similar surgical procedures. C57BL/6 mice were deeply anesthetized using intraperitoneal injections of urethane (Sigma Aldrich). The first injection (1.3g/kg urethane dissolved in 0.9% NaCl solution) was followed by a total of 3-4 booster injections (10% of the induction dose), each performed after 30 minutes from one another, in order to stabilize deep anesthesia. The level of anesthesia was monitored by testing the absence of leg withdrawal reflex after pinching and spontaneous whisking. The mouse was then positioned on a stereotaxic table covered with a heating plate (HP-1M: RTD/157, Physitemp Instruments Inc, Clifton, NJ, USA) and a feedback temperature controller connected to a rectal probe allowed to maintain body temperature at around 36°C (TCAT-2LV controller, Physitemp Instruments Inc, Clifton, NJ, USA). After reduction of cutaneous reflexes by subcutaneous application of lidocaine (0.2ml; Astrazeneca), skin and muscles were removed to expose the skull. The head was

fixed over the Bregma to a metal bar connected to a custom-built stereotaxic table.

Craniotomy was performed over the cerebellum and, when necessary, on mPFC area to expose their surface and finally place the electrodes (from Bregma: FN -5.8 AP, +0.50 ML, +2.4 DV; DN: -5.8 AP, +2.25 ML, +2.35 DV; PrL: +2.8 AP, 0.25 ML, +0.6 DV).

2.2 Extracellular recordings

Extracellular electrodes have the capability to detect action potentials, or "spikes", produced by active neurons due to currents flowing over their membrane. The difference in the electric potential between the intracellular and extracellular environment is defined as membrane potential. At a resting state the neuronal membrane potential is normally around -70 mV, meaning that the intracellular space is 70 mV more negative than the outside. The origin of extracellular signal and current flowing around the axon of an active neuron can be modeled and explained using the volume conductor theory (Heinricher 2004; Lorente de No 1947; Rall 1962). In a simplified model, the axon can be conceptualized as surrounded by an extracellular saline bath, known as "volume conductor". The resting state of the axon is characterized by the absence of current flow and equally distributed membrane potential along its entire length (Fig. 2.1A). When an action potential is evoked at the level of the axon initial segment, the membrane of that region generates an inward current flow ("sink") that causes depolarization. If a microelectrode is placed close to the sink it will record a negative potential with respect to another electrode placed at distance. The current flowing through the depolarized region origins from areas of the membrane adjacent or distant to the sink. At the level of the "source" current flows outward, thus meaning that a microelectrode placed near the source will detect a positive potential, relatively to another distal electrode (Fig. 2.1B). The model of source and sink suggests that a microelectrode adjacent to an axon that is conducting an action potential will record a triphasic signal (+ - +).

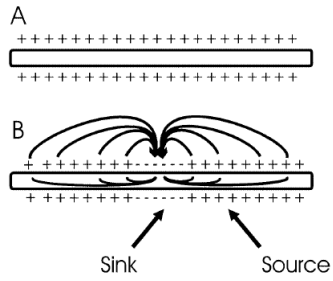

Figure 2.1| Volume conductor theory. *(A) Schematic representation of the extracellular currents flow around an axon at rest, surrounded by a low resistance volume conductor. (B) Schematic representation of the extracellular currents flow around an axon of an active neuron. Figure from (Heinricher 2004).*

Positive flexions always appear less evident than the negative ones because distal regions to the origin site of the action potential display lower density of current (Heinricher 2004; fig 2.2).

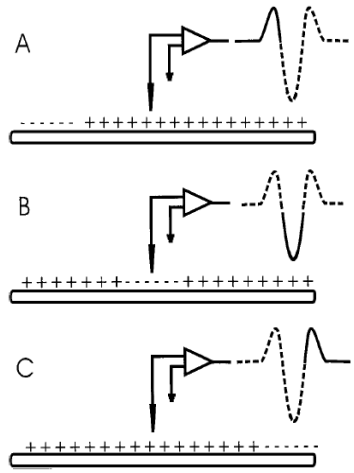

Figure 2.2| Triphasic extracellular signal recorded by a microelectrode adjacent to an axon that is conducting an action potential, according to the model of source and sink based on the volume conductor theory. *(A) Small positive flexion, reflecting the positive potential of the membrane under the electrode, which is not affected by the depolarization;* (B) *prominent negative deflection, representing the negative potential observed when the action potential reaches the membrane underlying the electrode;* (C) *small positive flexion when the action potential, which is propagating along the axon, overpasses the electrode and the membrane act as a source again. Figure from (Heinricher 2004).*

Interestingly, intracellular and extracellular potentials recorded simultaneously during antidromic activation of a motoneuron in the ventral horn of the cat unveiled that the negative deflection of the extracellular potential coincides with the depolarization detected by the intracellular-recording electrode, whilst the subsequent positive flexion corresponds with the repolarization phase recorded intracellularily (Heinricher 2004; fig 2.3). Action potentials can origin both at the level of soma or dendrites, with the model predicting a biphasic signal in which an initial negative component is followed by a positive phase (Fig. 2.4).

Nevertheless, it should be considered that in real conditions the morphology of the soma, the geometrical distribution of the dendrites and the conductance distribution along the membrane may diverge among different neurons. The position of the electrode relative to the cell also has an impact on several features of the recorded signal, thus complicating the picture of the simplified model described in the volume conductor theory.

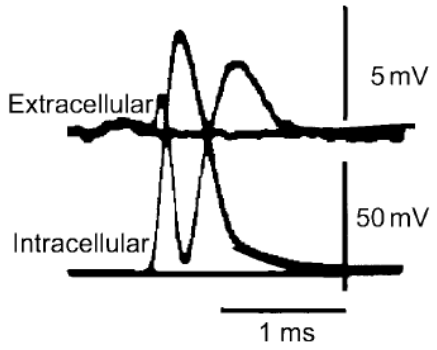

Figure 2.3| Simultaneous recordings of intracellular and extracellular potentials during antidromic activation of a motoneuron in the ventral horn of the cat. *The negative deflection of the extracellular spike corresponds to the depolarization seen by the electrode during intracellular recording whilst the late positive flexion coincides with the repolarization phase intracellularly recorded. Figure from (Heinricher 2004).*

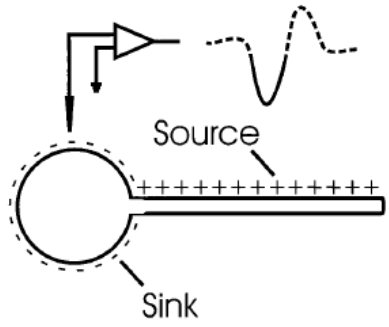

Figure 2.4| Spikes generated at the soma. *The model predicts a biphasic signal with an initial negative component corresponding to the sink followed by a positive late phase reflecting the source. Figure from (Heinricher 2004).*

The *in vivo* extracellular recording technique allows the acquisition of extracellular action potentials deriving from currents flowing through the neuronal membrane. Extracellular recordings of single neurons activity (single-unit; SU) or adjacent neurons potentials (local field potentials, LFP) allow the investigation of neuronal physiology and connectivity. The activity of neurons can be recorded for prolonged time in specific experimental conditions involving chronically implanted microelectrodes, thus allowing the correlation of neuronal activity with behaviors or physiological phenomena. Neuronal action potentials and discharge frequency serve as code to transmit informations through the nervous system. In particular, neurons are known to use two different strategies: the first, named "rate coding", exploits the firing rate as the key to decode incoming information, while "time coding" takes into account single spikes and their temporal latency as the key to decode the information.

For these reasons, extracellular recordings represent the major tool used to investigate neuronal discharge properties and functional connectivity within and across different brain areas. Nevertheless, it is important to consider its limitations, given the fact that this method cannot be exploited to investigate electrophysiological properties at the cellular level, in particular sub-threshold events, or physiological mechanisms involved in neuronal intrinsic excitability.

2.3 *In vivo* extracellular recordings from FN and PrL in mice

Depending on experimental requirements, plenty of different types of microelectrodes are available to record neuronal extracellular activity with a good signal-to-noise ratio. In this work, single-unit recordings were obtained using quartz-coated platinum/tungsten fiber microelectrodes (1-5MΩ; Thomas Recording, GmbH, Germany) mounted in a 16-channel multi-electrode array (MEA) system (system Eckhorn microdrive, Thomas Recording GmbH, Germany; Fig. 2.5). Microelectrodes were disposed in a 4x4 matrix with inter-electrode distance of 100 µm. Electrodes could be moved independently from one another allowing simultaneous and independent insertion into the exposed brain tissue.

Figure 2.5| Multielectrode Array (MEA). *The recording microelectrodes were placed in a 16-channel multielectrode array system, ending in a 4x4 matrix with inter-electrode distance of 100 µm.*

The detection and acquisition of electrophysiological activity was obtained using OpenEx software suite (Tucker-Davis Technologies, Alachua, FL, USA), then signals were digitized at 25 kHz, using a 300-5000 Hz band-pass filter, amplified and stored using a RZ5D processor multi-channel workstation (Tucker-Davis Technologies, Alachua, FL, USA).

Single-unit recordings were obtained from the FN or PrL region of mPFC in two different experimental series:

1. Single-neurons activity into the FN was monitored while performing a sensory tactile stimulation protocol using air-puffs delivered to the mouse peri-oral area. FN neurons showed a spontaneous firing activity that was recorded for 5 minutes, then low-frequency air-puffs (0.5 Hz- 30 ms- 30-60 psi) were delivered at the level of the mouse upper lip, lower lip or whisker pad to obtain the activation of the corresponding receptive fields and elicit neuronal responses. During the tactile stimulation peri-stimulus time histograms (PSTHs) were constructed online in order to detect a neuronal response in FN neurons. After the identification of a responsive unit, air-puff stimulation at 0.5 Hz was performed for additional 20 minutes. Then, a theta sensory stimulation (TSS) pattern (a burst of 100 air-puffs delivered at 4 Hz) was performed to induce plasticity, followed by post-induction recordings during tactile stimulation at 0.5 Hz lasting 40 minutes at least.

   In a subset of experiments AMPA and NMDA glutamate receptor antagonists, NBQX (100μM) and D-APV (250μM) respectively, were dissolved in Krebs solution with the following composition (in mM): 120 NaCl, 2 KCl, 1.2 $MgSO_4$, 26 $NaHCO_3$, 1.2 KH_2PO_4, 2 $CaCl_2$, and 11 glucose, equilibrated with 95% O_2-5% CO_2 (pH 7.4). Drugs were pre-loaded in a pneumatic picopump PV820, World Precision Instruments) ending in a 35G needle placed at the level of the FN using a Patch-Star micromanipulator (Scientifica, Ltd). After 15 minutes of single-unit recording, drugs were locally perfused at the rate of 1μl/5min during

tactile stimulation in order to allow a better carachterization of elicited excitatory responses. In another experimental set, the contribution of cerebellar cortex and PC activation onto FN neurons response patterns elicited by tactile stimulation was investigated using optogenetics (details reported in chapter 2.4);

2. Activity of PrL neurons was recorded during the electrical stimulation of the DN. PrL neurons spontaneous activity was recorded for about 5 minutes, then electrical stimulation of DN (21 pulses, 100 Hz, 100 μA) was performed every 5s using a co-axial platinum bi-polar tungsten electrode, in order to evoke neuronal responses into the PrL area. In a subset of experiments, the perfusion of dopaminergic receptor antagonists (SCH23390 hydrochloride, selective D1-like antagonist; (S)-(-)-Sulpiride, selective D2-like antagonist) onto the surface of the exposed mPFC allowed to investigate the putative role of DA release, induced presumably through the cerebello-VTA pathway, in the elicited responses. In these conditions, 5 minutes recording of mPFC neurons spontaneous activity was followed by DN electrical stimulation delivered every 5s for 20 minutes as control period. Drugs were applied locally using a micropipette immediately after the control period and maintained throughout the rest of the recording (about 30 minutes). In another subset of experiments the same protocol was performed for the perfusion of $GABA_A$ receptor antagonist gabazine (SR-95531, 3mM) onto the surface of mPFC, in order to investigate the inhibitory response elicited in PrL neurons presumably through cerebello-thalamic pathway onto PrL neurons activity.

2.4 Optogenetics

Optogenetics exploits the possibility to express light-sensitive proteins, such as microbial opsins, at the level of intact mammalian neurons membranes, allowing manipulation of neuronal firing on a millisecond time scale using light, both in *in vitro* and *in vivo conditions* (Boyden et al., 2005; Deisseroth, 2010).

Channelrhodopsin-2 (ChR2; and genetically modified variants), is a cation channel that induces neuronal depolarization upon illumination with pulses of blue light (Mattis et al., 2012). On the other side, hyperpolarization of neuronal membranes is achieved through the expression of the chloride pump Halorhodopsin (NpHR) or the proton pump Archaerhodopsin (Arch or ArchT) (Mattis et al., 2012).

It is possible to obtain cell-type specific expression of opsins by exploiting gene-based targeting strategies involving transgenic animals and/or viral constructs carrying opsin genes under control of tissue specific promoter sequences (Zhang et al., 2010). Another approach allows selective expression of light-sensitive proteins through the combination of rodents Cre-recombinase (Cre) driver lines with Cre-dependent viral opsin vectors. In *in vivo* conditions, light can be delivered to the the brain region of interest by a laser or LED light source coupled to a thin optical fiber (~100–300 μm) that has been implanted on the skull of the animal (Sparta et al., 2012). The wavelength and the opportune light source required for the experiments depend on the class of opsin expressed and the depth of the region that has to be illuminated. Moreover, since opsins expression is not restricted to neuronal somata but spreads also through neuronal projections, it is possible to specifically manipulate the terminals innervating a target region (Zhang et al., 2010).

Besides the possibility to rapidly photostimulate neurons in a reversible and repeatable manner, convenience in using optogenetics comes from the integration of photostimulation with electrophysiological recordings and anatomical tracing upon the expression of fluorescent reporter proteins integrated to opsins (Gradinaru et al., 2007). Nevertheless, there are important limitations to consider, such as the toxicity of viral vectors and the potential neuronal damage due to heating during photostimulation. Despite the limitations, the optogenetic technique provides the unique capacity to selectively and robustly modulate neuronal activity in behavioral models and acute slice preparations (Yizhar et al., 2011a).

2.4.1 ChR2 expression in the cerebellum

For our experimental purposes, optogenetics represented an ideal tool to interfere with PC activity and investigate the impact of the cerebellar cortex over DCN plasticity. Stereotaxic injection of the adeno associated viral construct AAV1-hSyn(H134N)-ChR2-EYFP (Penn Vector Core, University of Pennsylvania, USA) at the level of cerebellar molecular layer allowed ChR2 expression under a pan-neuronal promoter (thus common to molecular layer interneurons, PCs and parallel fibers). C57BL6 mice of either sex (30 days old, n=13) were deeply anesthetized with 1-2% isoflurane in oxygen 100% at 0.7 L/min delivered from a gas vaporizer (Ugo Basile S.R.L., Italy) and their head was fixed on the stereotaxic apparatus (Leica vernier stereotaxic instrument) using ear bars. The skull was then exposed and a burr hole was drilled in correspondence of cerebellar vermis lobule VI (from Lambda ML 0.0mm, AP -3.5mm; DV -0.3mm). The virus was loaded into a 10µl NanoFil syringe (World Precision Instruments) connected to an automatic syringe pump (Ugo Basile S.R.L., Italy). The injection needle (NF35BV, 35G, World Precision Instruments) was lowered into the vermis at 300 µm depth and 0.2 µl of virus solution was injected at a flow rate of 0.05 µl/min. This procedure allowed the expression of ChR2 selectively at the level of the cerebellar cortex. After surgical procedures and recovery from anesthesia mice returned to the animal facility. In order to ensure a good expression of ChR2, electrophysiological experiments were performed 21-28 days after viral injection.

2.4.2 Optogenetics *in vitro*

The efficacy of ChR2 expression in the cerebellar cortex was assessed *in vitro* by performing electrophysiological recordings in acute cerebellar slices (220µm thick). Cerebellar vermis from 5 mice that were injected with the construct but were not used for *in vivo* recordings was removed and sagittally cut using standard procedures (Mapelli et al. 2017). Then, extracellular recordings from PCs were performed using the patch-clamp technique. The recording of extracellular signals was operated using a Multiclamp 700B amplifier (Molecular Devices)

controlled by pClamp10 through a Digidata1440A (Molecular Devices). Since ChR2 was expressed all over the cerebellar cortical circuit, selective photoactivation of PCs somata or different cerebellar cortex regions was obtained through blue LED light illumination (473nm) of specific delimited areas determined using the PolyScan2 software (Polygon400, Mightex Systems). Successful ChR2 expression was confirmed not only by YFP fluorescence of the injected region but also by the increase in firing activity of PCs after photostimulation of the soma of the same PC or the activation of PFs in the molecular layer. (Fig 2.6)

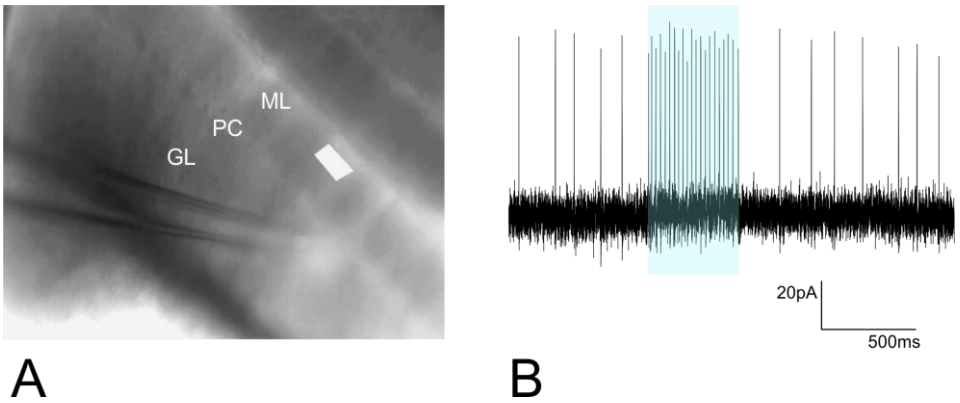

Figure 2.6| ChR2 expression in the cerebellar cortex of mice. A*) Acute brain slice in bright field, with the recording electrode placed near a Purkinje cell (PC). The white rectangle indicates the illuminated region, confined to the molecular layer.* ***B)*** *The trace shows the corresponding response in the recorded PC (single trace). Note the increase in PC firing frequency during optical stimulation (light blue rectangle), followed by a pause configuring a typical burst-pause PC response (Cao et al., 2012; Herzfeld et al 2015; Masoli and D'Angelo, 2017) GL, granular layer; ML, molecular layer.*

2.4.3 Optogenetics *in vivo*

During *in vivo* recordings, a 120µm diameter light-conducting glass fiber with 0.22 numerical aperture (Thomas Recording GmBh, Germany) was mounted in the Eckhorn Matrix (Thomas Recording GmBh, Germany), so that it was possible to insert the glass fiber down into the tissue with micrometric precision. A FC/PC patch cable (ThorLabs Ø105µm, 0.22NA, FC/PC-FC/PC Fiber Patch Cable, 1m) connected the optic fiber to a 473 nm MM laser (S1FC473MM fiber coupled laser, Thorlabs) with adjustable output power (50 mW maximum). Localized optical

stimulation of the molecular and PC layers was obtained after placing the tip of the fiber at about 250 µm from the surface of the cerebellum. Laser light pulses (50 ms) were applied at 0.5 Hz paired to the air-puff (delay of 30 ms) with a power of 0.5-1 mW. The laser pulse was triggered by a RZ5D bioamp processor (Tucker Davis Technologies, Alachua, FL, USA) driven by the OpenEx software controlling data acquisition. The output power, measured with a power meter (PM100D, with s130c sensor; Thorlabs) at the tip of the glass fiber, was 0.03mW (Kruse et al. 2014). The successful expression of ChR2 *in vivo* was assessed upon YFP fluorescence observed at the level of cerebellar vermis following craniotomy.

2.5 Histology

The location of recording sites at the level of DCN or PrL was confirmed by histological brain processing. At the end of every recording, electrical lesions were performed by applying a 20µA - 20s current pulse through the recording electrode connected to a stimulus isolator and a stimulator unit. Then, transcardial perfusion with Phosphate-Buffered Saline (PBS) was followed by perfusion of 4% paraformaldehyde (Sigma Aldrich). The fixed brains were dehydrated using 30% sucrose solution in PBS, embedded in OCT (Cryostat embedding medium, Killik, Bio-Optica) and stored at -80°C. Brains were cut to obtain 20-µm-thick histological sections that were stained with toluidine blue. The histological confirmation of recording sites was obtained by microscopic observation of the stained sections.

The same fixation procedures were performed to operate confocal microscopy analysis on 20-µm-thick brain sections obtained from injected mice, in order to validate ChR2 expression in the cerebellar cortex. Histological brain sections were counterstained with Hoechst 33258 (ThermoFisher Scientific- 2 µg/mL) and finally mounted with ProLong™ Gold Antifade Mountant (Thermo Fisher Scientific). A TCS SP5 II (Leica Microsystems) equipped with a DM IRBE inverted microscope (Leica Microsystems) was used to acquire images with 20X, 40X, or 63X objectives and visualized by LAS-AF Lite software (Leica Microsystems Application Suite

Advanced Fluorescence Lite version 2.6.0) or with ImageJ (Fiji distribution, SciJava). Fluorescence microscopy confirmed that the site of injection was confined to the molecular layer.

2.6 Data analysis

In each experimental series, the analysis of single-unit recordings was performed offline. Single-unit traces were extracted individually using SpikeTrain (Neurasmus B.V., Rotterdam the Netherlands) running under MATLAB (Mathworks, MA, USA), in order to proceed with the identification of action potentials ("spikes") over the background noise or stimulus artifacts. Spike sorting procedure required three fundamental operations:

1. Thresholding: a threshold line was positioned manually to isolate the events and assign a marker to each event;

2. Clustering: principal component analysis (PCA) allowed to automatically assign color-coded marker to each event, depending on their waveforms, in a way that allowed their clustering into groups.

3. Wave sorting: each color-coded waveform was individualized, then single events form each cluster were selected for further analysis operated manually.

For experiments requiring the application of the sensory tactile stimulation protocol, Openscope (belonging to OpenEx suite) was used to construct real-time PSTHs and allow the identification of neuronal responses triggered by air-puff stimulation.

After imposing 5 or 15 ms bin widths, responses of FN neurons to tactile stimulation were identified either as a pause or a peak in the PSTH. Raster plots of 300 trials obtained offline were also used for an accurate analysis of FN neurons responses. The presence of changes in neuronal response after TSS was assessed

by comparing the duration and the amplitude of peaks and pauses in PSTHs belonging to the pre- and post-induction periods. Responses to air-puff stimuli were considered statistically significant when the post-stimulus mean basal frequency of a bin exceeded twice the value of the mean standard deviation of the pre-stimulus period. Comparative statistical analysis was operated by applying paired or unpaired Student's *t* test, or one-way ANOVA using Origin software. For all single-unit recordings, MATLAB routine *xcorr* was run to perform autocorrelation analysis on post-stimulus PSTHs, with the feature of oscillation peaks normalized to 1. MATLAB routine for *k-means* clustering was used to operate clustering analysis, by inserting as input parameters the latency and duration of responses, or frequency and magnitude obtained from autocorrelation analysis. The *k-means* analysis of the autocorrelation results identified two distinct clusters of units characterized by low frequency - high magnitude and high frequency - low magnitude oscillations, that proved to be statistically different when subjected to Student's *t* test.

In the set of experiments in which electrical stimulation of the DN was performed while recording single-unit activity into the PrL region, responses were analyzed offline by constructing PSTHs using 100 ms bin widths. Changes in neuronal firing rate in PrL units caused by DN stimulation were investigated by comparing the spontaneous firing rate of each neuron to that measured during the stimulation period. The coefficient of variation of the inter-spike interval (CV2) was taken as indicator of the regularity of the firing. The value of CV2 referred to spontaneous activity of each unit was then compared to that measured from the correspondent stimulation period.

For subsets of experiments requiring perfusion of selective antagonists for dopamine or $GABA_A$ receptors, the amplitude of PrL neurons responses to DN stimulation was obtained from the PSTHs constructed using 100 ms bin widths. Amplitude changes in neuronal response were considered statistically significant when the mean basal frequency of a bin exceeded once the value of the mean standard deviation of the pre-stimulus period. Putative changes in response

amplitude following drugs perfusion were measured by comparing the reciprocal values before and during drug action.

Statistical comparisons were operated through the paired or unpaired Student's *t* test. Data were fitted using routines written in OriginPro8 (OriginLab co., MA, USA) and reported as mean ± SEM (standard error of the mean).

Chapter 3

Scope of the thesis

This thesis is focused on the cerebellum and its plasticity mechanisms as well as its functional and anatomical interconnection with the prefrontal cortex (a detailed description has been provided in chapter 1) and offers an interpretation on two key aspects of cerebellar functions.

The first aspect is related to the role of the cerebellum in processing and learning of sensory inputs. In particular, DCN represent the regions in which sensory information originating from several pathways is ultimately integrated and elaborated before being relayed as cerebellar output. Interestingly, the observation in several brain regions, including the cerebellum, of oscillations belonging to the theta band during particular behavioral states, such as active motion and cognition, suggests that theta-frequency stimulation pattern might represent an interesting element to consider for the investigation of learning processes in the cerebellum.

Neural activity resonant in the theta band frequency has been reported in the cerebellar network and may be related to long-lasting changes underlying cerebellar learning. Following this hypothesis, chapter 4 describes the impact of theta band frequency sensory stimulation on DCN neurons firing pattern *in vivo.* The aim of the project was to give a deep insight of the theta sensory stimulation influence on cerebellar nuclei neurons activity *in vivo*. Indeed, previous studies reported that sensory tactile stimulation patterns in the theta band are able to induce long-lasting plasticity in GrCs (Roggeri et al. 2008), PCs and MLIs (Ramakrishnan et al. 2016) in *in vivo* conditions. Despite these evidences, the mechanisms implicated in DCN neurons ability to modify their discharge properties in response to theta patterned sensory stimulation are still under debate. The employment of pharmacological tools and optogenetics helped to better characterize some of the processes underlying plasticity in the DCN.

The second part of this thesis addresses cerebellar involvement in cognition. Both anatomical tracing in humans (*Palesi et al. 2015*) and *in vivo* electrophysiological recordings in rodents (*Watson et al, 2009; 2014*) provided evidence of the existence of anatomical and functional connections between the cerebellum and the prefrontal cortex, a region of the nervous system that is well known to be involved in higher cognitive functions. Following these observations, chapter 5 is focused on the functional connectivity of fastigial and dentate nuclei with the prefrontal cortex. Herein, we characterized the single-unit pattern changes in medial prefrontal cortex neurons following electrical stimulation of the contralateral fastigial or dentate nuclei. Two main anatomical pathways connect the cerebellum to the prefrontal area: the dopaminergic pathway, passing through the ventral tegmental area and the glutamatergic pathway arising from mediodorsal and ventrolateral nuclei of the thalamus. Pharmacological approaches helped to discriminate these two pathways and investigate whether and how specific neuromodulators or neurotransmitters affect prefrontal neurons responses to cerebellar stimulation. These preliminary results open new perspectives on cerebellar contribution to cognitive functions, enlighting the fact that the impact of the cerebellum over the correct functioning of the cerebral cortex might be more relevant than previously thought.

In conclusion, chapter 6 summarizes the findings reported in the previous chapters and provides a general discussion.

Chapter 4

Long-lasting changes in deep cerebellar nuclei correlate with low-frequency oscillations *in vivo*

*Letizia Moscato[1 *], Ileana Montagna[1 *], Simona Tritto[1], Lisa Mapelli[1**], Egidio D'Angelo[1, 2**]*

[1] University of Pavia, Dept. of Brain and Behavioral Sciences, Italy

[2] IRCCS Mondino Foundation, Pavia, Italy

**co-first authors ** co-last authors*

Published on Frontiers in Cellular Neuroscience, 2019 Mar 6; 13:84.

The deep cerebellar nuclei (DCN) have been suggested to play a critical role in sensorimotor learning and some forms of long-term synaptic plasticity observed *in vitro* have been proposed as a possible substrate. However, till now it was not clear whether and how DCN neuron responses manifest long-lasting changes *in vivo*. Here, we have characterized DCN unit responses to tactile stimulation of the facial area in anesthetized mice and evaluated the changes induced by theta-sensory stimulation (TSS), a 4Hz stimulation pattern that is known to induce plasticity in the cerebellar cortex *in vivo*. DCN units responded to tactile stimulation generating bursts and pauses, which reflected combinations of excitatory inputs most likely relayed by mossy fiber collaterals, inhibitory inputs relayed by Purkinje cells, and intrinsic rebound firing. Interestingly, initial bursts and pauses were often followed by stimulus-induced oscillations in the peri-stimulus time histograms (PSTH). TSS induced long-lasting changes in DCN unit responses. Spike-related potentiation and suppression (SR-P and SR-S), either in units initiating the response with bursts or pauses, were correlated with stimulus-induced oscillations. Fitting with resonant functions suggested the existence of peaks in the theta-band (burst SR-P at 9 Hz, pause SR-S at 5 Hz). Optogenetic stimulation of the cerebellar cortex altered stimulus-induced oscillations suggesting that Purkinje cells play a critical role in the circuits controlling DCN oscillations and plasticity. This observation complements those reported before on

the granular and molecular layers supporting the generation of multiple distributed plasticities in the cerebellum following naturally patterned sensory entrainment. The unique dependency of DCN plasticity on circuit oscillations discloses a potential relationship between cerebellar learning and activity patterns generated in the cerebellar network.

4.1 Introduction

Two functional aspects of the cerebellum, that have been emphasized in turn but proved hard to reconcile, are the pronounced oscillatory dynamics (Llinas 1988) and the role in sensorimotor learning (Albus 1971a; Ito 1972; Marr 1969). Key nodes in the cerebellar circuitry are the deep cerebellar nuclei (DCN). DCN convey rhythmic outputs to the motor system (Jacobson et al. 2008) and, at the same time, have been suggested to be the site of plasticity by studies using local lesions (Ohyama et al. 2003; Ohyama et al. 2006) or electrical stimulation of afferent fiber bundles (Racine et al. 1986). Multiple forms of plasticity have been reported in DCN synapses in vitro (Morishita and Sastry 1996; Ouardouz and Sastry 2000; Pugh and Raman 2009; Zhang and Linden 2006; Zhang et al. 2004)(reviewed in (D'Angelo 2014; D'Angelo et al. 2016b; Gao et al. 2012; Hansel et al. 2001b; Mapelli et al. 2015b) and have been proposed to play a critical role in animal associative behaviors by computational models (Antonietti et al. 2016b; Casellato et al. 2015; D'Angelo et al. 2016a; Medina and Mauk 1999). Despite this evidence, the demonstration that long-lasting changes can actually be measured in DCN in vivo and can be related to internal circuit oscillations and plasticity was still lacking.

DCN neurons are autorhythmic (Jahnsen 1986a; b) and receive both excitatory inputs from collaterals of mossy and climbing fibers and inhibitory inputs from Purkinje cells (PCs) (Llinas and Muhlethaler 1988). DCN neurons respond to tactile stimulation generating discharge patterns, which reflect the combination of inhibitory and excitatory inputs (Canto et al. 2016; Chen et al. 2010; Rowland and Jaeger 2005; 2008; Yarden-Rabinowitz and Yarom 2017). DCN neurons send

output fibers to thalamus and to various precerebellar nuclei, influencing neuronal activity both in descending systems and in the cerebral cortex (Gao et al. 2018; Watson et al. 2014). Specific pathways also connect DCN with the inferior olive (Jacobson et al. 2008) and cerebellar granular layer (Ankri et al. 2015; Gao et al. 2016). These connections form the basis for reverberating loops that have been predicted to sustain rebound excitation and oscillatory cycles (Hoebeek et al. 2010; Kistler and De Zeeuw 2003; Llinas and Muhlethaler 1988; Marshall and Lang 2004; Witter et al. 2013).

In the DCN, long-term synaptic plasticity (long-term potentiation and depression, LTP and LTD) has been identified both at excitatory and inhibitory connections in vitro. Interestingly, excitatory plasticity depended on post-inhibitory rebound bursts (Pugh and Raman 2006) and inhibitory plasticity required co-activation of mossy fibers (Morishita and Sastry 1996; Ouardouz and Sastry 2000), so that plasticity at the two synapses appears to be correlated and to require precise activation sequences.

In this work, we asked whether long-lasting changes could be induced in DCN single unit responses in anesthetized mice in vivo using facial theta sensory stimulation (TSS), which proved able in previous works to induce long-lasting changes in responses recorded from the cerebellum granular layer and molecular layer (Ramakrishnan et al. 2016; Roggeri et al. 2008). TSS actually induced long-lasting changes in DCN unit responses. Interestingly, these changes were uniquely correlated with the frequency of stimulus-induced oscillations, suggesting a close relationship between oscillatory dynamics and plasticity (Cheron et al. 2016; D'Angelo and De Zeeuw 2009) reminiscent of induction schemes identified in hippocampus and neocortex (Buzsaki 2006; Roy et al. 2014).

4.2 Materials and methods

Multiple single-unit recordings were performed from the fastigial nucleus of C57BL/6 mice of either sex (40.2±1.8 days old; n=51) under urethane anesthesia. Urethane was used as its anesthetic action is exerted through multiple weak

effects (including a 10% reduction of NMDA, 18% reduction of AMPA and 23% enhancement of GABA-A receptor-mediated currents) (Hara and Harris 2002) compared to ketamine or isoflurane, which act by powerfully blocking NMDA receptors (up to 80 and 60%, respectively; (Hara and Harris 2002)) and could therefore severely compromise the induction of plasticity (Bengtsson and Jorntell 2007; Godaux et al. 1990; Marquez-Ruiz and Cheron 2012; Mawhinney et al. 2012; Muller et al. 1993). Moreover, urethane was successfully used before in similar recording conditions to investigate plasticity in the granular layer (Roggeri et al. 2008) and molecular layer (Ramakrishnan et al. 2016) of cerebellum.

All experimental protocols were conducted in accordance with international guidelines from the European Union Directive 2010/63/EU on the ethical use of animals and were approved by the ethical committee of Italian Ministry of Health (638/2017-PR; 7/2018-PR).

Surgical procedures

Mice were deeply anesthetized with intraperitoneal injections of urethane (Sigma Aldrich). Induction (1.3g/kg urethane dissolved in 0.9% NaCl) was followed by booster injections (10% of the induction dose) in order to stabilize anesthesia, starting 30 minutes after induction and repeating 3-4 times every 30 minutes. The level of anesthesia was monitored by evaluating the leg withdrawal after pinching and spontaneous whisking. The animal was then placed on a custom-built stereotaxic table covered with a heating plate (HP-1M: RTD/157, Physitemp Instruments Inc, Clifton, NJ, USA). Body temperature was monitored with a rectal probe and maintained at 36°C through a feedback controller (TCAT-2LV controller, Physitemp Instruments Inc, Clifton, NJ, USA). The mouse head was fixed over the Bregma to a metal bar connected to a pedestal anchored to the stereotaxic table. This arrangement allowed open access to the peri-oral area for air-puff stimulation. Surgery was performed to expose the cerebellar surface: local reflexes were reduced by subcutaneous application of lidocaine (0.2ml; Astrazeneca), then the skin and muscles were removed. Craniotomy of the occipital bone (-5.8 AP, +0.5 ML from Bregma, in order to record from the

fastigial nucleus) allowed to expose the cerebellar surface over the vermis. The *dura mater* was carefully removed and the surface was covered with saline (NaCl 0.9%; Sigma) to prevent drying.

Single-unit recordings *in vivo*

Quartz-coated platinum/tungsten fiber electrodes (1-5MΩ) organized in a multi-electrode array (MEA) of 4x4, with inter-electrode distance of 100 µm (Eckhorn matrix, Thomas Recording, GmBh, Germany) were used for neuronal recordings. Recording electrodes were positioned over the vermis, ipsilateral to the air puff stimulator, and lowered perpendicularly to the surface down to a depth of 2109.1±65.5 µm (n=33). The electrophysiological signals were digitized at 25 kHz, using a 300-5000 Hz band-pass filter, amplified and stored using a RZ5D processor multi-channel workstation (Tucker-Davis Technologies, Alachua, FL, USA). DCN neurons were identified online by assessing recording depth, spontaneous activity, and stimulus-evoked responses. At the end of recordings, an electric lesion was made by injecting current through the recording electrode. The recording site was then confirmed by histological tissue processing (see below).

Sensory stimulation

Tactile sensory stimulation was performed using air-puffs (30ms pulses, 30-60 psi) delivered through a small tube ending with a nozzle (0.5 mm diameter) positioned 2-3 mm away from the snout area of the animal and connected to a MPPI-2 pressure injector (Applied Scientific Instrumentation, Eugene, OR, USA) (Ramakrishnan et al. 2016; Roggeri et al. 2008). While cerebellar cortical responses to skin receptive fields stimulation are organized in the so-called "fractured somatotopy" in the granular layer and in zonal or small regions in the molecular layer (Ekerot and Jorntell 2001; Jörntell and Ekerot 2002; Kassel et al. 1984; Shambes et al. 1978), DCN neurons have been described to respond to large portions of the body surface, both ipsi- and contra-lateral (Rowland and Jaeger

2005). We nevertheless limited the sensory stimulation area to mouse upper lip, lower lip or whisker pad of the ipsilateral region. Following 5 minutes of spontaneous activity recording, low frequency stimuli (0.5 Hz) were delivered over the mouse upper lip, lower lip or whisker pad to activate the corresponding receptive fields and evoke the neuronal response (Bower and Woolston 1983; Morissette and Bower 1996; Ramakrishnan et al. 2016; Roggeri et al. 2008; Vos et al. 1999) (see Fig.1A). DCN single unit responses were monitored online by building peri-stimulus time histograms (PSTHs) triggered by the air-puffs. Once a responsive unit was detected, control stimuli were delivered for 20 minutes at 0.5 Hz, in order to characterize unit responses to tactile sensory stimulation. Then, the theta sensory stimulation (TSS) pattern (a burst of 100 air-puffs at 4 Hz) was delivered, followed by post-induction recordings for at least 40 minutes at 0.5 Hz. Since the air puff has been reported to elicit a brief spike burst in the mossy fibers (Chadderton et al. 2004; Vos et al. 1999), the TSS is likely to determine short bursts repeated at 4Hz. This pattern is known to induce plasticity in the cerebellar cortex (see (Prestori et al. 2013; Ramakrishnan et al. 2016; Roggeri et al. 2008; Romano et al. 2018). In 12 recordings TSS was not delivered, monitoring the stability of responses for at least 60 minutes.

Pharmacology

In a subset of experiments, the AMPA and NMDA receptor antagonists, 100μM NBQX (Abcam) (Guo et al. 2016) and 250μM D-APV (Tocris Bioscience) (Zhang et al. 2017), were injected in the fastigial nucleus near the recording electrodes. APV and NBQX were added to a Krebs solution with the following composition (in mM): 120 NaCl, 2 KCl, 1.2 $MgSO_4$, 26 $NaHCO_3$, 1.2 KH_2PO_4, 2 $CaCl_2$, and 11 glucose, equilibrated with 95% O_2-5% CO_2 (pH 7.4). The solution containing the drugs was pre-loaded in a pneumatic picopump (PV820, World Precision Instruments), operated through adjustable air pressure, terminating in a 35G needle, positioned using a Patch-Star micromanipulator (Scientifica, Ltd). After 15 minutes of single-unit recording, the solution was injected at the rate of

1μl/5min. It should be noted that the injection of GABAergic antagonists in the fastigial nucleus would not help discerning the origin of the pause, as it would affect the synapses coming from both local interneurons and PCs.

Optogenetics

Adeno associated virus injection and expression. The expression of ChR2 in the cerebellar vermis was obtained through local injection of the adeno associated viral construct pAAV-hSyn-hChR2-EYFP (AAV1 serotype; Penn Vector Core, University of Pennsylvania, USA). C57BL6 mice of either sex (30 days old, n=13) were anesthetized with 1-2% isoflurane in oxygen 100% at 0.7 L/min delivered from a gas vaporizer (Ugo Basile S.R.L., Italy) and were placed in a stereotaxic apparatus (Leica vernier stereotaxic instrument), where they constantly received isoflurane from a nose cone and had their head fixed with ear bars. Mice body temperature was constantly monitored by a heating pad connected to a rectal thermal probe (TCAT-2LV controller, Physitemp Instruments Inc, Clifton, NJ, USA) and maintained at 36°C. After testing the absence of withdrawal reflexes, a sagittal incision on the head was performed to expose the cranium, and a burr hole was drilled to target lobule VI of cerebellar vermis 3.5 mm posterior to Lambda. The virus was loaded into a 10μl NanoFil syringe (World Precision Instruments) that was connected to an automatic syringe pump (Ugo Basile S.R.L., Italy).

The injection needle (NF35BV, 35G, World Precision Instruments) was positioned into the vermis at 300 μm depth and 0.2 μl of virus solution at a titer of 1.168^{13} genome copies/ml was injected at a flow rate of 0.05 μl/min. This procedure ensured a localized expression of ChR2 at the level of cerebellar molecular and PC layers. A good incorporation of the virus in the tissue was assured by keeping the needle in place for 10 min after the end of perfusion. The head was sutured and mice were kept under observation until recovery from the anesthesia, before returning to the animal facility. In order to ensure a good expression of ChR2, electrophysiological experiments were performed 21-28 days after viral injection.

ChR2 expression in acute cerebellar slices. In 5 mice that were injected with the construct but were not used for *in vivo* recordings, after 30 days the cerebellum was removed and used to prepare acute slices (220µm thick) following standard procedures *(Mapelli et al. 2017).* The efficacy of ChR2 expression was tested by extracellular recordings from PCs. The PC soma was selectively illuminated with blue led light (Polygon400, Mightex Systems). The extracellular signals were recorded using a Multiclamp 700B amplifier (Molecular Devices) controlled by pClamp10 through a Digidata1440A (Molecular Devices). When illuminated, the PCs increased firing activity as expected from effective ChR2 expression causing membrane depolarization (Fig. S1).

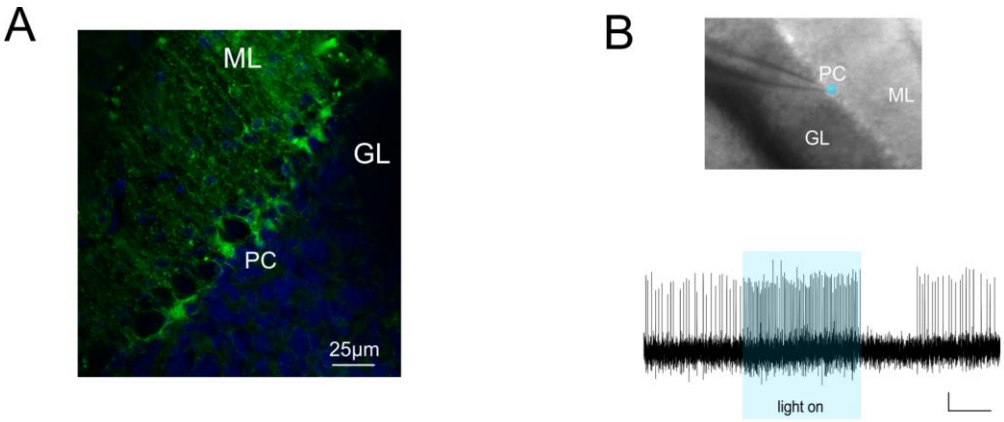

Fig S1. ChR2 expression in the cerebellar cortex of mice used for optogenetics. (A) Confocal image of green fluorescence (YFP) in the cerebellar cortex of a mouse sacrificed after *in vivo* recordings. Since YFP is expressed under the same promoter, YFP fluorescence reports the place of ChR2 expression. Note that fluorescence is mostly confined to the molecular and Purkinje cell layers. GL, granular layer; ML, molecular layer; PC, Purkinje cell. **(B)** Acute brain slice in bright field, with the recording electrode placed near a Purkinje cell (PC). The blue circle indicates that illuminated region is confined to PC soma and the trace shows the corresponding response in the stimulated PC (single trace, scale bars: 10 pA/200 ms). Note the increase in PC firing frequency during optical stimulation, followed by a pause configuring a typical burst-pause PC response (*Cao et al., 2012; Herzfeld et al 2015; Masoli and D'Angelo, 2017*). GL, granular layer; ML, molecular layer.

General aspects of optogenetics experiments. Since our aim was to interfere with PC activity, the site of AAV1 injection was limited to restricted regions of the molecular layer (Fig.S1A). The ChR2 was expressed under a generic neuronal promoter in common to molecular layer interneurons, PCs and parallel fibers. Since local circuit wiring in the molecular layer is not homogeneous (Valera et al. 2016), optogenetic activation was not expected to sort out the same effect in all cases (cfr. Fig.1A for a scheme of the circuit). Indeed, depending on the individual experiment, optogenetic stimulation could either increase or decrease PC activity and the pause and, in 2 out of 8 cases, no response modification was detected.

Light application during in vivo recordings. A light-conducting glass fiber with 120µm diameter cladding and numerical aperture NA=0.22 (Thomas Recording GmBh, Germany) was mounted in the Eckhorn Matrix (Thomas Recording GmBh, Germany). Just as the recording electrodes, it was possible to drive the tip of the glass fiber down into the tissue with micrometric precision. The optic fiber was connected though a FC/PC patch cable (ThorLabs Ø105µm, 0.22NA, FC/PC-FC/PC Fiber Patch Cable, 1m) to a 473 nm MM laser (S1FC473MM fiber coupled laser, Thorlabs) with adjustable output power (50 mW maximum). The laser was gated by a (TTL) trigger signal generated by the RZ5D bioamp processor (Tucker Davis Technologies, Alachua, FL, USA) driven by the OpenEx software controlling data acquisition. YFP fluorescence allowed to determine the effectiveness of adenoviral expression *in vivo*. The tip of the fiber was placed at about 250 µm from the surface of the cerebellum, in order to obtain a localized optical stimulation of the molecular and PC layers. Laser light pulses (50 ms) were applied at 0.5 Hz paired to the air-puff (delay of 30 ms) with a power of 0.5-1 mW. The output power, measured with a power meter (PM100D, with s130c sensor; Thorlabs) at the tip of the glass fiber, was 0.03mW (Kruse et al. 2014).

Histology

The location of recording electrodes in the DCN was confirmed histologically. Electrical lesions were obtained at the end of recordings by applying a 20 µA - 20 sec current pulse through the same recording electrode connected to a stimulus isolator and a stimulator unit. Then, the mouse was perfused transcardially with Phosphate-Buffered Saline (PBS) followed by 4% paraformaldehyde (Sigma Aldrich) overnight at 4°C. The fixated brains were cryo-protected with 30% sucrose solution in PBS, embedded in OCT (Cryostat embedding medium, Killik, Bio-Optica), and stored at -80°C. 20-μm-thick histological sections were obtained and stained with toluidine blue. The histological confirmation of the recording sites was obtained by microscopic observation of the stained sections (see Fig. 1B). The identification of the viral expression was also analyzed histologically from the fixated brain of injected mice. Confocal images (see Fig. S1) were taken from 20-μm-thick sections washed with PBS (3 times for 5 min), counterstained with Hoechst 33258 (ThermoFisher Scientific- 2 µg/mL) for 15 min, washed again with PBS (3 times for 5 min) and finally mounted with ProLong™ Gold Antifade Mountant (Thermo Fisher Scientific). Images were acquired with a TCS SP5 II (Leica Microsystems) equipped with a DM IRBE inverted microscope (Leica Microsystems) with 20X, 40X, or 63X objectives and visualized by LAS-AF Lite software (Leica Microsystems Application Suite Advanced Fluorescence Lite version 2.6.0) or with ImageJ (Fiji distribution, SciJava). Fluorescence microscopy showed that the site of injection was confined to limited regions of the molecular layer (see Fig. S1).

Data analysis and statistics

Electrophysiological signals were acquired using OpenEx software (Tucker-Davis Technologies) and analyzed offline using custom-written routines in MATLAB (Mathworks, MA, USA) and Excel. Openscope (part of the OpenEx suite) was used to construct online peri-stimulus time histograms (PSTH) triggered by air-puffs, in order to identify responding units. The raw traces were analyzed and sorted

offline using SpikeTrain (Neurasmus BV, Rotterdam, Netherlands) running under MATLAB. The stability of recordings was carefully assessed (< ±20% amplitude fluctuation over the duration of the recording) and only units with stable spike size were considered for further analysis. PSTHs and raster plots were used for the analysis of responses to stimulation, normally consisting of peaks and pauses emerging from background discharge. To optimize PSTH resolution, a 5 ms bin width was used to analyze peaks and a 15 ms bin width was used to analyze pauses. The "burst" was defined as an increase in firing frequency generating a PSTH peak after the stimulus. The "pause" was defined as a decrease in firing frequency generating a PSTH pause after the stimulus. The threshold for peaks and pauses detection in PSTHs was set at twice the standard deviation of the basal frequency in the pre-stimulus period, calculated for each bin. No constraints on the number of bins showing significant changes compared to the pre-stimulus period were applied, since some response might show small duration (as the case of peaks, lasting 5-10ms and therefore described by one or few bins). Statistical comparisons of peak and pause changes in optogenetic experiments was performed against changes in the stability controls at the same experimental times (histograms in Figs. 3B, 4F).

The effect of TSS was evaluated by measuring the corresponding changes in PSTH peaks and pauses as the post-TSS responses (computed over the first 15 min after TSS) that exceeded twice the standard deviation of the pre-TSS response (computed over the last 15 min before TSS).

Positive changes were considered as a potentiation and negative changes were considered as a suppression of basal firing (a minority of units did not show any significant changes with respect to this criterion).

Statistical comparisons were carried out using paired or unpaired Student's *t*-test or Fisher's *F*-test. The normality of the data was assessed using the Shapiro-Wilk test. In the few cases data were not distributed normally, the Brown-Forsythe test was applied to assess the homogeneity of variances. Data in the text are reported as mean ± SEM. Clustering *k*-mean analysis and autocorrelation analysis on PSTHs were performed using MATLAB routines. Autocorrelations were performed

using a function (*xcorr*) yielding oscillation frequency and magnitude (with magnitudes normalized to 1). The statistical significance of the changes in oscillation frequency in pharmacological and optogenetic experiments was evaluated with respect to stability controls at the same experimental times.
Data fitting was performed using routines written in OriginPro8 (OriginLab co., MA, USA). A Lorentzian function was used to fit the frequency-dependence of plasticity changes:

$$y = y0 + \frac{2A}{\pi} \cdot \frac{w}{4(x - fc)^2 + w^2}$$

where *y0* and *A* are curve baseline and amplitude, *w* is curve width, *fc* is the resonance frequency.

4.3 Results

Single-unit recordings were performed from the cerebellar fastigial nucleus in urethane anesthetized mice (Fig.1A). All units were spontaneously active and showed a basal frequency of 8.19±0.99 Hz (range 2-27 Hz; n=51), in agreement with previous reports of spontaneous activity under urethane anesthesia (LeDoux et al. 1998; Raman et al. 2000; Sweeney et al. 1992). The recording site was confirmed by electric lesions made through the recording electrode and identified histologically (Fig.1B). Single-unit responses to low frequency tactile stimulation (0.5Hz) generated spike bursts and pauses modifying the basal discharge (Fig. 1C) that were likely to reflect the neuronal response to excitatory and inhibitory synaptic inputs impinging onto DCN neurons (Rowland and Jaeger 2005; 2008).

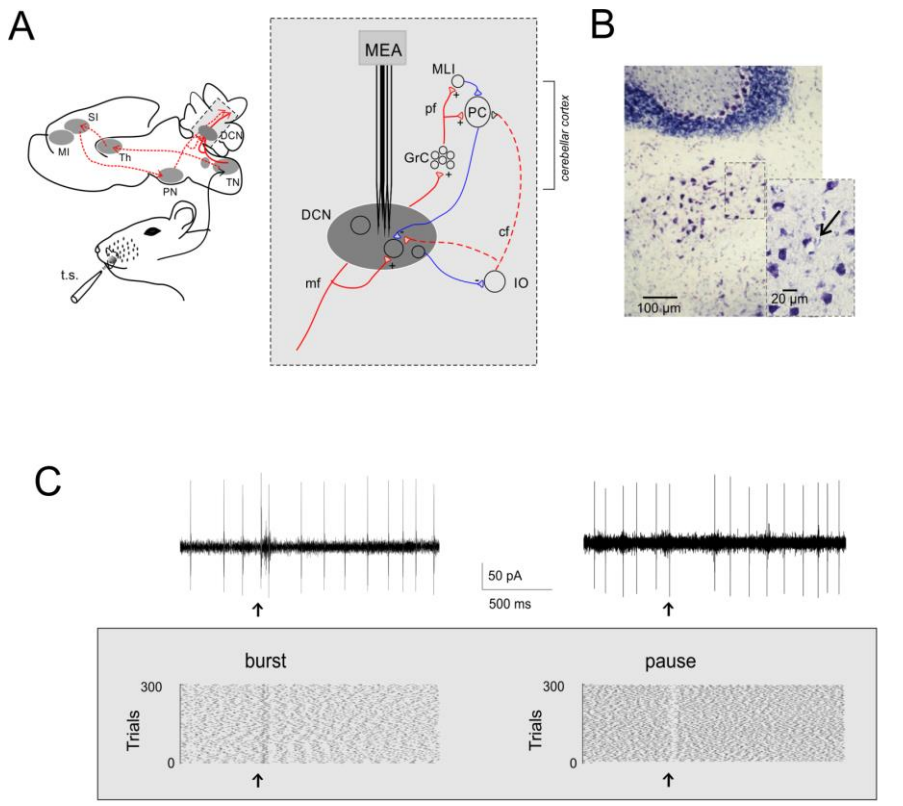

Fig.1 Extracellular recordings from DCN units *in vivo*. *(A) Schematic representation of the main pathways activated by air puff stimulation of the peri-oral region in mice: the trigemino-cerebellar (*solid red line*) and thalamo-cortical-pontine (*dashed red line*) pathways. The region in the gray box is expanded at the right to show the main circuit elements relevant to DCN neuron activity. MI, primary motor cortex; SI, primary sensory cortex; Th, thalamus, PN, pontine nuclei; TN, trigeminal nucleus, DCN, deep cerebellar nuclei; GrC, granule cells; MLIs, molecular layer interneurons; PC, Purkinje cell; IO, inferior olive; pf, parallel fibers; mf, mossy fibers; cf, climbing fiber; t.s., tactile stimulation. MEA, multi-electrode array (Eckhorn matrix, see section "Materials and Methods" for details). (B) Toluidine blue stained coronal cerebellar slice showing the electric lesion (*arrow*) made by the recording electrode in the fastigial nucleus. (C) Two single-unit recordings showing a burst and a pause in response to tactile stimulation (*arrow*). The raster plots show the spike discharge during ~2 s recordings and its change caused by tactile stimulation in 300 consecutive trials.*

Bursts and pauses in DCN unit responses

Single-unit responses to low frequency tactile stimulation generated combinations of peaks and pauses in peri-stimulus-time-histograms (PSTHs) and, in some cases, the response continued with an oscillation (see below). Over a total of 51 units, we

identified 2 fundamental categories of patterns, with either the burst or the pause as the initial response (Fig. 2A).

When the *burst* initiated the response ("burst-first" category, n=26), some units (n=18) showed a single PSTH peak with latency of 14.27±4.07 ms (duration 11.80±2.51 ms), while others (n=8) showed two PSTH peaks with latencies of 9.87±1.99 and 33±3.7ms (duration of 8.12±1.31 and 15±3.27ms). These peak latencies corresponded to those reported for trigeminal and cortical responses of granular layer neurons (Roggeri et al. 2008; Vos et al. 1999), suggesting that the initial bursts most likely corresponded to synaptic excitation of DCN neurons through trigeminal and cortical mossy fibers (Fig. 2B; see Methods for details).

In a subset of experiments, selective AMPA and NMDA receptor antagonists (100μM NBQX + 250μM D-APV, respectively) were injected in the fastigial nucleus close to the recording site. In 4 (out of 4) neurons that initiated the response with a burst, the burst was abolished (peak change -95.9±12.8%, n=4; paired Student's *t* test p=0.026), while pauses remained unaltered (pause depth change -16.2±10.2%; n=4, paired Student's *t* test p=0.14; see below) (Fig. 3A).

When the *pause* initiated the response ("pause-first" category, n=25), it occurred with a latency of 28.8±5.2 ms (duration 25.0±3.8 ms). This delay was compatible with signal transmission along the mossy fiber - granule cell - PC - DCN neuronal pathway (Ramakrishnan et al. 2016), rather than resulting from local interneurons, suggesting that the initial pause most likely corresponded to DCN neuron inhibition by PCs. In a subset of experiments (n=8), optogenetic stimulation of the molecular layer was applied to disrupt the cortical output, by delivering a light impulse 30 ms after the air-puff, i.e. in coincidence with the pause.

In 6 of these recordings optogenetic stimulation caused a change in pause depth and duration exceeding 3 times the standard deviation of time-matched controls (see Methods and histograms in Fig.3B). It should be noted that the pause in three cases increased and in three cases decreased, possibly reflecting the balance between optogenetic activation of PCs and molecular layer interneurons (see Methods and Fig. 1A and Fig. S1 for details). In the remaining 2 units, no evident effect of optogenetics was observed.

Several units initiating the response with a burst (21 out of 26) showed a pause following peak(s), and some units initiating the response with a pause (8 out of 24) showed a burst following the pause (Fig.2A). The nature of these *burst-pause* and *pause-burst* patterns showed peculiar properties.

In *burst-pause* responses, the pause was significantly delayed (58.17±5.52 ms, n=21, unpaired Student's *t* test p=0.00039) compared to that measured when it initiated the response. This longer delay suggests the intervention of additional mechanisms, like signal reentry through the recently discovered DCN - granule cells connections (Gao et al. 2016) or through precerebellar nuclei (Kistler and De Zeeuw 2003), capable of protracting and enhancing PCs activation through cerebello-cortical loops. Phase reset, an intrinsic electroresponsive phenomenon observed in neurons (e.g. see (Solinas et al. 2007)), was unlikely to be responsible for this effect, as explained below (see Fig.4D).

In *pause-burst* responses, the bursts followed with a latency of 90.61±20.63 ms (duration 12.14±3.54 ms, unpaired Student's *t* test p=0.01), that was significantly longer compared to that measured when it initiated the response. A positive correlation was found between pause depth and the subsequent peak amplitude (R^2=0.89, Fisher's F test *p*(F)<0.001, n=8) (Fig. 2C). A plausible explanation is that these bursts are non-synaptic and reflect post-inhibitory rebound discharge in DCN neurons (Alviña et al. 2008; Canto et al. 2016; Witter et al. 2013), which is the stronger the deeper the pause. This is supported by a recording in which the AMPA and NMDA receptor antagonists were injected in the fastigial nucleus while recording a pause-burst unit. In this case, the burst following the pause was unaffected (single observation, not shown).

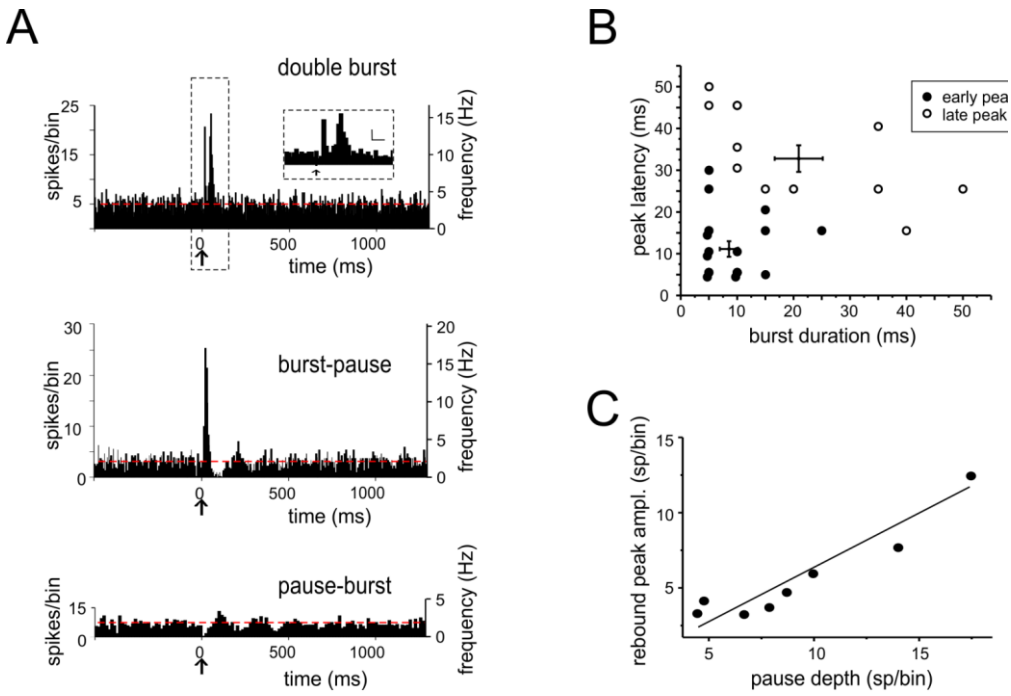

Fig 2. Bursts and pauses in DCN unit responses to tactile stimulation. *(A) Example of PSTHs obtained from DCN units showing different responses to tactile stimulation (*arrows*): double burst (5 ms-bin), burst-pause (5 ms-bin), and pause-burst (15 ms-bin). Red dashed lines show the basal discharge frequency. The scale bars in the inset on top are 5 sp/bin and 25 ms.* **(B)** *In the pool of responses starting with a burst, two groups were discriminated using cluster analysis (*k-means*) on peak latency and burst duration. This results in the identification of early and late peaks, whose latencies are compatible with inputs from the trigeminal and cortical pathways conveying sensory stimuli to the cerebellum (cfr. Figure 1A).* **(C)** *Characterization of pause-burst responses. A positive correlation was found between rebound-peak amplitude and pause depth [*R^2 *= 0.87, Fisher's* F*-test* p(*F*) *= 0.001,* n *= 8].*

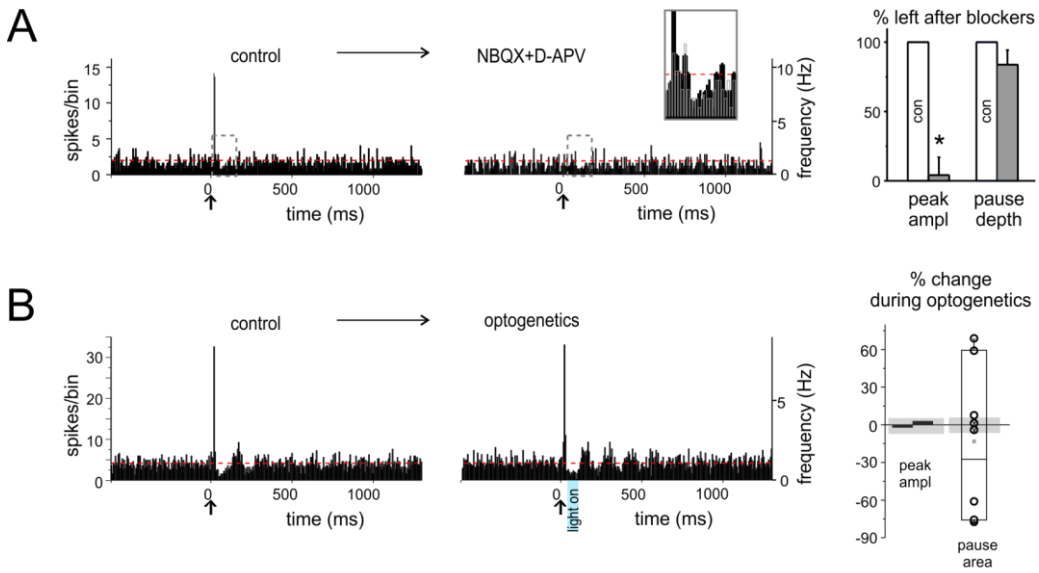

Fig.3. Pharmacological and optogenetic manipulations of burst and pause responses. *(A) Example of PSTHs from a DCN unit showing a burst as initial response (*left*), that was prevented (*right*) by excitatory transmission blockers (NBQX and D-APV) injection in the nucleus (*red dashed lines*show the basal discharge frequency). The gray dashed rectangles show the areas that are overlapped in the inset. The histogram shows the % of the response, whether PSTH peaks or pauses, left after blockers injection, compared to control (*n = 4 for both; paired Student's t-test; *p < 0.05). **(B)**Example of PSTHs from a DCN unit showing burst-pause response before (*left*) and during (*right*) optogenetic stimulation of the molecular layer (the blue rectangle showing the time and duration of laser activation;* red dashed lines *show the basal discharge frequency). The histograms on the right show the percent change on the peak amplitude of the excitatory response and on the pause area (obtained by multiplying pause depth and duration) during optogenetic stimulation compared to control, in the single units recorded. The gray shadows show the average % change observed at the same time points in the stability controls (see section "Materials and Methods"). Note that peak amplitude is not affected, while the pause is significantly modified.*

Spontaneous activity and stimulus-induced oscillations in DCN units

The PSTH elicited by tactile stimulation in several cases showed an *oscillation* following the initial peaks and pauses (Fig. 4A). This oscillatory pattern was apparent in autocorrelation analysis (Fig. 4B). The frequency / magnitude plot revealed a negative trend, with slower oscillations showing larger magnitude and *vice versa* (Fig. 4C). K-means analysis identified two significantly different clusters

of points (unpaired Student's *t* test p=0.00175), one at higher and the other at lower frequency. Low-frequency oscillations averaged 12.7±1.0 Hz, n=34.

The relationship between low-frequency stimulus-induced oscillations and spontaneous activity is shown in Figs 4D-E. No significant correlation was found either for frequency (R^2=0.03, Fisher's F test p(F)=0.89, n=34) or magnitude (R^2=0.25, Fisher's F test p(F)<0.08, n=34). It should be noted that, out of 34 units, 15 were of the burst-first and 19 of the pause-first category. At a closer analysis, the burst-first units showed a significantly higher magnitude (0.11±0.01 vs. 0.08±0.01; unpaired Student's *t* test p=0.037) and lower spontaneous frequency (6.2±0.8 Hz vs. 10.0±1.1 Hz, unpaired Student's *t* test p=0.01) than the pause-first units (Fig. 4C, D, E) suggesting the existence of two distinct functional classes of DCN neurons (see below).

The injection of AMPA and NMDA receptor antagonists in the fastigial nucleus did not modify the stimulus induced oscillation frequency of the units (average absolute variation from control of 5.1±0.6%, not different from that of stability controls of 5.1±0.5%, n=4 and n=10 respectively; unpaired Student's *t* test p=0.99). Conversely, optogenetic stimulation of the molecular layer caused a change in the stimulus induced oscillation frequency of the recorded units exceeding 3 times the standard deviation of time-matched controls (see Methods and Fig.4F). It should be noted that the induced-oscillation frequency in 2 cases increased and in 4 cases decreased, possibly reflecting the balance between optogenetic activation of PCs and molecular layer interneurons.

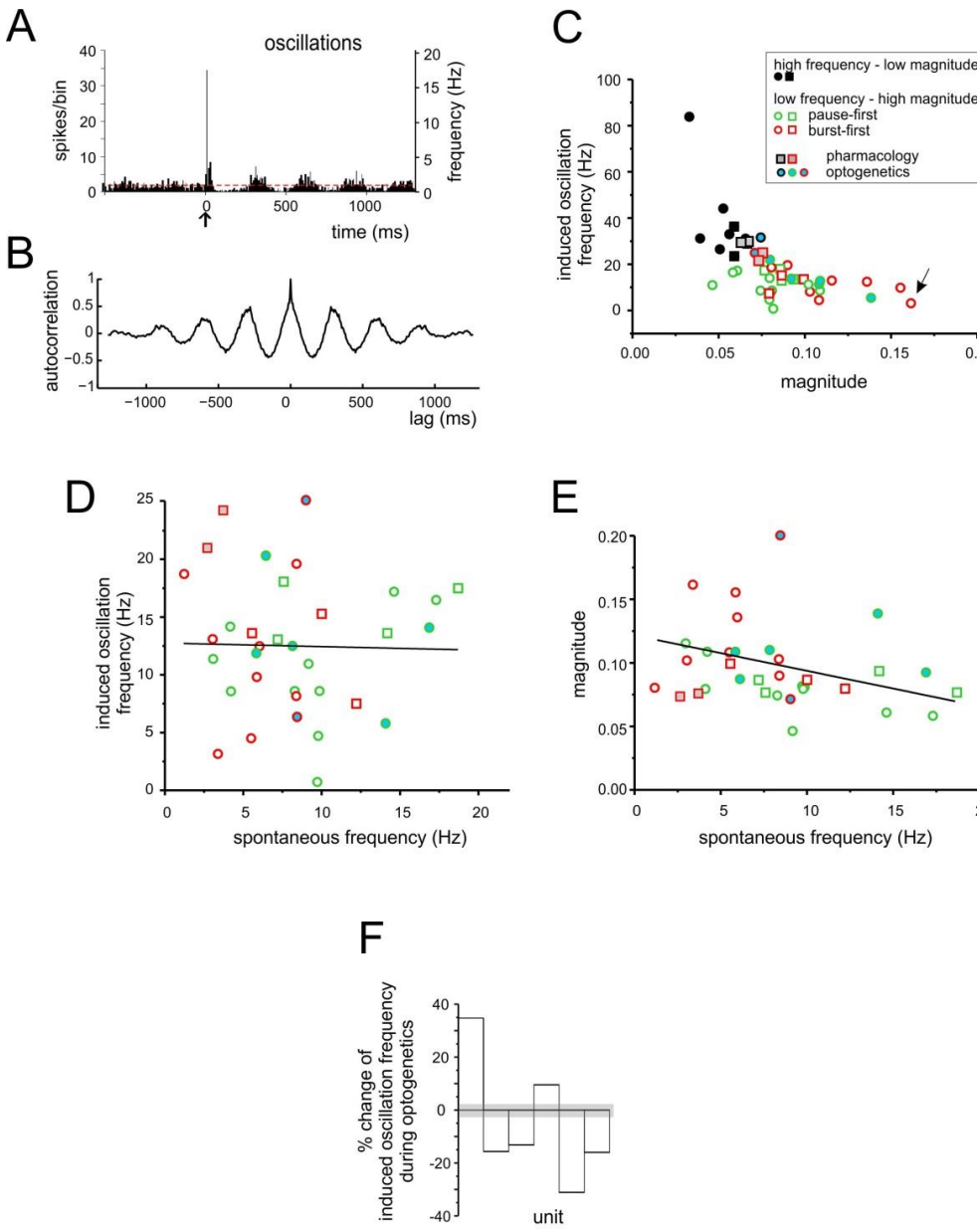

Fig. 4. Stimulus-induced oscillations in DCN units. *(A) PSTH obtained from a DCN unit showing low frequency oscillation following a burst-pause response. (B) Autocorrelogram obtained from the unit shown in (A)(oscillation frequency 3.15 Hz; magnitude 0.16). (C) The magnitude and frequency of oscillations deriving from the autocorrelation analysis shown in (B) were plotted for each unit. The k-means clustering revealed two groups of data, characterized by high frequency – low magnitude oscillations (black symbols) and low frequency – high magnitude oscillations (green and red symbols, for pause-first and burst-first responses respectively). The units in which the TSS was delivered are represented as circles, while those in which the TSS was not delivered are represented*

as squares. Gray filled symbols are used for the units in which pharmacology was applied, while blue-filled circles are used for the units in the optogenetics experiments. The arrow indicates the unit shown in ***(A,B)****.* ***(D)*** *Relationship between stimulus-induced oscillation frequency and spontaneous firing frequency for the low frequency – high magnitude oscillation units in* ***(C)****. The linear fitting shows no evident trend [*R^2 *= 0.03, Fisher's* F*-test* p*(F) = 0.89].* ***(E)*** *Relationship between magnitude of stimulus-induced oscillations and spontaneous firing frequency for the low frequency – high magnitude oscillation units in* ***(C)****. The linear fitting suggests a positive trend [*R^2 *= 0.25, Fisher's* F*-test* p*(F) < 0.08]. In* ***(C–E)****, the data points are divided into burst-first and pause-first units, and circles represent the units that were further used for plasticity induction (see Figure 5,6).* ***(F)*** *The histogram shows the percent change in stimulus-induced oscillation frequency during optogenetics in the same units reported in* ***(C–E)****. The gray shadow shows the average percent change observed at the same time points in the stability controls (see section "Materials and Methods").*

Long-lasting changes induced by TSS in DCN unit responses

The cerebellar cortex in rodents is known to respond to TSS of the whisker pad with long-lasting changes in the granular and molecular layers (Diwakar et al. 2011; Prestori et al. 2013; Ramakrishnan et al. 2016; Roggeri et al. 2008). We therefore investigated whether the delivery of the same TSS pattern was able to affect DCN neuron responsiveness. We defined Spike-Related Potentiation (SR-P) and Spike-Related Suppression (SR-S) as the increase or decrease in spike response probability with respect to baseline (cf. Ramakrishnan et al., 2016), both in bursts and pauses. For simplicity, we considered only the initial bursts and pauses, since their amplitude is not influenced by preceding electrical events. The values of changes were measured for each unit in the first 15 min following TSS with respect to the last 15 min before TSS.

TSS-induced changes in initial bursts. TSS was delivered in 13 recordings showing an initial excitatory burst (burst-first, Fig.5A). A significant SR-P of the first PSTH peak was observed in 4 units (45.27±10.73%, n=4, paired Student's *t* test p=0.01; Fig.5A), while a significant SR-S was observed in another 8 units (-27.16±5.34%, paired Student's *t* test p=0.01). Only in 1 out of these 13 units, no significant changes were observed.

TSS-induced changes in initial pauses. TSS was delivered in 13 recordings showing an initial pause in the response (pause-first, Fig.5B). A significant SR-P of the pause was observed in 4 units (48.43±14.77%, n=4, paired Student's *t* test p=0.004), while a significant SR-S of the pause depth was observed in another 7 units (-27.19±7.65%, n=7, paired Student's *t* test p=0.007; Fig.5B). In 2 units, no pause depth changes were found.

Stability controls. In 7 units showing an initial excitatory burst and in 5 units showing an initial pause, TSS was not delivered. In these units, the bursts and pauses remained stable for a duration similar to that of experiments in which the TSS was delivered (bursts: 4.7±11.7 % change, paired Student's *t* test, n=7, p=0.9; pauses: 5.6±10.0 % change, n=5, paired Student's *t* test p=0.1). These controls ruled out possible spurious changes due to intrinsic response amplitude fluctuations with time.

Average time course. The average time course for burst and pause changes was constructed by grouping all the units in each given category. The SR-P and SR-S of peaks and pauses reported above, which were statistically significant for the first 15 minutes after TSS, returned back to baseline within 30 minutes (Fig. 5C).

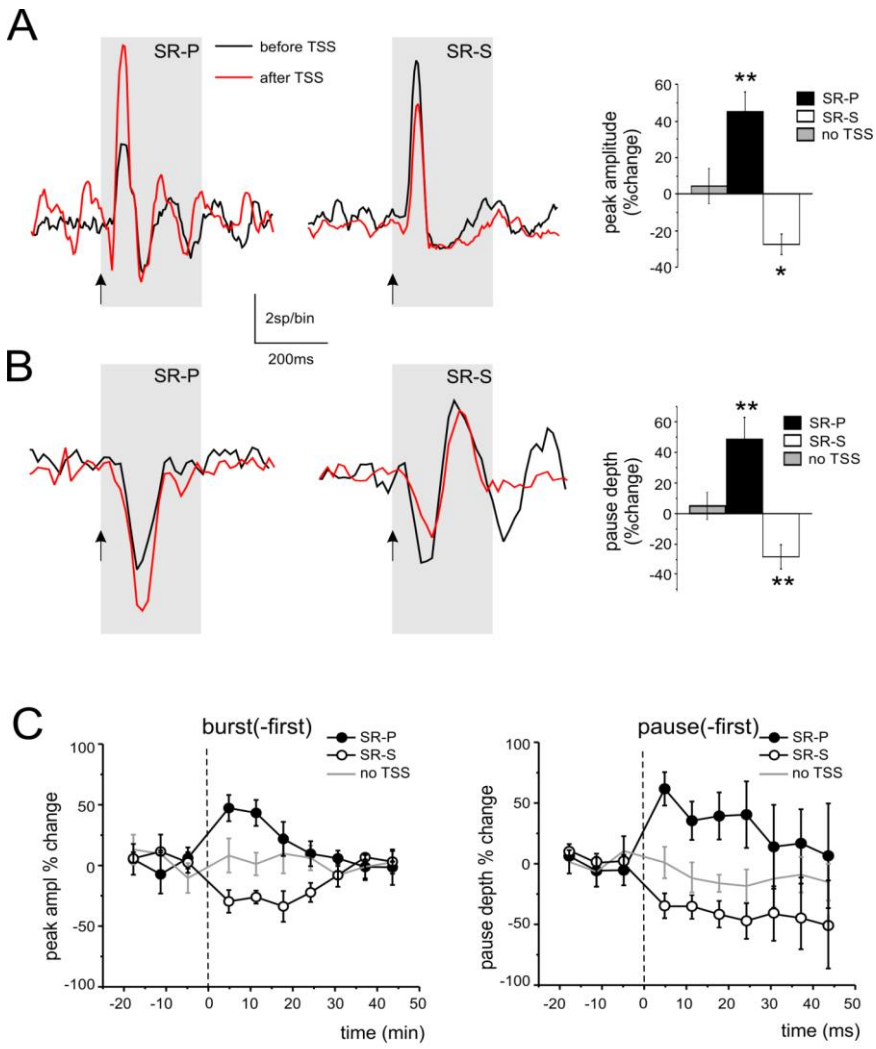

Fig. 5 Long-lasting changes induced by TSS in DCN unit responses. ***(A)*** *Example of PSTHs illustrating the* peak *changes (SR-P or SR-S) induced by TSS in DCN units of the burst-first category. The histogram shows the average percent changes in PSTH peak amplitude for all the units showing SR-P, SR-S, or stability controls (no TSS; paired Student's* t*-test; *p < 0.05, **p < 0.01).* ***(B)*** *Example of PSTHs illustrating the* pause *changes (SR-P or SR-S) induced by TSS in DCN units of the pause-first category. The histogram shows the average percent changes in PSTH peak amplitude for all the units showing SR-P, SR-S, or stability controls (no TSS; paired Student's* t*-test; **p < 0.01).* ***(C)*** *Average time-course of peak (in burst-first units,* left*) and pause (in pause-first units,* right*) amplitude percent changes normalized to the control period before TSS (*dashed line*) in the units showing SR-P, SR-S and in the stability group (TSS not delivered). Note that the response changes for peaks and pauses differed significantly from the stability controls in the first 15 min after the TSS.*

Correlation between long-lasting changes and stimulus-induced oscillations

In Fig. 4, two functional classes of units have been identified based on their response pattern and low frequency oscillatory properties, summing up to a total of 15 burst-first units and 17 pause-first units. Here we have considered the relationship between long-lasting changes and stimulus-induced oscillation frequency in the 8 burst-first and 10 pause-first units that received TSS in control condition (without pharmacological manipulation or optogenetics). The changes were weakly correlated to frequency, with larger changes occurring at lower frequencies (linear correlation: R^2=-0.07 and p(F)<0.05 for *burst-first* units; R^2=0.32 p(F)<0.03for *pause-first* units). The hypothesis that changes were centered on the theta-band was assessed by fitting the data using resonant functions. In particular, the Lorentzian distribution fitted the data better than linear, suggesting that peak and pause changes after TSS might be correlated with the frequency of stimulus-induced oscillations. By using a Lorentzian distribution, peak changes in the *burst-first* units (Fig.6A) peaked at 9.2 Hz with 53% SR-P and settled down to -17.2% SR-S at lower and higher frequencies (R^2=0.83; Fisher's F test p(F)<0.01). Pause changes in the *pause-first* units (Fig.6B) peaked at 5.5 Hz with -42% SR-S and settled to 26.2% SR-P at higher frequencies (R^2=0.78; Fisher's F test p(F)<0.02).

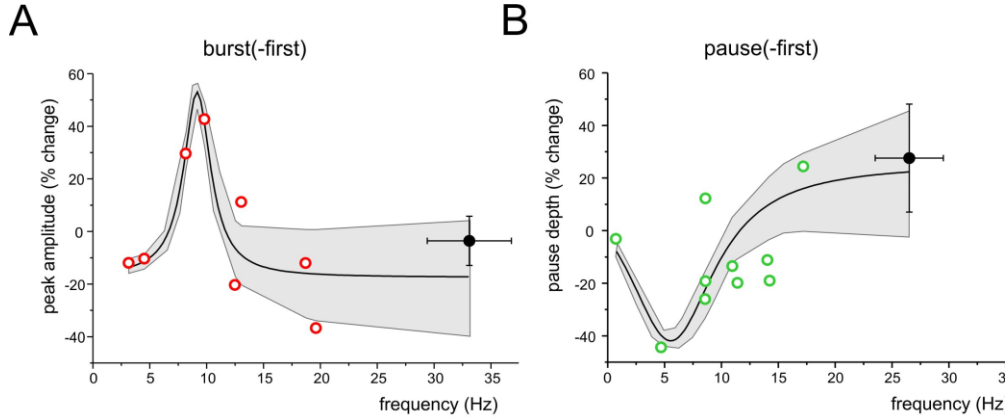

Fig. 6 Frequency-dependence of long-lasting changes after TSS. *(A) The plot shows the distribution of peak amplitude changes after TSS in burst-first units with respect to stimulus induced oscillation frequency. The Lorentzian fitting [R^2 = 0.83; Fisher's F-test p(F) = 0.01] shows a peak at 9.2*

Hz. ***(B)*** *The plot shows the distribution of pause amplitude changes after TSS in pause-first units with respect to stimulus induced oscillation frequency. The Lorentzian fitting [R^2 = 0.78; Fisher's F-test p(F) = 0.02] shows a peak at 5.5 Hz. Both in* ***(A,B)****, open symbols identify the same low-frequency units reported in Figure 4 and filled symbols are the average values (± SEM) of high frequency oscillation units. Both in* ***(A,B)****, the gray area shows the 95% confidence interval of the fitting.*

Thus, Lorentzian fitting of SR-P and SR-S distributions showed opposite changes in burst-first and pause-first units with peaks in the low frequency range of stimulus-induced oscillations. We then asked whether and how these long-lasting changes were influenced by cerebellar cortical activity. To this end, we used optogenetic stimulation of the cerebellar molecular layer, which allows a broader activation than electrical stimulation and is therefore more likely to capture neuronal chains involved in controlling the recorded DCN units. We have shown above that optogenetic stimulation of the molecular layer could indeed modify DCN responsiveness (see Figs. 3B, 4F), disrupting the cortical output by modifying PC firing. It should be noted that, as explained in Methods, this test was not expected to yield a deterministic increase or decrease in PC firing, but rather to impact on DCN units and change their ability to generate long-term response changes after TSS. We thus compared DCN units response changes with or without the use of optogenetics assuming the Lorentzian distribution as the best fit to our data. Optogenetic stimulation of the molecular layer during TSS altered the long-lasting changes compared to those expected from controls, in such a way that these always fell beyond the confidence limits predicted from control data, both for peaks in burst-first units (Fig. 7A) and for pauses in pause-first units (Fig.7B). The distance from the control curves in Fig.6A,B, estimated at the frequency of stimulus-induced oscillation recorded during optogenetic stimulation, was 45.1±7.0% (n=6, unpaired Student's *t* test p=0.03; significantly different from the distance from the same curve calculated from control data: 9.1±2.1 n=20, unpaired Student's *t* test p=0.0028; Fig.7C). Therefore, optogenetics did not seem to primarily address the same mechanism of frequency-dependent

induction of long-lasting changes occurring in DCN units but rather to affect different mechanisms, presumably located in the molecular layer (see Discussion).

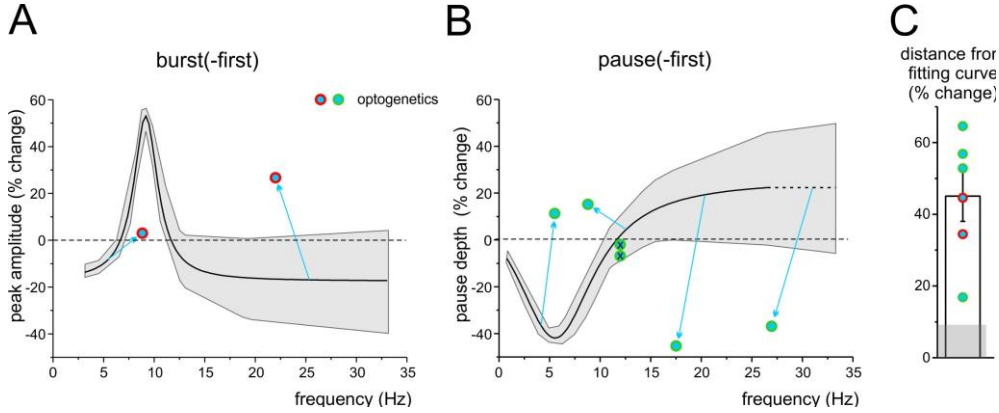

Fig.7.The impact of optogenetic stimulation on long-lasting response changes. *(A) The plot shows the Lorentzian fitting as Figure 6A, with the gray area showing the 95% confidence interval. Note that the data-points representing burst-first units in which the TSS was paired with optogenetics fall far outside the confidence interval.* ***(B)*** *The plot shows the Lorentzian fitting as in Figure 6B, with the gray area showing the 95% confidence interval, extrapolated beyond the last point of control to compare new data. Note that the data-points representing pause-first units in which the TSS was paired with optogenetics fall far outside the confidence interval (except for the two points representing the units in which optogenetics did not show any effect;* crossed circles*).* ***(C)*** *The histogram shows the average distance of the optogenetics data points from the fitting curves in* ***(A, B)****. The gray shadow shows the average distance of control data in Figure 6 from the same fitting curves.*

4.5 Discussion

DCN units were spontaneously active and responded to tactile sensory stimulation with different combinations of bursts, pauses and oscillations. Following theta-frequency stimulation (TSS), DCN units showed spike-related potentiation or suppression, SR-P or SR-S, both in bursts and pauses. To our knowledge, SR-P and SR-S are the first electrophysiological evidence that long-lasting changes can be observed following naturally patterned sensory entrainment in DCN neurons *in vivo*. Unique in the cerebellum among the other long-lasting changes observed *in vivo* (D'Angelo 2014; D'Angelo et al. 2016a; Gao et al. 2012; Ramakrishnan et al. 2016; Roggeri et al. 2008), the DCN SR-P/SR-S distributions were correlated to the

stimulus-induced oscillation frequency of DCN units through Lorentzian functions peaking in the theta-frequency range, disclosing the complex nature of the underlying plasticity mechanisms.

The nature of DCN unit responses

All DCN units responded to tactile stimulation with short delays typical of the fast cerebellar reaction to sensory inputs. In some units (53%), bursts were the first DCN response and occurred either as a single peak at 10-14ms or a double peak (in a third of cases) about 10ms later. This pattern closely matches that observed in the granular layer (Morissette and Bower 1996; Roggeri et al. 2008; Vos et al. 1999), suggesting that DCN neurons can receive double mossy fiber activation through the trigeminal pathway and the somato-sensory cortex (the trigeminal connection might not be direct for the fastigial nucleus though (Morcuende et al. 2002; Rowland and Jaeger 2005; 2008). The excitatory nature of these bursts was confirmed by their extinction after injection of AMPA and NMDA receptors blockers into the DCN. In the remaining units (47%), pauses were the first DCN response with delays of 25-29 ms, most likely reflecting signal transfer through the cerebellar cortex down to PCs and DCN. This delay can be accounted for by considering that PC excitation through mossy fibers and granule cells takes about 15ms (Ramakrishnan et al. 2016) and an additional time is required to inhibit DCN cells. Indeed, optogenetic stimulation of the molecular layer was able to modulate pause duration and depth.

It should be noted that, in principle, climbing fibers could also contribute to DCN excitation through axonal collaterals. However, in comparable recording conditions (Ramakrishnan et al. 2016), PC complex spikes that reflect climbing fiber activation were only sporadically observed and had a latency of 40-50ms, which is too long to explain the latency of the DCN unit responses. Although climbing fibers could contribute to DCN activation, when actively stimulated (Mogensen et al. 2017), it seems very unlikely that they took part to generate the PSTH peaks analyzed here.

The pauses occurring after initial bursts were also modified by optogenetic stimulation of the molecular layer and reflected therefore DCN inhibition by PCs. These pauses, which were evident about 50 ms after the stimulus, could have been protracted by signal reentry into the cerebellar cortex through intracerebellar (Ankri et al. 2015; Gao et al. 2016) or extracerebellar loops (Kistler and De Zeeuw 2003). The bursts following the pauses correlated with the depth of the preceding pause and were therefore probably rebound activities due to intrinsic electroresponsiveness (*Alviña et al. 2008; Hoebeek et al. 2010; Witter et al. 2013*) (this conclusion was supported by rebound burst persistence after injection of AMPA and NMDA receptors blockers into the DCN in a single experiment).

Some units continued their response with an oscillatory cycle independent on whether the responses started with a burst or a pause. The frequency and magnitude of oscillations induced by stimulation were not significantly correlated with spontaneous discharge in the same units. Therefore, oscillations could not be explained by phase reset, since in that case the two frequencies should coincide (Solinas et al. 2007). The origin of these oscillations should then reflect circuit mechanisms (see Fig. 1A). A first mechanism was hypothesized by Yarom (Chen et al. 2010; Jacobson et al. 2008) and involves DCN control of inferior olive (IO) oscillations that reverberate through climbing fibers into the DCN-PC-IO loop. Stimulus-induced oscillations similar to ours are indeed evident in the PSTH of DCN neurons following direct climbing fiber activation (Cheron and Cheron 2018). A second mechanism hypothesized by De Zeeuw could involve signal reentry through extra-cerebellar circuits (Gao et al. 2016; Kistler and De Zeeuw 2003) or through the more recently identified connections between DCN and granular layer (Ankri et al. 2015; Gao et al. 2016), therefore passing again through PCs. That PCs could actually be a node in the loops controlling the stimulus-induced oscillations was supported by their perturbation by optogenetic stimulation of the molecular layer.

There were two groups of units showing stimulus-induced ocillations, *burst-first* and *pause-first* units, which turned out to show opposite frequency-dependent changes following TSS. The potential relationship between these functional

groups and the DCN neuron subpopulations reported *in vitro* (Bagnall et al. 2009; Uusisaari and Knopfel 2012) remains to be determined.

Long-lasting changes in DCN unit responses and their relationship with plastic mechanisms

By being connected to the sensory input through multi-synaptic chains, the long-lasting changes in DCN unit responses could either be generated locally or occur upstream in the cerebellar cortex.

On one hand, according to fittings using Lorentzian functions, SR-P peaked at 9.2 Hz in *burst-first* units and SR-S at 5.5 Hz in *pause-first* units. This property favors the engagement of local mechanisms, since no similar frequency-dependent changes have ever been observed either in the granular or molecular layer *in vivo* (Ramakrishnan et al. 2016; Roggeri et al. 2008) or *in vitro* (for review see (D'Angelo 2014; D'Angelo et al. 2016b; Gao et al. 2012; Hansel et al. 2001a). Moreover, LTP and LTD reported in DCN neurons *in vitro* are based on specific sequences of excitation, inhibition and rebounds (Morishita and Sastry 1996; Ouardouz and Sastry 2000; Pugh and Raman 2006; Zhang and Linden 2006). Therefore, the different synapses impinging on DCN neurons could reciprocally influence one each other, providing a plausible mechanism for SR-P and SR-S induction during stimulus-induced oscillations. The robust potentiation in PC responses observed *in vivo* following TSS (Ramakrishnan et al. 2016) is likely to contribute to DCN plasticity in *pause-first* units, independently of the frequency of stimulus-induced oscillations.

On the other hand, SR-P and SR-S of the initial burst and pause were remarkably altered by optogenetic stimulation of the molecular layer. Optogenetic stimulation caused long-lasting changes in DCN unit responses that went much beyond those expected from the alteration of stimulus-dependent oscillation frequency. This suggests the engagement of additional mechanisms. For example, similar to electrical stimulation, optogenetic stimulation might cause a broad set of long-lasting changes in the molecular layer [for details see (Ramakrishnan et al. 2016)]

modifying the PC output, which would eventually perturb the long-lasting changes observed in DCN unit responses. Further insights on the role of cortical input on DCN responses to TSS might derive from the use of genetically modified models with known alterations in the cerebellar cortex (e.g. mice lacking the phosphatase PP2B in PCs, that show selective loss of PC potentiation, as in (Romano et al. 2018; Schonewille et al. 2010).

A further issue is about the time course of SR-P and SR-S, which decayed over 30min. Both in rodents and humans, cerebellar learning has been predicted to occur in two steps, a faster one in the cerebellar cortex and a slower one in DCN (Attwell et al. 2001; Medina and Mauk 2000; Monaco et al. 2014; Smith et al. 2006). Mathematical modeling further predicts that fast plasticity at the parallel fiber-PC synapse would be able to tune slow and more stable plasticity in DCN (Casellato et al. 2014; Garrido et al. 2013; Medina et al. 2001). So why *in vivo* recordings have shown more persistent changes in the granular layer (Roggeri et al. 2008) and molecular layer (Ramakrishnan et al. 2016) than in DCN? There are three key issues to consider. First, more intense or repeated stimulation may be needed to promote plasticity consolidation in DCN. Secondly, here DCN was not entrained in active sensorimotor feedback that can enhance cerebellar oscillations (Marshall and Lang 2004). Thirdly, there was no attentional or motivational state, as the animal was anesthetized. Indeed, neuromodulation by noradrenaline, acetylcholine or serotonin is thought to be critical to drive oscillations and plasticity and promote learning (Schweighofer et al. 2004; Sugihara et al. 1995). It should also be noted that a similar trend, with a stimulus inducing long-term plasticity in the cerebellar cortex but having less effects on the cerebellar nuclei, has been recently described for the anterior interposed nucleus in cats (Mogensen et al. 2017). It cannot be excluded that stimulus-induced oscillations and the induction or expression of long-lasting changes in DCN neuron responses might have been influenced by anesthesia. We notice, however, that urethane is very conservative on the NMDA and GABA-A receptor-dependent mechanisms of neurotransmission and has been successfully used to demonstrate long-lasting changes at other cerebellar synapses *in vivo* (Ramakrishnan et al. 2016; Roggeri et

al. 2008). Moreover, stimulus-induced oscillations in DCN neurons have been recently shown using ketamine-xylidodihydrothiazin anesthesia (Cheron and Cheron 2018).

4.6 Conclusions

The identification of a possible relationship between DCN long-lasting changes and oscillatory dynamics engaged by tactile stimuli suggests that two key cerebellar functions can be reconciled: oscillatory activity in DCN may not just be needed to gate motor activity (Llinas 1988; Marshall and Lang 2004) but also to control plasticity and acquisition of sensorimotor engrams (Cheron et al. 2016; D'Angelo and De Zeeuw 2009). Interestingly, the preferential frequency of long-lasting DCN response changes identified by Lorentzian fittings was in the theta-band, i.e. the characteristic oscillatory frequency of the IO-PC-DCN circuit (Jacobson et al. 2008) and of the cerebello-extracerebellar loops (Kistler and De Zeeuw 2003) following mossy fiber inputs. It is tempting to speculate that the cerebellum uses oscillating and resonant mechanisms similar to those that are known to favor the induction of plasticity in hippocampal and cortical synapses (Buzsaki 2006; Roy et al. 2014) and that the frequency of oscillations provides a signal binding DCN plasticity to specific neuronal ensembles and brain states (Buzsaki 2006; Buzsaki 2005; Timofeev 2011). This would be eventually reflected into neuro-muscular coherence on the systemic scale (Gruart et al. 2000; Koekkoek et al. 2002; Sánchez-Campusano et al. 2009; 2007; Wang et al. 2018). The frequency dependence of burst and pause changes in DCN units *in vivo* prompts for a further characterization of LTP and LTD mechanisms in DCN neurons *in vitro,* also considering the existence of functionally distinct DCN neuronal populations. New experiments may also be conducted in awake animals and combined with computational modeling (Casellato et al. 2014; D'Angelo et al. 2016a; Luque et al. 2014; Medina and Mauk 2000) to address the impact of frequency-dependent forms of plasticity during cerebellar adaptation and learning.

Additional information

Acknowledgments. This project/research received funding from the European Union's Horizon 2020 Framework Program for Research and Innovation under the Framework Partnership Agreement No. 650003 (HBP FPA); the European Union's Horizon 2020 Framework Program for Research and Innovation under the Specific Grant Agreement No. 720270 (Human Brain Project SGA1), and under the Specific Grant Agreement No. 785907 (Human Brain Project SGA2). This work was supported by grant [7(17)] of Centro Fermi to ED, Blue-Sky Research grant of the University of Pavia (BSR77992) to LM.

Author Contributions. LeM performed *in vivo* recordings, data analysis, and wrote the first draft of the manuscript; IM performed the sets of *in vivo* recordings with pharmacology and optogenetics, and data analysis; LDP performed the initial *in vivo* recordings; ST performed histology and image analysis; LiM and ED coordinated the work and wrote the manuscript. All authors approved the final version of the manuscript.

Conflict of Interest Statement. The authors declare that the research was conducted in the absence of any personal, professional or financial relationship that could be constructed as a potential conflict of interest.

Chapter 5

Investigation of cerebello - prefrontal cortex physiological interaction *in vivo*

Ileana Montagna[1], Letizia Moscato[1], Simona Tritto[1], Lisa Mapelli[1], Egidio D'Angelo[1, 2]

[1] University of Pavia, Dept. of Brain and Behavioral Sciences, Italy

[2] IRCCS Mondino Foundation, Pavia, Italy

In preparation

The physiological interaction between the cerebellum and neo-cortical areas subserving cognitive functions, such as the medial prefrontal cortex (mPFC), strongly stands for a critical cerebellar role in cognition. The existence of alterations in cerebello-mPFC connections have been reported in several cognitive dysfunctions, suggesting that the cerebellum has a crucial impact on the mPFC appropriate functioning. Herein, cerebellar impact on mPFC activity was investigated by single-unit recordings *in vivo* in the prelimbic area (PrL) of the mPFC of anesthetized mice, following electrical stimulation of the contralateral fastigial or dentate nuclei. We identified two typical discharge patterns in PrL neurons, elicited by cerebellar nuclei stimulation, both characterized by an initial pause, wich can be followed by a rebound excitation in some cases. Furthermore, the nature of PrL neurons responses to cerebellar stimulation was investigated using pharmacological tools. The co-application of selective dopamine D1-like and D2-like receptor antagonists (SCH23390 and sulpiride, respectively) during cerebellar stimulation did not abolish pause responses. Nevertheless, dopamine receptors antagonists exerted a significant effect on PrL neurons spontaneous firing rate, thus confirming a modulatory effect of dopamine on cortical neurons. Notably, pause responses were mostly abolished following perfusion of gabazine, a $GABA_A$ receptor selective antagonist. A plausible explanation to the PrL pause responses to cerebellar stimulation could rely on the contribution of cerebello-prefrontal projections activating local inhibitory interneurons in the mPFC, that in turn elicit inhibitory responses in cortical pyramidal neurons. Overall, these

findings demonstrate physiological interactions between the cerebellum and the PrL of the mPFC, providing insights of a complex functional interplay between these two regions.

5.1 Introduction

Although the role of the cerebellum is mainly considered as related to sensorimotor integration, several findings suggest a fundamental cerebellar role in cognitive functions as well. Anatomical tracing studies in humans revealed the existence of a prominent interconnection between the cerebellum and neocortical areas involved in cognition, including the mPFC (Palesi et al. 2015). In recent years, an increasing number of studies questioned about the nature and relevance of cerebello-prefrontal connection. Abnormal functionality of prefrontal-cerebellar pathway has been reported in several cognitive disorders, ranging from schizophrenia to autism spectrum disorders (Andreasen et al. 1996; Andreasen and Pierson 2008; Fatemi et al. 2012; Whitney et al. 2008). These observations lead to new perspectives for understanding neuronal mechanisms underlying these pathologies. Structural and functional alterations such as reduced number of Purkinje cells (PCs), cerebellar hypoplasia, and increased volume of frontal lobe cortex, positively correlate with autistic symptoms (Palmen et al. 2004; Vargas et al. 2005; Whitney et al. 2008) whilst abnormalities in the cerebellar vermis (Henze et al. 2011; Lawyer et al. 2009; Okugawa et al. 2007) and a reduction in cerebellar projections at the level of the cerebellar peduncle, have been related to schizophrenia (Kyriakopoulos et al. 2008).

The existence of a bidirectional connection between cerebellum and mPFC has been revealed through electrophysiological and amperometric studies in rodents *in vivo* (Watson et al. 2014; Watson et al. 2009). In particular, it has been reported that electrical stimulation of the fastigial nucleus (FN) is able to elicit responses in the prelimbic subdivision (PrL) of the mPFC (Watson et al. 2014). This connection appeared to be reciprocal, since electrical stimulation of the PrL in turn evokes field potential responses in PCs of the cerebellar vermis, although

responses with smaller amplitude were also detected in the paravermal and lateral cerebellar cortex (Watson et al. 2009). In addition, stimulation of the dentate nucleus (DN) in urethane-anesthetized mice is shown to provoke dopamine release in the mPFC either via cerebello-activated ventral tegmental area (VTA) projections or glutamatergic projections from thalamic nuclei (Rogers et al. 2011). Recent studies revealed that the dopamine release in mPFC induced by optogenetic activation of cerebellar terminals over the VTA in freely moving mice is not sufficient to promote prosocial behaviour (Carta et al., 2019). Hence, putative cognitive functions related to cerebellar drive onto mPFC activity cannot be explained by the sole contribution of dopaminergic pathway.

Thalamocortical interactions are fundamental for processing sensation, perception, and consciousness (John, 2002; Alitto and Usrey, 2003). Cerebellar projections from deep cerebellar nuclei also reach thalamic nuclei, which in turn are reported to elicit strong, sustained synaptic responses from mPFC neurons, thus suggesting that their prolonged activation is necessary for working memory function (Cruikshank et al., 2012). In particular, the majority of thalamocortical projections reaching the mPFC originate from the mediodorsal nucleus (MD) of the thalamus (Ferguson ad Gao, 2018). MD glutamatergic projections contact both pyramidal neurons in layer V and interneurons in layers III and V of mPFC, which in turn form inhibitory synapses with pyramidal excitatory neurons, regulating their discharge patterns (Rotaru et al., 2005; Povysheva et al., 2006). Indeed, mPFC interneurons exert a crucial role in excitatory/inhibitory balance over pyramidal neurons firing in mPFC through feed forward inhibition and gain control activity (Ferguson and Gao, 2018).

Therefore, the cerebellum may affect the mPFC activity via different pathways, though the underlying mechanisms are largely unknown. On one hand, dopamine exerts a mixture of contrasting effects on pyramidal cells and local interneurons in mPFC engaging different classes and subtypes of dopamine receptors (mostly D1 or D2-like) which are also heterogeneously distributed among prefrontal neurons (Floresco and Magyar 2006; Floresco et al. 2006).

Moreover, it has been shown that dopamine may exert its neuromodulatory action on mPFC neurons either by decreasing spontaneous and evoked activity (Gulledge and Jaffe 1998), or by increasing neuronal excitability (Buchta et al. 2017; Otani et al. 2015; Trantham-Davidson et al. 2008). On the other hand, thalamic projections reach different layers in the mPFC, thus exerting different effects over cortical activity. In this perspective, it becomes difficult to assess whether the cerebello-thalamo-cortical pathway is related to direct excitation of mPFC pyramidal neurons or indirect modulation via local interneurons, due to the complexity of mPFC circuitry.

Herein, we characterized PrL neurons responses following electrical stimulation of contralateral cerebellar FN and DN *in vivo* in mice. Cerebellar nuclei stimulation generated two types of discharge patterns in PrL neurons, both characterized by an initial pause in spontaneous activity, that in some cases was followed by a burst. The possible involvement of dopamine receptors in mediating these responses was investigated. Our results are compatible with a purely modulatory role of dopamine on PrL neurons excitability. The role of local synaptic inhibition was revealed by blocking GABA receptors, which almost completely abolished PrL neurons response to cerebellar stimulation.

These results could be explained considering that pause responses in PrL neurons might derive from the activation of mPFC interneurons inhibiting pyramidal cells by virtue of thalamo-cortical projections activated by cerebellar stimulation.

Overall these findings demonstrate the existence of functional connection between the cerebellum and the PrL of the mPFC, providing new evidence on the nature of this functional interaction between these two regions. In particular, our results show that the cerebellar impact over the mPFC transcends the solely dopaminergic control, evidencing the existence of more complex mechanisms through which the cerebellum might affect cortical activity.

5.2 Materials and methods

Multiple single-unit recordings were performed from the PrL of C57BL/6 mice of either sex (30.02±0.21 days old; n=84) under urethane anethesia. No statistical difference was found between males and females neuronal properties and responsivity (in a cohort of 22 males and 13 females, unpaired Student's t test resulted in p=0.1 for spontaneous frequency; p=0.3 for response amplitude as pause depth; p=0.2 for the percent change after pharmacological treatment). Therefore, the results in this paper were considered independent from the sex or the oestrus cycle stage of female animals. Concerning the anesthesia used, urethane is characterized by overall weak effects on glutamatergic and GABAergic receptors (Hara and Harris 2002), making improbable an influence on stimulus-evoked responses in mPFC neurons in our recordings.

Surgical Procedures

Urethane (Sigma Aldrich) was dissolved in saline solution (1.3g/kg urethane dissolved in 0.9% NaCl, Sigma Aldrich) and administered through intraperitoneal injections, each performed 30 minutes from one another. Induction was followed by 3-4 booster injections (10% of the induction dose) in order to stabilize deep anesthesia. The level of anesthesia was checked by testing the leg withdrawal reflex after pinching and the presence of spontaneous whisking. Then, the animal was placed on a custom-built stereotaxic table covered with a heating plate (HP-1M: RTD/157, Physitemp Instruments Inc, Clifton, NJ, USA). A rectal probe allowed to control body temperature, that was maintained at 36°C through a feedback controller (TCAT-2LV controller, Physitemp Instruments Inc, Clifton, NJ, USA). Subcutaneous application of lidocaine (0.2ml; Astrazeneca), reduced cutaneous reflexes. After skull exposure, the mouse head was fixed to a metal bar connected to a pedestal anchored to the stereotaxic table. Then, the skin and muscles were surgically removed and craniotomy was performed over the cerebellum and mPFC to grant exposure of their surface and subsequent placement of electrodes (From Bregma, FN: -5.8 AP, +0.50 ML, +2.4 DV; DN: -5.8

AP, +2.5 ML, +2.4 DV; PrL: +2.8 AP, 0.25 ML, +0.6 DV). The *dura mater* was carefully removed and the surface was perfused with saline solution (NaCl 0.9%; Sigma Aldrich) to prevent drying.

Electrophysiological extracellular recordings

Multiple quartz-coated platinum/tungsten fiber electrodes (1-5MΩ; Thomas Recording GmBh, Giessen, Germany) were inserted in a 4x4 Eckhorn Matrix and positioned over the exposed mPFC area, contralaterally to the stimulus source. Each recording electrode was moved independently of each another and lowered to the surface down to a depth of 682.27±34.50 µm (n=95) in order to reach the PrL. The electrophysiological signals were digitized at 25 kHz, using a 300-5000 Hz band-pass filter, amplified and stored using a RZ5D processor multi-channel workstation (Tucker-Davis Technologies, Alachua, FL, USA). Histological tissue processing performed after electric lesions at the end of each experiment allowed the identification of the exact placement of electrodes in PrL, FN or DN.

Electrical stimulation

The electrical stimulation of FN and DN (21 pulses, 100Hz, 100 µA, repeated every 5 s) was performed using a bipolar tungsten electrode (0.5 MΩ; World Precision Instruments Inc, Sarasota, FL, USA) connected through a stimulus isolator to a stimulator unit. This stimulation protocol was modified from (Watson et al. 2014), where 100 pulses at 100Hz were used.

Similar stimulation parameters (10 stimuli, 50Hz) also drive FN output to the vestibular nuclei (Bagnall et al. 2009). Moreover, high-frequency cerebellar stimulation (100 pulses, 50 Hz) has been related to dopamine efflux in the mPFC (Mittleman et al. 2008). Following these reports, we have defined a similar stimulation protocol that showed to be efficient in evoking cortical neurons responses and is likely to elicit dopamine release in mPFC (Mittleman et al. 2008). The intensity of the electrical stimulation delivered to FN and DN was set as

slightly suprathreshold , compared to that sufficient to evoke a response in the mPFC (data not shown).

The stimulating electrode was mounted on a Patch-star micromanipulator (Scientifica, Ltd) and lowered into the cerebellum with micrometric precision to a depth of 2400 or 2600 μm from the surface, in order to stimulate FN or DN, respectively.

Once a PrL neuron was detected, 5 minutes recording of spontaneous activity was followed by control recording during cerebellar stimulation, in order to characterize the evoked response patterns in PrL neurons. Each control recording had a duration of 8 minutes approximately.

Over a total of 95 neurons recorded, the effect of FN and DN stimulation on PrL were detected and characterized in 10 and 44 units, respectively. In 36 units, no significant response to stimulation was detected.

Pharmacology

All drugs were added to a Krebs solution with the following composition (in mM): 120 NaCl, 2 KCl, 1.2 $MgSO_4$, 26 $NaHCO_3$, 1.2 KH_2PO_4, 2 $CaCl_2$, and 11 glucose, equilibrated with 95% O_2-5% CO_2 (pH 7.4) and perfused onto the exposed PrL surface using a micropipette. Pharmacological testing of PrL responses was performed in experiments involving DN stimulation, but not FN stimulation. In a first subset of experiments, the selective dopamine receptors antagonists SCH23390 hydrochloride (selective D1-like receptor antagonist, 44 mM; Abcam) and (S)-Sulpiride (selective D2-like receptor antagonist; 36mM; Abcam) were co-perfused on PrL surface immediately after control recordings. The effects of these selective antagonists on PrL response pattern during DN stimulation was monitored for at least 20 minutes.

In 11 out of 75 cells dopamine receptors antagonists were not applied while stimulating the DN, to rule out possible spurious changes due to intrinsic response amplitude fluctuations overtime which may create bias against the effects of the drugs. In a second subset of experiments the GABAergic contribution to PrL responses detected following DN stimulation was assessed

through the perfusion on mPFC surface of the selective $GABA_A$ receptor antagonist gabazine (SR-95531, Abcam, 3mM (Kurt et al.,2006). As for dopamine receptors antagonists, following drug perfusion PrL neuron activity was recorded for other 30 min, during which the same pattern of electrical stimuli was delivered to the DN.

Histology

Histological analysis was used to verify the precise location of both recording and stimulating electrodes in PrL and FN or DN, respectively. At the end of every experiment, an electric lesion was performed applying 20 μA current for 20s through the same electrodes used for electrophysiological recordings in the PrL. The stimulating electrode placed at the level of FN or DN produced itself a detectable electrical signature to the tissue due to the current injection (100 μA) during experimental procedures. Mouse brains were fixed by transcardial perfusion of Phosphate-Buffered Saline (PBS) solution and 4% formaldehyde. Brains were dehydrated using a 30% sucrose solution and cryoconserved at -80°C. Then, coronal brain 20-μm-thick histological sections were obtained and stained with toluidine blue. The correct localization of recording/stimulation sites was assessed through hystological analysis performed using an optical microscope.

Data analysis

The electrophysiological signals from PrL neurons were acquired by OpenEx software (Tucker-Davis Technologies) and analyzed offline using SpikeTrain (Neurasmus BV, Rotterdam, Netherlands) running under MATLAB (Mathworks, MA, USA). PrL responses to cerebellar stimulation were analyzed through the construction of peri-stimulus time histograms (PSTHs) with 100 ms bin width, for convenience. This analysis approach evidenced that PrL response patterns to the incoming stimulus were consistently characterized by a pause, sometimes followed by bursts emerging from background activity.

PSTHs constructed using 20 ms bin width allowed the measurement of latency and duration of the detected responses. PrL responses to cerebellar stimulations were identified as pauses or peaks in PSTHs when values exceeded once the standard deviation of the basal frequency measured in the pre-stimulus period. 36 out of 95 units did not show any significant change with respect to this criterion. The effects of selective antagonists on detected responses were evaluated by comparing changes in pause amplitude and area in PSTHs with respect to control. To this aim, we measured changes in response parameters over 10, 20 and 30 min after drugs perfusion, considering significant only those values in the PSTH that exceeded once the standard deviation of the control response. Antagonist-mediated increase or decrease in neuronal responsiveness to cerebellar stimulation were detected as positive or negative changes compared to control, respectively.

To test whether selective antagonists influence spontaneous firing rate and coefficient of variation of the inter-spike interval (CV2, which provides information about the spiking regularity), firing rate and CV2 were measured after antagonists perfusion and compared to control measurements. Data were fitted using OriginPro8 (OriginLac co., MA, USA) and statistical analysis was performed using paired or unpaired Student's *t*-test. All data are reported as mean ± SEM.

5.3 Results

Single-unit recorded from the PrL in urethane anesthetized mice displayed spontaneous activity with a basal frequency of 1.63±0.20 Hz (n=95; Fig. 1). This observation is in agreement with previous reports of PrL neurons spontaneous firing in urethane anesthetized rodents *(Watson et al. 2014).*

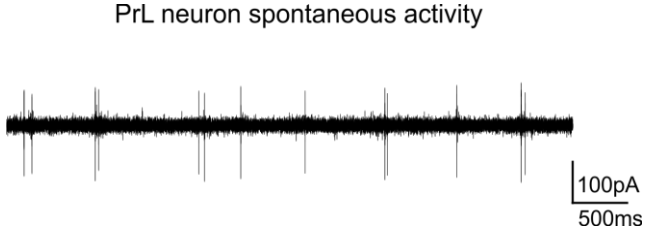

Figure 1. Extracellular recordings from PrL neurons *in vivo*. *Example of PrL neuron spontaneous activity.*

Both sites of recordings and stimulation were marked through electrical lesions and confirmed by histological analysis (Fig.2, 3).

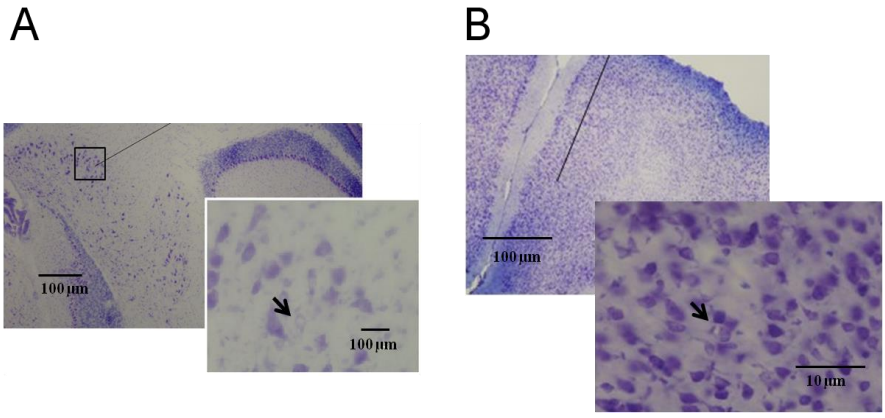

Figure 2. Histological confirmation of stimulation site in the FN and recording site in PrL. A) T*oluidine blue stained coronal cerebellar slice showing the electrical lesion (arrow) made by the stimulating electrode in the fastigial nucleus. B) Toluidine blue stained coronal section showing electrical lesion made by the recording electrode in the PrL. Note that the histological sections in A and B were obtained from a single animal.*

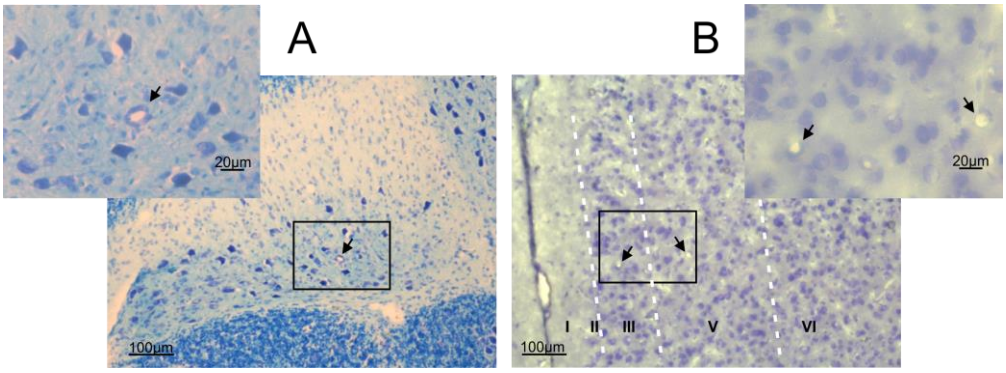

Figure 3. Histological confirmation of stimulation site in the DN and recording site in PrL. *A) Toluidine blue stained coronal section of the cerebellum. The region in the rectangle is magnified on top left; the black arrow indicates the electrical lesion made by the stimulating electode at the level of DN.* B) *Toluidine blue stained coronal section of PrL region. The black arrows indicate lesions made through two electrodes used for simultaneous recordings of PrL neurons. The lesions indicate that recording sites were located in layers III and V of the PrL. The region in the rectangle is magnified on top right. Note that the histological sections in A and B were obtained from a single animal.*

Impact of FN stimulation on PrL neurons

FN stimulation was performed while recording PrL neurons activity in 10 cases. PrL neurons responded to FN stimulation in 5 of 10 recordings, with two typical response patterns: 3 units showed pure inhibition, consisting in a pause in the PSTH respresenting the suppression of neuronal firing following the income of the stimulus (Fig.4A); 2 units showed a biphasic response consisting in a long-latency excitation following the initial pause, represented by a peak following the initial pause in the PSTH (Fig.4B).

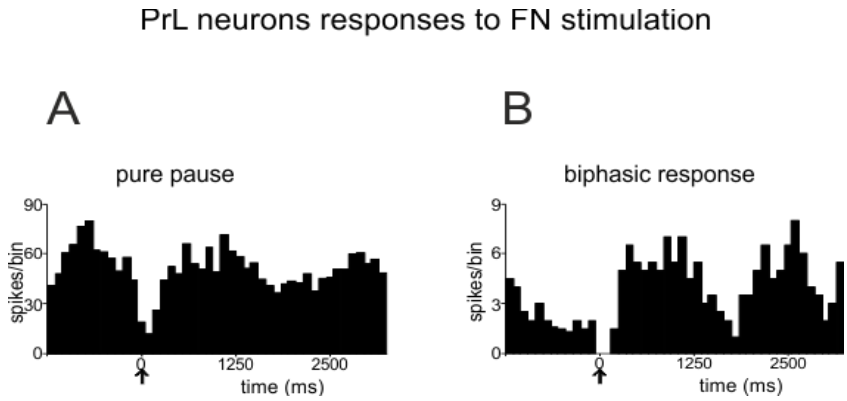

Figure 4. PrL response patterns to FN stimulation. *Exemples of PSTHs obtained from PrL neurons showing two different response patterns to the electrical stimulation of FN. The black arrow indicates the stimulus onset.* ***A)*** *Pure inhibition.* ***B)*** *Biphasic response.*

The remaining cells (n=5) did not respond to the stimulation, with respect to our criterion of analysis (see materials and methods for detailed description). Pure pause responses occurred with a latency of 12±4.8 ms (duration: 220±20 ms; n=3). Biphasic responses showed a pause latency of 13.33±3.33 ms (duration: 140±60 ms; n=2) and peak latency of 250±10 ms (duration 110±90 ms; n=2). The values of spontaneous firing rate and CV2 measured before and after FN stimulation did not differ significantly (p=0.3 and p=0.1, n=5; respectively; paired Student's t test), suggesting that the stimulation protocol did not modify PrL spontaneous activity. These data are in agreement with those previously reported for PrL neurons responses to FN stimulation *in vivo (Watson et al. 2014)*.

This comparison was useful to validate the stimulation pattern used, in order to approach the study of PrL neurons responses to DN stimulation.

Impact of DN stimulation on PrL neurons

In 75 out of 95 cells, we characterized PrL neurons firing during DN stimulation. Over the responding units recorded (n=44), we identified two response patterns in PTSHs, characterized either by pure inhibition (61%) or by a pause followed by a burst (biphasic response, 39%) (Fig.5 A, B). Pure pause responses occurred with a latency of 4.80±2.09 ms (duration: 183.33±12.94 ms, n=27; Fig.4A). Biphasic responses showed a pause latency of 18.66±0.20 ms (duration: 144±12.97 ms, n=17 and peak latency of 262.66±19.01ms (duration 129.33±31.64 ms; n=17; Fig.4B). The stimulation of DN failed in eliciting responses in 41% of recorded PrL neurons (n=31) with respect to our criterion.

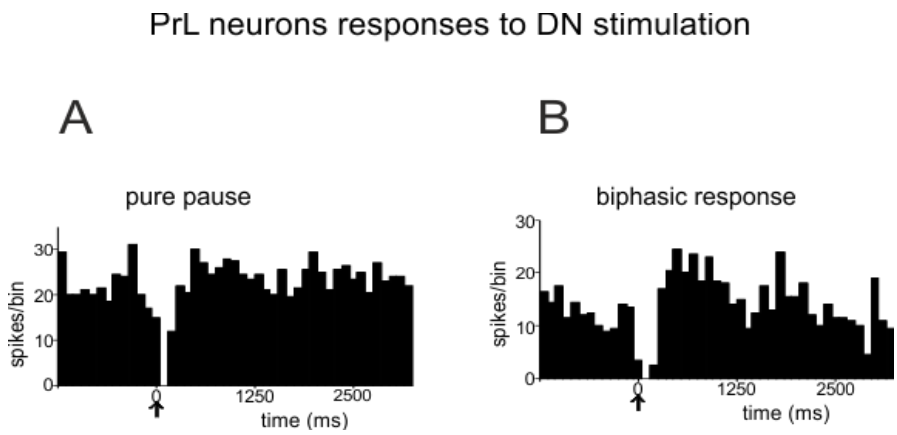

Figure 5. PrL response patterns to DN stimulation. *Exemples of PSTHs obtained from PrL neurons showing two different response patterns to DN electrical stimulation. The black arrow indicates the stimulus onset.* ***A)*** *Pure inhibition.* ***B)*** *Biphasic response.*

The PrL units dispalying biphasic responses to DN stimulation showed a positive correlation between pause depth and peak amplitude in the PSTH, suggesting that the burst following the initial pause is likely to represent rebound excitation (Fig. 6). Latency and duration of pause in both types of responses did not differ significantly (p=0.2 and p=0.1, respectively; paired Student's t-test).

As a consequence, pause responses were considere for the analysis independent from the presence of a rebound peak (pause latency: 13.10±4.46, pause duration: 159.28±10.95; n=44). Spontaneous firing rate and CV2 values measured before

and after 20 minutes of DN stimulation did not differ significantly (p=0.1 and p=0.6, respectively; paired Student's t-test) suggesting that the stimulation protocol did not affect PrL spontaneous activity. This observation was confirmed for both PrL response patterns.

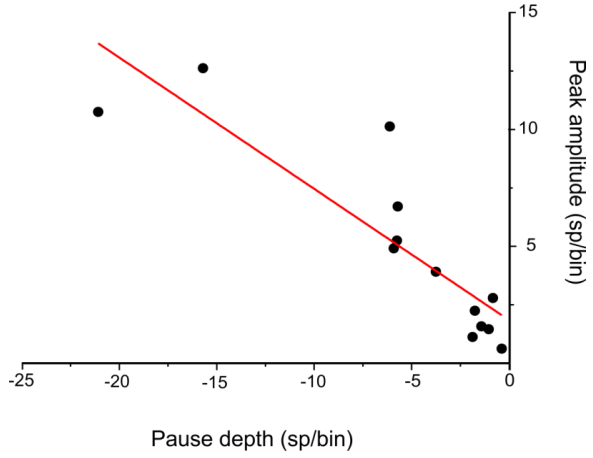

Figure 6. Characterization of PrL biphasic responses. *Positive correlation found between pause depth and peak amplitude in cells showing biphasic responses (R^2=0.73, p(F)=0.003).*

Effect of D1-like and D2-like receptor antagonists on evoked PrL inhibitory responses

In order to characterize the nature of these responses, we first addressed whether the dopaminergic cerebello-prefrontal pathway could be involved. To this purpose, the effects of selective dopamine receptors antagonists over PrL inhibitory responses were investigated, focusing on DN stimulation experiments.

After recording PrL neuronal responses to DN stimulation for a control period of at least 15 minutes, D1-like and D2-like dopamine receptor antagonists were co-perfused over the surface of the mPFC area (9 out of 75 cells) and PrL neurons responses were recorded for further 30 min.

The results confirmed that DN stimulation is able to elicit two types of response patterns in PrL units, characterized either by pure inhibition or by a biphasic response in which the initial pause was followed by a burst. Over 9 cells recorded, 78% (n=7) showed initial pause only, 22% (n=2) showed biphasic responses. Again, no difference was found between the pauses in the two patterns of responses and therefore they were pooled together for the subsequent analysis. The effect of dopamine antagonists on PrL responses were analyzed in terms of changes in pause depth. The blockade of D1-like and D2-like dopamine receptors induced a significant increase in 5 out of 9 PrL neurons spontaneous activity (after 20 min from drugs perfusion: +86.9±23.6 %, n=5, p=0.04). Conversely, in 4 out of 9 PrL neurons D1-like and D2-like antagonists perfusion caused a decrease in spontaneous firing (-57.5±13.54%, p=0.14). The divergent effects of drugs onto PrL neurons activity might reflect the different distribution of D1-like and D2-like receptors among PrL neuronal subpopulations. Interestingly, the inhibitory evoked responses in PrL by DN stimulation were not abolished following the perfusion of the selective dopamine receptors antagonists (Fig.7 A, B).

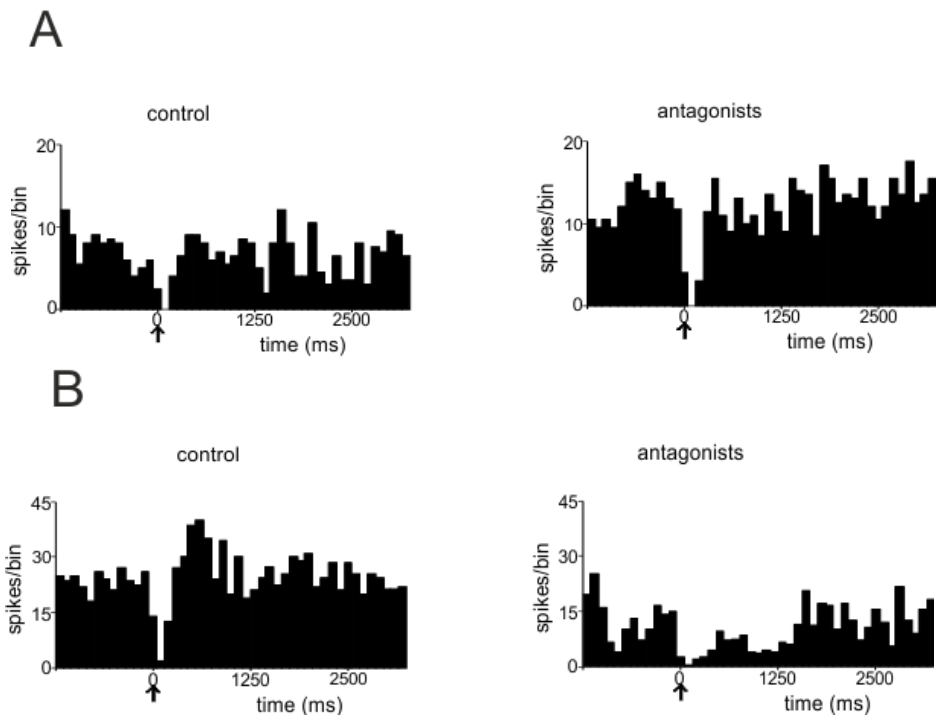

Figure 7. *Comparative exemples of PSTHs of PrL response patterns before and 20 minutes after D1-like and D2-like receptors antagonists perfusion, showing that evoked inhibitory responses are not abolished by drugs application while basal frequency is either increased* ***(A)*** *or decreased* ***(B).***

The pause response showed a tendency to increase or decrease following drugs perfusion reflecting the same tendency observed for basal frequency (Fig. 8A). A strong positive correlation was found between the changes in pause depth and basal frequency (Fig.8B), supporting the idea that the response itself is not directly modified by dopamine. These results suggest that dopamine efflux in PrL more likely reflects a modulatory effect on neuronal firing, rather than on the pause response itself. Stability recordings, in which antagonists were not applied, were performed for a duration similar to the experiments in which dopamine receptors antagonists were co-applied (40 min). Over 11 PrL units recorded for stability recordings, 73% (n=8) responded with an initial pause only, 18% (n=2) exhibited biphasic response, 9% (n=1) did not respond.

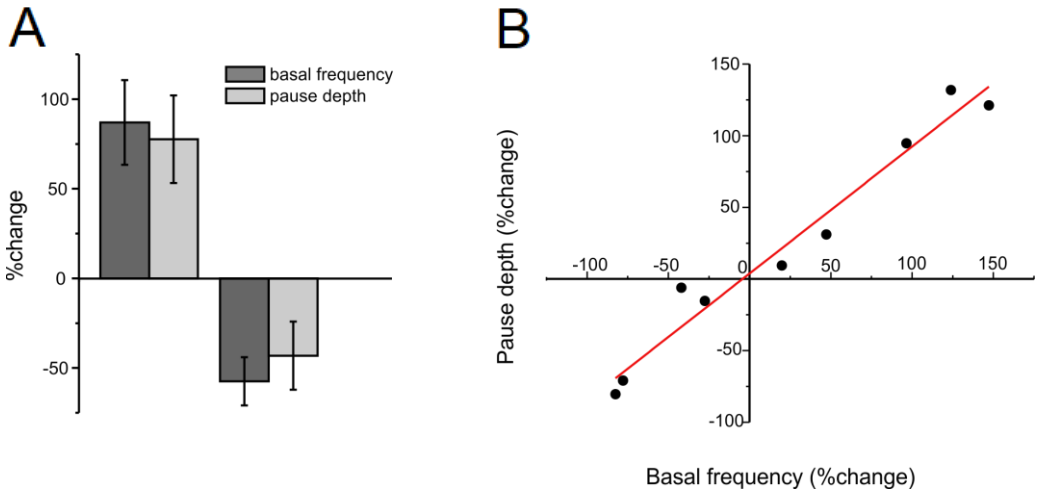

Figure 8. Basal frequency changes following D1-like and D2-like antagonists perfusion. A) *The histograms show that %changes in basal frequency and pause depth for increases (left) and decreases (right). B) The plot shows the positive correlation between changes in PrL neurons basal frequencies and response amplitude following D1-like and D2-like antagonists perfusion (R^2=0.95, n=9)*

Effect of $GABA_A$-receptor antagonist on evoked PrL inhibitory responses

Since dopamine receptors antagonist did not affect the inhibitory response in PrL units during DN stimulation, we tested whether the inhibitory component of the response could be related to synaptic activation of local interneurons (presumably from the cerebello-thalamo-cortical pathway).

Therefore, we measured the depth of PrL responses before and during the perfusion of the selective $GABA_A$ receptor blocker gabazine (SR-95531, 3mM). Possible changes in basal frequency rate and CV2 were also measured comparing values before and after antagonist perfusion.

Experiments were conducted following the same procedures applied during dopamine antagonists perfusion. After acquiring PrL units responses to DN stimulation in control, gabazine was perfused over the surface of the mPFC region and PrL neurons activity was recorded for further 30 minutes. Again, we detected two types of responses, a pure pause and a biphasic response in which the initial pause was followed by a burst. Over a total of 19 units recorded in this subset of experiments, 5 showed pure inhibition, 9 showed biphasic responses, whilst 5 cells did not respond with respect to our criterion. Again, we considered for the analysis changes in initial pause responses following inhibition blockade after 20 minutes of gabazine perfusion in all PrL responding units.

The blockade of GABA receptors induced an increase in 15 of 19 PrL neurons spontaneous activity (+132±46.3%, p=0.015) and a reduction of pause depth in 11 over 14 responding units (Fig. 9; after 20 min of drugs perfusion: -75.4±8.27%, p=0.001). In this case, no correlation was found between pause depth changes and basal frequency changes after gabazine perfusion (Fig.10). These results suggest that the PrL pause responses to DN stimulation described here are mainly mediated by local synaptic inhibition.

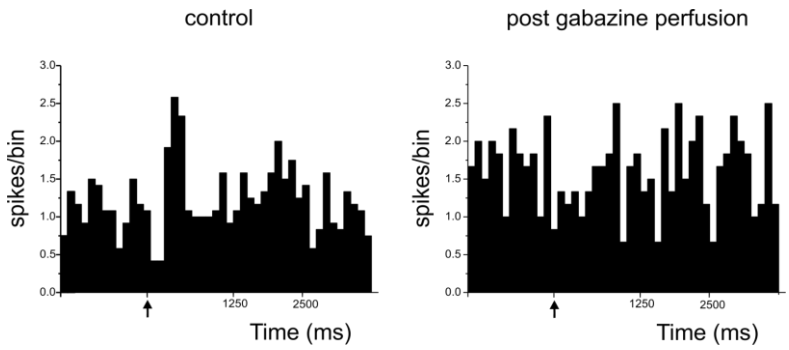

Figure 9. Average PSTHs of PrL responses patterns before and 20 min after gabazine perfusion. *The PSTHs show that inhibitory responses in PrL neurons were significantly reduced whilst basal frequency notably increased following gabazine perfusion (n=8). Note that the peak following the pause in control is abolished after gabazine perfusion.*

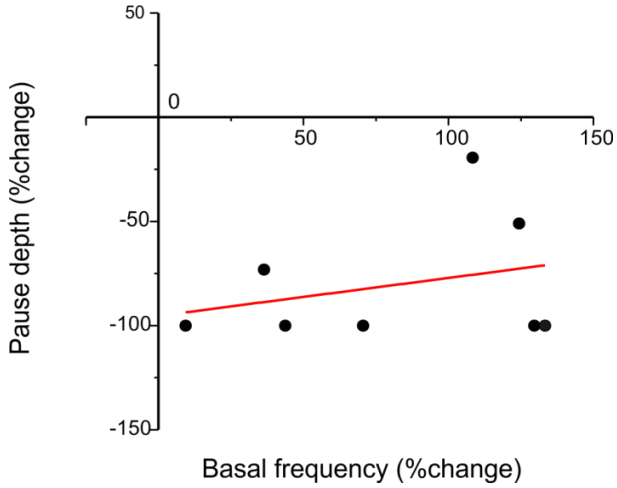

Figure 10. Correlation in PrL responding units between changes in basal frequency and in pause depth following gabazine perfusion. *Inhibitory blockade provoked an overall increase in basal frequency and reduction of the amplitude of detected responses after DN stimulation. The plot shows that reduction in pause amplitude following gabazine perfusion is not correlated to the increase in firing frequency (R^2=0.07).*

Interestingly, in all PrL units showing a biphasic response (n=8) the peak following the pause was completely abolished after 20 min from gabazine perfusion over mPFC (Fig. 9).

This observation provides further confirmation of the excitatory rebound nature of peaks following pauses in this type of response patterns, as previously reported in

correlation analysis between pause depth and peak amplitude in biphasic responding units (Fig 6).

5.4 Discussion

PrL neurons showed spontaneous activity and responded to electrical stimulation of cerebellar FN and DN with two response patterns, both characterized by an initial pause, in some cases followed by a rebound excitation detected as a peak in PSTHs. In biphasic responses peak amplitude correlated with pause depth, suggesting that rebound activity could explain the peaks. Since no significant differences were found between the pauses in the two patterns of response, all pauses were pooled together for the analyses, independent from the presence of a rebound peak following the pause. The cerebello-prefrontal functional connection is expected to recruit the dopaminergic pathway, thorugh the VTA, or the thalamic pathway. The dopaminergic influence over PrL responses to cerebellar stimulation was assessed through the perfusion of selective dopamine receptors antagonists. The local synaptic origin of the PrL pause response was investigated by perfusion of a $GABA_A$ receptor antagonist. Our results allow to speculate on cortical processes underlying the patterns of responses evoked in PrL by cerebellar stimulation.

Nature of the PrL responses evoked by cerebellar stimulation

PrL responses elicited by cerebellar stimulation occurred with a latency of about 13 ms, in agreement with previous electrophysiological studies in rodents *in vivo* (Watson et al. 2014). Neurons in mPFC receive multiple connections from various subcortical regions, including VTA and several thalamic nuclei, which in turn represent two major targets for cerebellar output projections (Rogers et al. 2011; Hoover and Vertes 2007; Kuroda et al., 1996). Further studies also report cerebellar connections to the basal ganglia (Nieoullon et al. 1978) whose efferences also reach the mPFC (Maurice et al. 1999; Middleton and Strick 1994).

Hence, the co-existence of several pathways reaching the mPFC might be a possible explanation for the heterogeneity of observed responses.

Dopaminergic component in PrL neurons responses

The electrical stimulation of DN in urethane-anesthetized mice is reported to exert modulatory activity on mPFC neurons through dopamine release, either via the VTA pathway or via glutamatergic projections from the mediodorsal (MD) and ventrolateral nuclei of the thalamus (Rogers et al. 2011). Dopamine exerts its neuromodulatory effect mainly affecting intrinsic excitability and input resistance, which in turn results in facilitation or suppression of spontaneous and evoked spiking over PrL neurons. In particular several *in vivo* studies report that decrease or increase in the activity of pyramidal neurons and local interneurons in PrL result from the engagement of different classes and subtypes of dopamine receptors (D1-like and D2-like) that are heterogeneously distributed among neuronal subpopulations (Gulledge and Jaffe 1998; Parfitt et al. 1990; Seamans et al. 2001; Sesack and Bunney 1989). Indeed, our results following perfusion of selective dopamine receptors blockers over mPFC revealed that the major contribution of dopamine to PrL activity is mediated by changes in basal firing activity, presumably due to changes in intrinsic excitability. Indeed, the co-perfusion of D1-like and D2-like receptors antagonists did not abolish PrL neurons responses. In conclusion, our data support the hypothesis that dopamine released in PrL modulates neuronal responses elicited by cerebellar stimulation, presumably affecting neurons intrinsic excitability. Nevertheless, the sole contribution of the dopaminergic pathway is not sufficient to explain the impact of cerebellar drive over mPFC activity.

Inhibitory component in PrL neurons responses

Following previous results, showing limited impact of dopamine release over PrL responses to cerebellar stimulation, we focused our attention on the contribution of GABAergic synaptic inhibition within the PrL, presumably mediated by thalamic projections activated by DN stimulation (Rogers et al. 2011). MD

thalamus is reported as the major contributor to glutamatergic projections reaching the mPFC at the level of interneurons in cortical Layers III/V (Ferguson and Gao, 2018), although part of glutamatergic fibers from MD thalamus is also reported to directly excite pyramidal neurons in Layer V (Ferguson and Gao, 2018). Pyramidal cells represent the 80-90% of the total neuronal population in the mPFC, whilst the remaining 10–20% consists of inhibitory GABAergic interneurons (Ascoli et al., 2008; DeFelipe et al., 2013). Following these considerations, and taking into account the smaller soma of interneurons, recording electrodes lowered into the PrL had a much higher probability to detect pyramidal neurons activity rather than that of local interneurons. Nevertheless, the impact of inhibitory interneurons on overall cortical activity seems to be prominent due to their role in excitation/inhibition balance exerted through feedforward inhibition and gain control activity on pyramidal neurons firing (Ferguson and Gao, 2018). Herein, the activation of cortical inhibitory interneurons via the cerebello-thalamic pathway might provide a plausible explanation to inhibitory response patterns detected in PrL following DN stimulation. Indeed, our results show that for all PrL responding units the inhibitory component of PrL responses was almost entirely abolished by blocking $GABA_A$ receptors. Therefore, a reasonable explanation of our data is that the impact of cerebellar activation on PrL activity is mainly exerted through the activation of inhibitory cells regulating pyramidal neurons activity. However, the pause response was not completely abolished (on average 25% of the pause persisted) and in 3 over 14 responding units, no change in pause depth was detected after gabazine perfusion. This could simply be a consequence of the impossibility to determine the final concentration of the drug perfused on the target region where the electrode is recording, making feasible that in some cases said concentration was partially or totally ineffective. Anyway, we cannot rule out the possibility that other mechanisms play a minor role in generating the responses reported here.

Potential pathways involved in PrL neurons responses

The cerebellum affects neuronal activity in mPFC by activating several pathways (Fig. 11) passing through different brain areas such as VTA or thalamus (Rogers et al, 2011; Schmahmann 1996). Dopamine release in mPFC following cerebellar activation mainly derives from the VTA pathway (Rogers et al, 2011). Interestingly, both the electrical stimulation of the VTA and local perfusion of dopamine were reported to inhibit spontaneous activity in most mPFC neurons (Pirot et al. 1992). This observation helps to validate our results reporting an increase in PrL neurons firing activity following blockade of D1-like and D2-like receptors, thus confirming the neuromodulatory effect of dopamine release in mPFC.

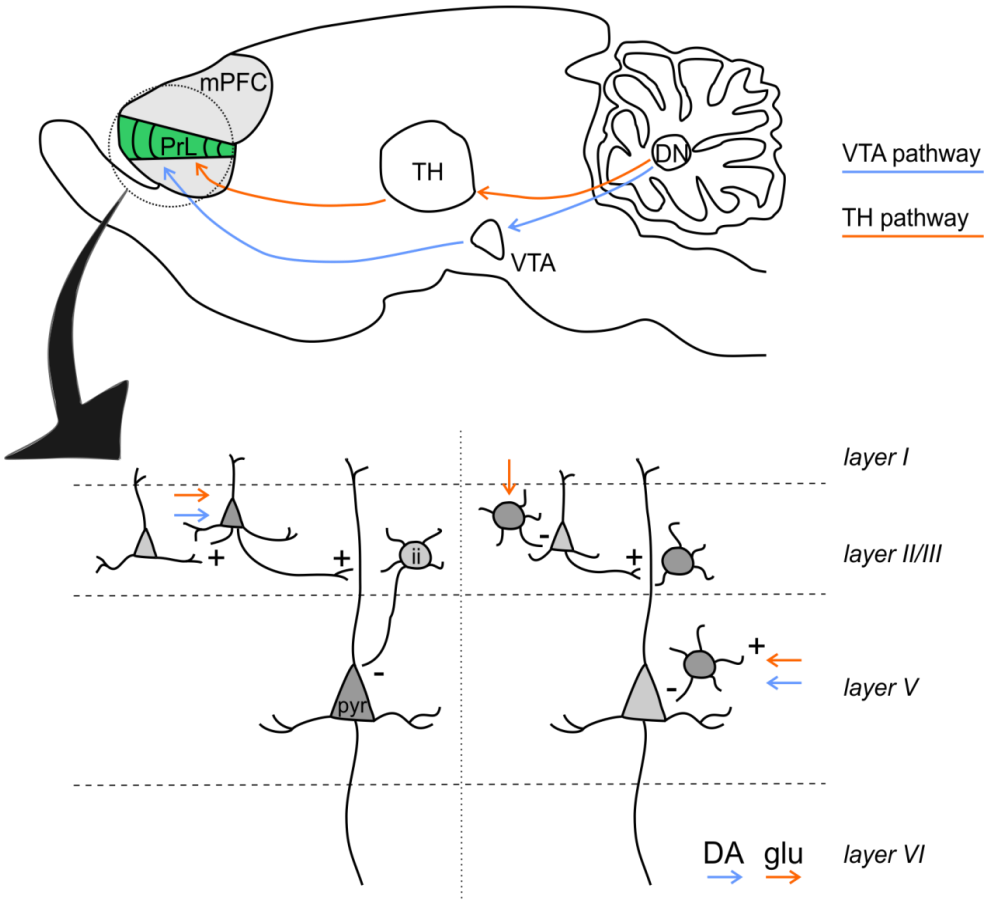

Figure 11. Cerebellar pathways involved in PrL neurons activity. *Two main pathways connect the cerebellum to PrL: the one passing through the VTA (mainly dopaminergic, blue) and the one passing through the thalamus (TH, glutamatergic, red). Both pathways reach PrL neurons at the level of layers III or V, influencing excitation/inhibition balance, as represented in the bottom scheme.*

Dark grey represents high levels of activity, vs the light grey that indicates reduced or lower ativity (redrawn from Ferguson and Gao, 2018)

Tracing studies identified bilateral projections from VTA that are directed either to mPFC or to DN and interposed cerebellar nuclei, but not to FN, with a contralateral predominance (Ikai et al. 1992). Moreover, the discovery that VTA contains GABAergic neurons projecting to the mPFC (Hnasko et al. 2012; Omelchenko and Sesack 2009) might explain the contribution of cerebello-VTA pathway to the observed inhibitory responses in PrL following DN stimulation. Hovewer, since VTA is not reached by FN projections, this explanation is not valid for PrL responses to FN stimulation. The GABAergic projections from the VTA might then represent a possible candidate involved in the inhibitory response pattern detected in PrL units by DN stimulation, although the exclusive contribution of this pathway to PrL responses is unlikely believable. Therefore, inhibitory pattern of responses in PrL following both FN and DN stimulation might be evoked via thalamic pathway indirectly promoting pyramidal neurons inhibition through local inhibitory interneurons activation. The FN lies in the white matter of vermal lobule VII, a cerebellar region notoriously involved in ocular adaptation and movements. Thalamus represents the intermediate station relaying cerebellar motor-sensory information to higher functioning brain areas. It seems reasonable then to assume that the connection between FN and associative brain regions, such as the PrL, passing through the thalamus takes part into the control of eye movements in goal-directed behaviour instead of cognitive information processing *per se*.

Conversely, DN connection with both VTA and MD thalamus suggests that these pathways are more likely directly involved in cognitive functions. In particular, the prominent MD innervations over mPFC notably play a fundamental role in cognitive processes (Parnaudeau et al., 2018). Remarkably, reduction of inhibition/excitation balance in mPFC due to the increase in cortical interneurons excitability is reported to impair working memory, cognitive flexibility and social interaction (Ferguson and Gao, 2018). Since our data support the idea that

cerebellar stimulation provides inhibition of PrL neurons activity, it is reasonable to consider the cerebellum as involved in the regulation of inhibition/excitation balance in the cortical network. Hence, the functional role of the cerebellum in cognition gains a prominent value considering the global effects exerted by inhibitory pathways over mPFC correct functioning.

5.5 Conclusions

Our findings show effective interactions between the cerebellum and the PrL of the mPFC, providing insights of a functional interplay between these two regions. The presented results suggested the existence of two response patterns among the PrL neurons that receive functional connection from the cerebellum. Our data confirm that dopaminergic release, that might be also induced through the cerebellar-VTA pathway, has a role in modulating PrL neurons spiking. The suppression of both types of responses in PrL neurons following $GABA_A$ receptors antagonist perfusion demonstrated that cerebellar influence over mPFC involves the activation of inhibitory neurons, presumably local cortical interneurons activated thorugh the thalamic pathway. Indeed, the disruption of correct excitation/inhibition balance in mPFC is reported to be determinant in various cognitive disorders. Certainly, the finding of GABAergic neurons in VTA projecting to the mPFC (Hnasko et al. 2012; Omelchenko and Sesack 2009) complicates the picture, making more difficult to clearly discern dopaminergic and thalamic pathways, suggesting complex mechanism through which cerebellar stimulation affects cortical neuronal acivity.

Further analysis is required to investigate the influence of cerebellar stimulation and application of D1/D2-like and GABA antagonists on rhythmic firing between PrL cells. Autocorrelation analysis might be useful to investigate changes in PrL neuros rhythmic firing not only during cerebellar stimulation and drugs perfusion but also to investigate putative effects over cortical up-down states linked to the anesthesia. Moreover, the performance of simultaneous recordings

from multiple units allows cross-correlation analysis for possible network rhythmicity linked to cerebellar stimulation.

The present study shows that the cerebellum may have indeed a prominent role in regulating activity of cortical areas involved in cognitive functions and provides new insights for understanding neuronal mechanisms underlying cognitive processes related to cerebello-prefrontal interactions. However, although electrical stimulation is widely employed in brain research, it has to be considered that it might lack specificity, due to current spread and *en passant* fiber activation, and its effect might be associated with either modifications in local neural activity as well as changes spreading within the entire neural network (Trevathan et al. 2018).

For these reasons, the next step in the characterization of cerebello-prefrontal physiological interaction should include optogenetics. The virally-driven expression of light-sensitive ionic channels specifically onto cerebellar projections to MD thalamus or VTA, would allow the selective activation of separate cerebellar pathways involved in modulation of mPFC activity, thus giving a better characterization of the cerebellar role in cognitive processes and overall brain functioning.

Additional information

Acknowledgments. This project/research received funding from the European Union's Horizon 2020 Framework Program for Research and Innovation under the Specific Grant Agreement No. 785907 (Human Brain Project SGA2) to ED; Blue-Sky Research grant of the University of Pavia (Università degli Studi di Pavia; BSR77992) to LiM.

Author Contributions. IM performed recordings using D1/D2-like receptor antagonists, the entire set of recordings with gabazine, data analysis and wrote the manuscript; LeM performed the initial recordings, pharmacology with selective D1/D2-like receptor antagonist, and data analysis; ST performed histology and

image analysis; LiM and ED coordinated the work, wrote the manuscript and approved the final version of the manuscript.

Conflict of Interest Statement. The authors declare that the research was conducted in the absence of any personal, professional or financial relationship that could be constructed as a potential conflict of interest.

Chapter 6

General discussion

Over the years, a large number of studies thoroughly described the role of the cerebellum in learning and memory of sensory-motor information. It is a general assumption to consider long-term modifications in the strength of synaptic transmission, in terms of potentiation (LTP) or depression (LTD), together with increase or decrease in neuronal intrinsic excitability, as the biological basis for learning in the neuronal circuits. Initially, the principal mechanism for cerebellar motor learning was assumed to reside in LTD at parallel fiber-Purkinje cell (PF-PC) synapse, controlled by theaching signals originating from the climbing fibers (CFs) (Albus 1971b; Marr and D. 1969). Nevertheless, the idea that a single form of plasticity at a single synapse is sufficient to explain the cerebellar motor learning was recently revised in order to support the existence of a more complex picture in cerebellar learning involving various forms of long-term plasticity not confined to the sole cerebellar cortex (D'Angelo et al. 2016a). Indeed, further investigations revealed the existence of several forms of synaptic and non-synaptic plasticity in the cerebellum both *in vivo* and *in vitro* (D'Angelo 2014; Gao et al. 2012; Mapelli et al., 2015). In agreement with experimental observations, computational models accounting for plastic changes at the level of deep

cerebellar nuclei (DCN) show faster and more stable learning capabilities compared to previous models with only cortical plasticity sites. This finding provides a more realistic reproduction of human-like behavior during cerebellar learning of associative task, enlighting the crucial role of DCN neurons in cerebellar functioning (Antonietti et al. 2016a). Both LTP and LTD have been described in the inhibitory synapses between PCs and DCN neurons and in the excitatory synapses between MFs and DCN *ex vivo* (Medina and Mauk 1999; Morishita and Sastry 1996; Ouardouz and Sastry 2000; Pugh and Raman 2009; Zhang and Linden 2006). Moreover, the presence of persistent changes in the intrinsic excitability of nuclear neurons has also been described (Zhang et al. 2004).

Despite plasticity in cerebellar cortical neurons has been investigated in detail over the years, the capability of DCN neurons to modify their discharge properties in response to patterned sensory stimulation were still under debate. Previous studies reported that sensory tactile stimuli delivered in theta patterns (TSS) in anesthetized mice were able to induce long-term changes in cerebellar granule cells (Roggeri et al. 2008), PCs and molecular layer interneurons (Ramakrishnan et al. 2016). One of the aims of this thesis project was the investigation of putative changes underlying DCN neurons capability to integrate sensory information. We showed that TSS is able to evoke several discharge patterns in DCN neurons *in vivo*, likely depending on the synaptic pathways engaged by the stimulation. Moreover, our results show that long-lasting changes detected in DCN following TSS were related to oscillations in the theta frequency range. Our findings provide the first evidence that DCN neurons are able to modify their discharge properties following a patterned sensory stimulation, thus giving a more detailed description of the mechanisms involved in cerebellar sensory integration *in vivo*.

In the second part of this work we investigated the potential contribution of the cerebellum to neocortical processing, starting from the considerable amount of studies providing evidence of the interconnection between the cerebellum and

cerebral associative areas of the brain, such as the medial prefrontal cortex (mPFC). The integral tractographic reconstruction of human cerebellar projections originating from the DCN and passing through the superior cerebellar peduncle showed a prominent cerebello-prefrontal cortex connection (Palesi et al. 2015). The same conclusion was sustained by *in vivo* electrophysiological studies in rodents reporting a bidirectional functional connection between these brain regions (Watson et al. 2014; Watson et al. 2009). Moreover, clinical studies support the hypothesis of a cerebellar role in cognitive function following the observation that cerebellar abnormalities are related to several cognitive dysfunctions. Despite this recent interest in cerebello-prefrontal connections, the cerebellar role in mPFC functioning is still highly neglected in the majority of investigations (Laubach et al. 2018, Fig 6.1).

Figure 6.1| Research focus on publication on the prefrontal cortex. *Wordcloud with functional color grouping for papers published on the PFC of mice, rats, mokeys and umans since 2000. Orange=anatomical terms; Purple=pharmacological terms; Blue=diseases and other medical conditions; Green= psychological constructs; Red=other terms. Note that the cerebellum is missing. (Laubach et. al.2018).*

Following these observations, we characterized neuronal responses in the prelimbic region (PrL) of the mPFC, during electrical stimulation of DCN in anesthetized mice.

In particular, a pharmacological approach allowed to explore whether and how PrL neurons spontaneous and evoked activities are influenced by different

pathways driven by cerebellar activation. Our results suggest that the cerebellum may exert a crucial role in regulating mPFC activity, by controlling the level of excitation/inhibition in mPFC circuitry and presumably the intrinsic excitability of cortical neurons. Herein, our findings demonstrate the existence of physiological interactions between the cerebellum and the PrL of the mPFC, thus allowing to speculate that the functional interplay between these two regions might have indeed an important role in cognition. Importantly, cerebellar activation seems to preferentially lead to mPFC inhibition. The understanding of neuronal correlates underlying cerebello-prefrontal connectivity might explain the involvement of cerebellar abnormalities in various cognitive deficits.

Overall, the findings reported in this thesis provide new insights for understanding DCN role in cerebellar functioning and in driving PrL neurons activity. As reported in chapter 4, DCN neurons are able to modify their responsiveness following sensory stimulation, depending on stimulus-induced oscillations. These results are relevant not only for understanding cerebellar functioning itself, but also for understanding cerebellar contribution to higher order cognitive processes. Indeed, the results described in chapter 5 provide strong evidence of a cerebellar drive over neuronal activity in PrL, presumably involving both the dopaminergic neuromodulatory system and the thalamic glutamatergic system activating cortical interneurons. Therefore, it is evident that the cerebellum should be considered as an important contributor to general brain processing, including higher order cognitive functions, going beyond its role in the sensori-motor system.

Further investigations on physiological cerebello-prefrontal interactions should include the application of optogenetics in order to specifically address the impact of cerebello-thalamic pathway and cerebello-VTA pathway onto mPFC activity. The viral-induced expression of opsins in cerebellar axons projecting to other brain areas would allow their selective photostimulation and recording from the mPFC *in vivo* in both anesthetized and awake animals, thus ensuring the

detection of responses elicited by specific stimulation of afferent projections thorugh different pathways.

Moreover, considering the amount of studies reporting abnormal cerebello-prefrontal interaction in several cognitive disorders such as autism and schizophrenia (Schmahmann 2004, D'Angelo and Casali 2012), it would be interesting to investigate the contribution of each cerebellar pathway onto mPFC in both normal and pathological condition in animal models. The IB2 (Islet Brain 2)-KO mouse model of autism could represent a good starting point since its behavioral deficits reminiscent of Phela-McDermid syndrome are proved to be linked to alterations in cerebellar morphology and synaptic transmission (Giza et al., 2010). *In vivo* recordings of mPFC neurons activity during activation of cerebellar afferents to thalamus or VTA might represent a good approach to give better insights into the pathophysiology of cognitive impairments related to cerebellar dysfunction. Pharmacological tools might be employed to analyze the impact of cerebellum-mediated release of neurotrasmitters and neuromodulators in mPFC in both normal and pathological conditions.

Moreover, starting from the observation that cerebellar stimulation can be used to rescue neural mechanisms underlying cognition and alleviate symptoms in epilepsy (Cooper et al. 1976) and schizophrenia (Demirtas-Tatlidede et al., 2010) patients, another interesting approach in studying cerebellar contribution to autism might be represented by cerebellar stimulation in awake, freely-behaving animals. Once again, optogenetics could represent the finest tool to specifically stimulate the cerebellar ciruit either at the level of the cortex or DCN, in such a way to restore cerebellar physiological activity and see if cerebellar stimulation in autistic mice models is able to elicit evident impact on their behaviour.

In conclusion, the cerebellar contribution in cortical activity has been demonstrated to represent a crucial component in processes of sensation, movement and cognition, thus enlighting the needing of further investigation in cerebellar physiology and interaction with other cortical areas in order to better understand overall brain function.

References

Albus JS. A theory of cerebellar function. *Math Biosci 10, 25-61* 1971b.

Alviña K, Walter J, Kohn A, Ellis-Davies G, and Khodakhah K. Questioning the role of rebound firing in the cerebellum. *Nat Neurosci* 11: 1256-1258, 2008.

Alitto H. J., Usrey W. M. (2003). Corticothalamic feedback and sensory processing. Curr. Opin. Neurobiol. 13, 440–445.

Ambrosi G, Flace P, Lorusso L, Girolamo F, Rizzi A, Bosco L, Errede M, Virgintino D, Roncali L, and Benagiano V. Non-traditional large neurons in the granular layer of the cerebellar cortex. *Eur J Histochem* 51 Suppl 1: 59-64, 2007.

Andreasen NC, O'Leary DS, Cizadlo T, Arndt S, Rezai K, Ponto LL, Watkins GL, and Hichwa RD. Schizophrenia and cognitive dysmetria: a positron-emission tomography study of dysfunctional prefrontal-thalamic-cerebellar circuitry. *Proc Natl Acad Sci U S A* 93: 9985-9990, 1996.

Andreasen NC, and Pierson R. The role of the cerebellum in schizophrenia. *Biol Psychiatry* 64: 81-88, 2008.

Ankri L, Husson Z, Pietrajtis K, Proville R, Lena C, Yarom Y, Dieudonne S, and Uusisaari MY. A novel inhibitory nucleo-cortical circuit controls cerebellar Golgi cell activity. *Elife* 4: 2015.

Antonietti A, Casellato C, Garrido JA, Luque NR, Naveros F, Ros E, D' Angelo E, and Pedrocchi A. Spiking Neural Network With Distributed Plasticity Reproduces Cerebellar Learning in Eye Blink Conditioning Paradigms. *IEEE Trans Biomed Eng* 63: 210-219, 2016a.

Antonietti A, Casellato C, Garrido JA, Luque NR, Naveros F, Ros E, E DA, and Pedrocchi A. Spiking Neural Network With Distributed Plasticity Reproduces Cerebellar Learning in Eye Blink Conditioning Paradigms. *IEEE Trans Biomed Eng* 63: 210-219, 2016b.

Apps R, and Hawkes R. Cerebellar cortical organization: a one-map hypothesis. *Nat Rev Neurosci* 10: 670-681, 2009.

Ascoli G. A., Alonso-Nanclares L., Anderson S. A., Barrionuevo G., Benavides-Piccione R., Burkhalter A., et al. (2008). Petilla terminology: nomenclature of features of GABAergic interneurons of the cerebral cortex. Nat. Rev. Neurosci. 9, 557–568.

Armano S, Rossi P, Taglietti V, and D'Angelo E. Long-term potentiation of intrinsic excitability at the mossy fiber-granule cell synapse of rat cerebellum. *J Neurosci* 20: 5208-5216, 2000.

Attwell PJE, Rahman S, and Yeo CH. Acquisition of Eyeblink Conditioning Is Critically Dependent on Normal Function in Cerebellar Cortical Lobule HVI. *The Journal of Neuroscience* 21: 5715-5722, 2001.

Bagnall M. W., du Lac S. (2006). A new locus for synaptic plasticity in cerebellar circuits. Neuron 51, 5–7.

Bagnall MW, Zingg B, Sakatos A, Moghadam SH, Zeilhofer HU, and du Lac S. Glycinergic projection neurons of the cerebellum. *J Neurosci* 29: 10104-10110, 2009.

Bengtsson F, and Jorntell H. Ketamine and xylazine depress sensory-evoked parallel fiber and climbing fiber responses. *J Neurophysiol* 98: 1697-1705, 2007.

Bohne P., Scwarz MK, Herlitze S, Mark MD. A new projection from the deep cerebellar nuclei to the hippocampus via the Ventrolateral and Laterodorsale thalamus in mice. Front Neural circuit 2019 Aug 9; 13:51.

Bosman LW, Koekkoek SK, Shapiro J, Rijken BF, Zandstra F, van der Ende B, Owens CB, Potters JW, de Gruijl JR, Ruigrok TJ, and De Zeeuw CI. Encoding of whisker input by cerebellar Purkinje cells. *J Physiol* 588: 3757-3783, 2010.

Bower JM, and Woolston DC. Congruence of spatial organization of tactile projections to granule cell and Purkinje cell layers of cerebellar hemispheres of the albino rat: vertical organization of cerebellar cortex. *J Neurophysiol* 49: 745-766, 1983.

Boyden ES, Zhang F, Bamberg E, Nagel G, Deisseroth K. Millisecond-timescale, genetically targeted optical control of neural activity. Nature neuroscience, 2005. 8(9): p. 1263–8.

Brincat SL, Miller EK. Prefrontal Cortex Networks Shift from External to Internal Modes during Learning. J Neurosci. 2016;36(37):9739–54

Britt J. P., Benaliouad F., McDevitt R. A., Stuber G. D., Wise R. A., Bonci A. (2012). Synaptic and behavioral profile of multiple glutamatergic inputs to the nucleus accumbens.

Buchta WC, Mahler SV, Harlan B, Aston-Jones GS, and Riegel AC. Dopamine terminals from the ventral tegmental area gate intrinsic inhibition in the prefrontal cortex. *Physiol Rep* 5: 2017.

Buzsaki G. *Rhythms of the brain*. New York: Oxford University Press US, 2006.

Buzsaki G. Theta rhythm of navigation: link between path integration and landmark navigation, episodic and semantic memory. *Hippocampus* 15: 827-840, 2005.

Caligiore D, Pezzulo G, Baldassarre G, Bostan AC, Strick PL, Doya K, Helmich RC, Dirkx M, Houk J, Jörntell H, Lago-Rodriguez A, Galea JM, Miall RC, Popa T, Kishore A, Verschure PF, Zucca R, and Herreros I. Consensus Paper: Towards a Systems-Level View of Cerebellar Function: the Interplay Between Cerebellum, Basal Ganglia, and Cortex. *Cerebellum* 16: 203-229, 2017.

Canto CB, Witter L, and De Zeeuw CI. Whole-Cell Properties of Cerebellar Nuclei Neurons In Vivo. *PLoS One* 11: e0165887, 2016.

Cao Y., Maran S. K., Dhamala M., Jaeger D., Heck D. H. (2012). Behavior-related pauses in simple-spike activity of mouse Purkinje cells are linked to spike rate modulation. *J. Neurosci.* 32 8678–8685.

Carta I., Chen C.H., Schott A.L., Dorizan S., Khodakhah K. Cerebellar modulation of the reward circuitry and social behavior. Science. 2019;363

Casellato C, Antonietti A, Garrido JA, Carrillo RR, Luque NR, Ros E, Pedrocchi A, and D'Angelo E. Adaptive robotic control driven by a versatile spiking cerebellar network. *PLoS One* 9: e112265, 2014.

Casellato C, Antonietti A, Garrido JA, Carrillo RR, Luque NR, Ros E, Pedrocchi A, and D'Angelo E. Distributed cerebellar plasticity implements generalized multiple-scale memory components in real-robot sensorimotor tasks. *Front Comput Neurosci* in press: 2015.

Chadderton P, Margrie TW, and Häusser M. Integration of quanta in cerebellar granule cells during sensory processing. *Nature* 428: 856-860, 2004.

Chen H, Wang Y, Yang L, Sui J, Hu Z, Hu B. Theta synchronization between medial prefrontal cortex and cerebellum is associated with adaptive performance of associative learning behavior. Sci. Rep. 2016;6:20960.

Chen X, Kovalchuk Y, Adelsberger H, Henning HA, Sausbier M, Wietzorrek G, Ruth P, Yarom Y, and Konnerth A. Disruption of the olivo-cerebellar circuit by Purkinje neuron-specific ablation of BK channels. *Proc Natl Acad Sci U S A* 107: 12323-12328, 2010.

Cheron G, Marquez-Ruiz J, and Dan B. Oscillations, Timing, Plasticity, and Learning in the Cerebellum. *Cerebellum* 15: 122-138, 2016.

Cheron J, and Cheron G. Beta-gamma burst stimulations of the inferior olive induce high-frequency oscillations in the deep cerebellar nuclei. *Eur J Neurosci* 2018.

Cruikshank S. J., Ahmed O. J., Stevens T. R., Patrick S. L., Gonzalez A. N., Elmaleh M., et al. (2012). Thalamic control of layer 1 circuits in prefrontal cortex. J. Neurosci. 32, 17813–17823.

Contreras D, Timofeev I, Steriade M. Mechanisms of long-lasting hyperpolarizations underlying slow sleep oscillations in cat corticothalamic networks. The Journal of Physiology. 1996;494 (Pt 1):251–264.

Cooper IS, Amin I, Riklan M, Waltz JM, Poon TP. Chronic cerebellar stimulation in epilepsy. Clinical and anatomical studies. Arch Neurol (1976)

Cornew L, Roberts TPL, Blaskey L, Edgar JC. Resting-state oscillatory activity in autism spectrum disorders. J. Autism Dev. Disord. 2012;42:1884–1894,

Courtemanche R, Robinson JC, Aponte DI. Linking oscillations in cerebellar circuits. Front Neural Circuits 7:125, 2013.

Cunningham MO, Pervouchine DD, Racca C, Kopell NJ, Davies CH, Jones RS, Traub RD, Whittington MA. Neuronal metabolism governs cortical network response state. PNAS. 2006;103:5597–5601.

D'Angelo E. The organization of plasticity in the cerebellar cortex: from synapses to control. *Prog Brain Res* 210: 31-58, 2014.

D'Angelo E, Antonietti A, Casali S, Casellato C, Garrido JA, Luque NR, Mapelli L, Masoli S, Pedrocchi A, Prestori F, Rizza MF, and Ros E. Modeling the Cerebellar Microcircuit: New Strategies for a Long-Standing Issue. *Front Cell Neurosci* 10: 176, 2016a.

D'Angelo E, and Casali S. Seeking a unified framework for cerebellar function and dysfunction: from circuit operations to cognition. *Front Neural Circuits* 6: 116, 2012.

D'Angelo E, and De Zeeuw CI. Timing and plasticity in the cerebellum: focus on the granular layer. *Trends Neurosci* 32: 30-40, 2009.

D'Angelo E, Koekkoek SK, Lombardo P, Solinas S, Ros E, Garrido J, Schonewille M, De Zeeuw CI. Timing in the cerebellum: oscillations and resonance in the granular layer. Neuroscience. 2009;162:805–815.

D'Angelo E, Mapelli L, Casellato C, Garrido JA, Luque N, Monaco J, Prestori F, Pedrocchi A, and Ros E. Distributed Circuit Plasticity: New Clues for the Cerebellar Mechanisms of Learning. *Cerebellum* 15: 139-151, 2016b.

David F, Schmiedt JT, Taylor HL, Orban G, Di Giovanni G, Uebele VN, Renger JJ, Lambert RC, Leresche N, Crunelli V. Essential thalamic contribution to slow waves of natural sleep. Journal of Neuroscience. 2013;33:19599–19610.

DeFelipe J., Lógaopez-Cruz P. L., Benavides-Piccione R., Bielza C., Larrañaga P., Anderson S., et al. . (2013). New insights into the classification and nomenclature of cortical GABAergic interneurons. Nat. Rev. Neurosci. 14, 202–216.

Deisseroth K. Optogenetics. Nat Methods. 2011;8:26–29

Dembrow N, and Johnston D. Subcircuit-specific neuromodulation in the prefrontal cortex. *Front Neural Circuits* 8: 54, 2014.

Demirtas-Tatlidede A, Freitas C, Cromer JR, Safar L, Ongur D, Stone WS, et al. Safety and proof of principle study of cerebellar vermal theta burst stimulation in refractory schizophrenia. Schizophr Res (2010) 124:91

Devor A, Yarom Y. GABAergic modulation of olivary oscillations. In: Gerrits N, Ruigrok T, De Zeeuw CI, editors. Cerebellar Modules: Molecules, Morphology and Function. Elsevier; 2000. pp. 213–220.

De Zeeuw CI, Hoogenraad CC, Koekkoek SKE, Ruigrok TJH, Galjart N, Simpson JI. Microcircuitry and function of the inferior olive. Trends Neurosci. 1998;21:391–400

Diwakar S, Lombardo P, Solinas S, Naldi G, and D'Angelo E. Local field potential modeling predicts dense activation in cerebellar granule cells clusters under LTP and LTD control. *PLoS One* 6: e21928, 2011.

Douglas R. J., Martin K. A. (2004). Neuronal circuits of the neocortex. *Annu. Rev. Neurosci.* 27 419–451.

Dykstra S, Engbers JD, Bartoletti TM, and Turner RW. Determinants of rebound burst responses in rat cerebellar nuclear neurons to physiological stimuli. *J Physiol* 594: 985-1003, 2016.

Ekerot CF, and Jorntell H. Parallel fibre receptive fields of Purkinje cells and interneurons are climbing fibre-specific. *Eur J Neurosci* 13: 1303-1310, 2001.

Engel TA, Steinmetz NA, Gieselmann MA, Thiele A, Moore T, Boahen K. Selective modulation of cortical state during spatial attention. Science. 2016;354:1140–1144.

Fatemi SH, Aldinger KA, Ashwood P, Bauman ML, Blaha CD, Blatt GJ, Chauhan A, Chauhan V, Dager SR, Dickson PE, Estes AM, Goldowitz D, Heck DH, Kemper TL, King BH, Martin LA, Millen KJ, Mittleman G, Mosconi MW, Persico AM, Sweeney JA, Webb SJ, and Welsh JP. Consensus paper: pathological role of the cerebellum in autism. *Cerebellum* 11: 777-807, 2012.

Ferguson B. R., Gao W. J. (2018). PV interneurons: critical regulators of E/I balance for prefrontal cortex-dependent behavior and psychiatric disorders. *Front. Neural Circuits* 12:37.

Ferguson BR, Gao W-J. (2018) Thalamic Control of Cognition and Social Behavior Via Regulation of Gamma-Aminobutyric Acidergic Signaling and Excitation/Inhibition Balance in the Medial Prefrontal Cortex. Biological psychiatry. 2018;83:657–669.

Floresco SB, Grace AA. Gating of hippocampal-evoked activity in prefrontal cortical neurons by inputs from the mediodorsal thalamus and ventral tegmental area. J Neurosci. 2003;23:3930–3943.

Floresco SB, and Magyar O. Mesocortical dopamine modulation of executive functions: beyond working memory. *Psychopharmacology (Berl)* 188: 567-585, 2006.

Floresco SB, Magyar O, Ghods-Sharifi S, Vexelman C, and Tse MT. Multiple dopamine receptor subtypes in the medial prefrontal cortex of the rat regulate set-shifting. *Neuropsychopharmacology* 31: 297-309, 2006.

Gall D, Prestori F, Sola E, D'Errico A, Roussel C, Forti L, Rossi P, and D'Angelo E. Intracellular calcium regulation by burst discharge determines bidirectional long-term synaptic plasticity at the cerebellum input stage. *J Neurosci* 25: 4813-4822, 2005.

Gao Z, Davis C, Thomas AM, Economo MN, Abrego AM, Svoboda K, De Zeeuw CI, and Li N. A cortico-cerebellar loop for motor planning. *Nature* 2018.

Gao Z, Proietti-Onori M, Lin Z, Ten Brinke MM, Boele HJ, Potters JW, Ruigrok TJ, Hoebeek FE, and De Zeeuw CI. Excitatory Cerebellar Nucleocortical Circuit Provides Internal Amplification during Associative Conditioning. *Neuron* 89: 645-657, 2016.

Gao Z, van Beugen BJ, and De Zeeuw CI. Distributed synergistic plasticity and cerebellar learning. *Nat Rev Neurosci* 13: 619-635, 2012.

Garrido JA, Luque NR, D'Angelo E, and Ros E. Distributed cerebellar plasticity implements adaptable gain control in a manipulation task: a closed-loop robotic simulation. *Front Neural Circuits* 7: 159, 2013.

Gaspar P, Bloch B, and Le Moine C. D1 and D2 receptor gene expression in the rat frontal cortex: cellular localization in different classes of efferent neurons. *Eur J Neurosci* 7: 1050-1063, 1995.

Giza J, Urbanski MJ, Prestori F, Bandyopadhyay B, Yam A, Friedrich V, Kelley K, D'Angelo E, and Goldfarb M. Behavioral and cerebellar transmission deficits in mice lacking the autism-linked gene islet brain-2. *J Neurosci* 30: 14805-14816, 2010.

Godaux E, Cheron G, and Mettens P. Ketamine induces failure of the oculomotor neural integrator in the cat. *Neurosci Lett* 116: 162-167, 1990.

Gowen E, and Miall RC. The cerebellum and motor dysfunction in neuropsychiatric disorders. *Cerebellum* 6: 268-279, 2007.

Gradinaru V, Zhang F, Ramakrishnan C, Mattis J, Prakash R, Diester I, Goshen I, Thompson KR, Deisseroth K . Molecular and cellular approaches for diversifying and extending optogenetics. Cell. 2010;141:154–165.

Grishkat HL, and Eisenman LM. Development of the spinocerebellar projection in the prenatal mouse. *J Comp Neurol* 363: 93-108, 1995.

Gruart A, Guillazo-Blanch G, Fernandez-Mas R, Jimenez-Diaz L, and Delgado-Garcia JM. Cerebellar posterior interpositus nucleus as an enhancer of classically conditioned eyelid responses in alert cats. *J Neurophysiol* 84: 2680-2690, 2000.

Gulledge AT, and Jaffe DB. Dopamine decreases the excitability of layer V pyramidal cells in the rat prefrontal cortex. *J Neurosci* 18: 9139-9151, 1998.

Guo A, Feng JY, Li J, Ding N, Li YJ, Qiu DL, Piao RL, and Chu CP. Effects of norepinephrine on spontaneous firing activity of cerebellar Purkinje cells in vivo in mice. *Neurosci Lett* 629: 262-266, 2016.

Hansel C, Linden DJ, and D'Angelo E. Beyond parallel fiber LTD: the diversity of synaptic and non-synaptic plasticity in the cerebellum. *Nat Neurosci* 4: 467-475, 2001a.

Hansel C, Linden DJ, and D'Angelo E. Beyond parallel fiber LTD: the diversity of synaptic and nonsynaptic plasticity in the cerebellum. *Nature Neuroscience* 4: 467-475, 2001b.

Hara K, and Harris RA. The anesthetic mechanism of urethane: the effects on neurotransmitter-gated ion channels. *Anesth Analg* 94: 313-318, table of contents, 2002.

Heidbreder C. A., Groenewegen H. J. (2003). The medial prefrontal cortex in the rat: evidence for a dorso-ventral distinction based upon functional and anatomical characteristics. Neurosci. Biobehav. Rev. 27, 555–579

Heinricher MM. *Principles of Extracellular Single-Unit Recording*. Thieme Verlagsgruppe, Stuttgart, New York, Delhi, Rio, 2004.

Herzfeld D. J., Kojima Y., Soetedjo R., Shadmehr R. (2015). Encoding of action by the Purkinje cells of the cerebellum. *Nature* 526 439–442.

Henze R, Brunner R, Thiemann U, Parzer P, Richterich A, Essig M, Resch F, and Stieltjes B. Gray matter alterations in first-admission adolescents with schizophrenia. *J Neuroimaging* 21: 241-246, 2011.

Hnasko TS, Hjelmstad GO, Fields HL, and Edwards RH. Ventral tegmental area glutamate neurons: electrophysiological properties and projections. *J Neurosci* 32: 15076-15085, 2012.

Hoebeek FE, Witter L, Ruigrok TJ, and De Zeeuw CI. Differential olivo-cerebellar cortical control of rebound activity in the cerebellar nuclei. *Proc Natl Acad Sci U S A* 107: 8410-8415, 2010.

Hoover WB, and Vertes RP. Anatomical analysis of afferent projections to the medial prefrontal cortex in the rat. *Brain Struct Funct* 212: 149-179, 2007.

Houck BD, and Person AL. Cerebellar loops: a review of the nucleocortical pathway. *Cerebellum* 13: 378-385, 2014.

Hübner C., Bosch D., Gall A., Lüthi A., Ehrlich I. (2014). Ex vivo dissection of optogenetically activated mPFC and hippocampal inputs to neurons in the basolateral amygdala: implications for fear and emotional memory. Front. Behav. Neurosci. 8:64

Humeau Y., Herry C., Kemp N., Shaban H., Fourcaudot E., Bissiere S., et al. . (2005). Dendritic spine heterogeneity determines afferent-specific Hebbian plasticity in the amygdala. Neuron 45, 119–131.

Ikai Y, Takada M, Shinonaga Y, and Mizuno N. Dopaminergic and non-dopaminergic neurons in the ventral tegmental area of the rat project, respectively, to the cerebellar cortex and deep cerebellar nuclei. *Neuroscience* 51: 719-728, 1992.

Ito M. Control of mental activities by internal models in the cerebellum. Nat. Rev. Neurosci. 9, 304–313; 2008.

Ito M. Neural design of the cerebellar motor control system. *Brain Res* 40: 81-84, 1972.

Jacobson GA, Rokni D, and Yarom Y. A model of the olivo-cerebellar system as a temporal pattern generator. *Trends Neurosci* 31: 617-625, 2008.

Jahnsen H. Electrophysiological characteristics of neurones in the guinea-pig deep cerebellar nuclei in vitro. *J Physiol* 372: 129-147, 1986a.

Jahnsen H. Extracellular activation and membrane conductances of neurones in the guinea-pig deep cerebellar nuclei in vitro. *J Physiol* 372: 149-168, 1986b.

Jercog D, Roxin A, Barthó P, Luczak A, Compte A, de la Rocha J. UP-DOWN cortical dynamics reflect state transitions in a bistable balanced network. eLife. 2017;p. e22425

Jirenhed DA, Bengtsson F, and Hesslow G. Acquisition, extinction, and reacquisition of a cerebellar cortical memory trace. *J Neurosci* 27: 2493-2502, 2007.

John ER. The neurophysics of consciousness. Brain Res Rev. 2002;39:1–28.

Jörntell H, and Ekerot CF. Reciprocal bidirectional plasticity of parallel fiber receptive fields in cerebellar Purkinje cells and their afferent interneurons. *Neuron* 34: 797-806, 2002.

Kansal K, Yang Z, Fishman AM, Sair HI, Ying SH, Jedynak BM, Prince JL, and Onyike CU. Structural cerebellar correlates of cognitive and motor dysfunctions in cerebellar degeneration. *Brain* 140: 707-720, 2017.

Kassel J, Shambes GM, and Welker W. Fractured cutaneous projections to the granule cell layer of the posterior cerebellar hemisphere of the domestic cat. *J Comp Neurol* 225: 458-468, 1984.

Kehr W, Lindqvist M, and Carlsson A. Distribution of dopamine in the rat cerebral cortex. *J Neural Transm* 38: 173-180, 1976.

Kelly R. M., Strick P. L.. Cerebellar loops with motor cortex and prefrontal cortex of a nonhuman primate. *J. Neurosci.* 23 8432–8444, 2003

Kishore A, Meunier S, and Popa T. Cerebellar influence on motor cortex plasticity: behavioral implications for Parkinson's disease. *Front Neurol* 5: 68, 2014.

Kistler W, De Zeeuw C. Gap junctions synchronize synaptic input rather than spike output of olivary neurons. In: De Zeeuw CI, Cicirata F, editors. Creating Coordination in the Cerebellum. Elsevier; 2005. pp. 189–197.

Kistler WM, and De Zeeuw CI. Time windows and reverberating loops: a reverse-engineering approach to cerebellar function. *Cerebellum* 2: 44-54, 2003.

Koekkoek SK, Den Ouden WL, Perry G, Highstein SM, and De Zeeuw CI. Monitoring kinetic and frequency-domain properties of eyelid responses in mice with magnetic distance measurement technique. *J Neurophysiol* 88: 2124-2133, 2002.

Konarski JZ, McIntyre RS, Grupp LA, and Kennedy SH. Is the cerebellum relevant in the circuitry of neuropsychiatric disorders? *J Psychiatry Neurosci* 30: 178-186, 2005.

Koziol L. F., Budding D., Andreasen N., D'Arrigo S., Bulgheroni S., Imamizu H., et al. Consensus paper: the cerebellum's role in movement and cognition. *Cerebellum* 13 151–177; 2014.

Kruse W, Krause M, Aarse J, Mark MD, Manahan-Vaughan D, and Herlitze S. Optogenetic modulation and multi-electrode analysis of cerebellar networks in vivo. *PLoS One* 9: e105589, 2014.

Kuljis RO, Rakic P. Distribution of neuropeptide Y-containing perikarya and axons in various neocortical areas in the macaque monkey. J Comp Neurol. 1989;280:383–392.

Kuroda M., Murakami K., Oda S., Shinkai M., Kishi K. (1993). Direct synaptic connections between thalamocortical axon terminals from the mediodorsal thalamic nucleus (MD) and corticothalamic neurons to MD in the prefrontal cortex. Brain Res. 612, 339–344.

Kuroda M., Murakami K., Igarashi H., Okada A. (1996). The convergence of axon terminals from the mediodorsal thalamic nucleus and ventral tegmental area on pyramidal cells in layer V of the rat prelimbic cortex. Eur. J. Neurosci. 8, 1340–1349.

Kurt S, Crook JM, Ohl FW, Scheich H, Schulze H. Differential effects of iontophoretic in vivo application of the GABA(A)-antagonists bicuculline and gabazine in sensory cortex. Hear Res. 2006;212(1-2):224–235.

Kvitsiani D., Ranade S., Hangya B., Taniguchi H., Huang J. Z., Kepecs A. (2013). Distinct behavioural and network correlates of two interneuron types in prefrontal cortex. Nature 498, 363–366.

Kyriakopoulos M, Vyas NS, Barker GJ, Chitnis XA, and Frangou S. A diffusion tensor imaging study of white matter in early-onset schizophrenia. *Biol Psychiatry* 63: 519-523, 2008.

Larouche M, Che PM, and Hawkes R. Neurogranin expression identifies a novel array of Purkinje cell parasagittal stripes during mouse cerebellar development. *J Comp Neurol* 494: 215-227, 2006.

Laubach M., Amarante L.M., Swanson K., White S.R, What, if anything, is rodent prefrontal cortex? *eNeuro 5(5) e0315-18. 2018.*

Lawyer G, Nesvåg R, Varnäs K, Okugawa G, and Agartz I. Grey and white matter proportional relationships in the cerebellar vermis altered in schizophrenia. *Cerebellum* 8: 52-60, 2009.

LeDoux MS, Hurst DC, and Lorden JF. Single-unit activity of cerebellar nuclear cells in the awake genetically dystonic rat. *Neuroscience* 86: 533-545, 1998.

Lee A. T., Gee S. M., Vogt D., Patel T., Rubenstein J. L., Sohal V. S. (2014a). Pyramidal neurons in prefrontal cortex receive subtype-specific forms of excitation and inhibition. Neuron 81, 61–68.

Lee A. T., Vogt D., Rubenstein J. L., Sohal V. S. (2014c). A class of GABAergic neurons in the prefrontal cortex sends long-range projections to the nucleus accumbens and elicits acute avoidance behavior. J. Neurosci. 34, 11519–11525.

Lemieux M, Chen JY, Lonjers P, Bazhenov M, Timofeev I. The impact of cortical deafferentation on the neocortical slow oscillation. Journal of Neuroscience. 2014;34:5689–5703.

Lisman J, Grace AA. The hippocampal-VTA loop:controlling the entry of information into long-term memory. Neuron 46, 703-713; 2005.

Little J. P., Carter A. G. (2012). Subcellular synaptic connectivity of layer 2 pyramidal neurons in the medial prefrontal cortex. J. Neurosci. 32, 12808–12819.

Little J. P., Carter A. G. (2013). Synaptic mechanisms underlying strong reciprocal connectivity between the medial prefrontal cortex and basolateral amygdala. J. Neurosci. 33, 15333–15342.

Llinas R, and Muhlethaler M. An electrophysiological study of the in vitro, perfused brain stem-cerebellum of adult guinea-pig. *J Physiol* 404: 215-240, 1988.

Llinás RR. Inferior olive oscillation as the temporal basis for motricity and oscillatory reset as the basis for motor error correction. Neuroscience. 2009;162(3):797–804.

Llinas RR. The intrinsic electrophysiological properties of mammalian neurons: insights into central nervous system function. *Science* 242: 1654-1664, 1988.

Lorente de No R. A study of nerve physiology. *Stud Rockefeller Inst Med Res Repr* 131: 1-496, 1947.

Luczak A, Barthó P, Marguet SL, Buzsáki G, Harris KD. Sequential structure of neocortical spontaneous activity in vivo. PNAS. 2007;104:347–352.

Luque NR, Garrido JA, Carrillo RR, D'Angelo E, and Ros E. Fast convergence of learning requires plasticity between inferior olive and deep cerebellar nuclei in a manipulation task: a closed-loop robotic simulation. *Front Comput Neurosci* 8: 97, 2014.

Mapelli J, and D'Angelo E. The spatial organization of long-term synaptic plasticity at the input stage of cerebellum. *J Neurosci* 27: 1285-1296, 2007.

Mapelli L, Gagliano G, Soda T, Laforenza U, Moccia F, and D'Angelo EU. Granular Layer Neurons Control Cerebellar Neurovascular Coupling Through an NMDA Receptor/NO-Dependent System. *J Neurosci* 37: 1340-1351, 2017.

Mapelli L, Pagani M, Garrido JA, and D'Angelo E. Integrated plasticity at inhibitory and excitatory synapses in the cerebellar circuit. *Front Cell Neurosci* 9: 169, 2015a.

Mapelli L, Pagani M, Garrido JA, and D'Angelo E. Integrated plasticity at inhibitory and excitatory synapses in the cerebellar circuit. *Front Cell Neurosci* 9: 2015b.

Marquez-Ruiz J, and Cheron G. Sensory stimulation-dependent plasticity in the cerebellar cortex of alert mice. *PLoS One* 7: e36184, 2012.

Marr, and D. A theory of cerebellar cortex. *J Physiol* 1969.

Marr D. A theory of cerebellar cortex. *J Physiol* 202: 437-470, 1969.

Marshall SP, and Lang EJ. Inferior olive oscillations gate transmission of motor cortical activity to the cerebellum. In: *J Neurosci*. United States: 2004, p. 11356-11367.

Masoli S., D'Angelo E. (2017). Synaptic activation of a detailed purkinje cell model predicts voltage-dependent control of burst-pause responses in active dendrites. *Front. Cell. Neurosci.* 11:278.

Mason CA, and Gregory E. Postnatal maturation of cerebellar mossy and climbing fibers: transient expression of dual features on single axons. *J Neurosci* 4: 1715-1735, 1984.

Mattis J., Tye K. M., Ferenczi E. A., Ramakrishnan C., O'Shea D. J., Prakash R., et al. . (2012). Principles for applying optogenetic tools derived from direct comparative analysis of microbial opsins. Nat. Methods 9, 159–172.

Maurice N, Deniau JM, Glowinski J, and Thierry AM. Relationships between the prefrontal cortex and the basal ganglia in the rat: physiology of the cortico-nigral circuits. *J Neurosci* 19: 4674-4681, 1999.

Mawhinney LJ, de Rivero Vaccari JP, Alonso OF, Jimenez CA, Furones C, Moreno WJ, Lewis MC, Dietrich WD, and Bramlett HM. Isoflurane/nitrous oxide anesthesia induces increases in NMDA receptor subunit NR2B protein expression in the aged rat brain. *Brain Res* 1431: 23-34, 2012.

Medina JF, Garcia KS, and Mauk MD. A mechanism for savings in the cerebellum. *J Neurosci* 21: 4081-4089, 2001.

Medina JF, and Mauk MD. Computer simulation of cerebellar information processing. *Nat Neurosci* 3 Suppl: 1205-1211, 2000.

Medina JF, and Mauk MD. Simulations of cerebellar motor learning: computational analysis of plasticity at the mossy fiber to deep nucleus synapse. *J Neurosci* 19: 7140-7151, 1999.

Middleton FA, and Strick PL. Anatomical evidence for cerebellar and basal ganglia involvement in higher cognitive function. *Science* 266: 458-461, 1994.

Miller E. K., Cohen J. D. (2001). An integrative theory of prefrontal cortex function. Annu. Rev. Neurosci. 24, 167–202.

Mittleman G, Goldowitz D, Heck DH, and Blaha CD. Cerebellar modulation of frontal cortex dopamine efflux in mice: relevance to autism and schizophrenia. *Synapse* 62: 544-550, 2008.

Mogensen H, Bengtsson F, and Jorntell H. No Medium-Term Spinocerebellar Input Plasticity in Deep Cerebellar Nuclear Neurons In Vivo? *Cerebellum* 16: 638-647, 2017.

Monaco J, Casellato C, Koch G, and D'Angelo E. Cerebellar theta burst stimulation dissociates memory components in eyeblink classical conditioning. *Eur J Neurosci* 40: 3363-3370, 2014.

Morcuende S, Delgado-Garcia JM, and Ugolini G. Neuronal premotor networks involved in eyelid responses: retrograde transneuronal tracing with rabies virus from the orbicularis oculi muscle in the rat. *J Neurosci* 22: 8808-8818, 2002.

Morishita W, and Sastry BR. Postsynaptic mechanisms underlying long-term depression of GABAergic transmission in neurons of the deep cerebellar nuclei. *J Neurophysiol* 76: 59-68, 1996.

Morissette J, and Bower JM. Contribution of somatosensory cortex to responses in the rat cerebellar granule cell layer following peripheral tactile stimulation. *Exp Brain Res* 109: 240-250, 1996.

Muller T, Grosche J, Ohlemeyer C, and Kettenmann H. NMDA-activated currents in Bergmann glial cells. *Neuroreport* 4: 671-674, 1993.

Murray E, Wise S, and and Graham K. The Evolution of Memory Systems. edited by Press OU2017.

Nieoullon A, Cheramy A, and Glowinski J. Release of dopamine in both caudate nuclei and both substantia nigrae in response to unilateral stimulation of cerebellar nuclei in the cat. *Brain Res* 148: 143-152, 1978.

Ohyama T, Nores WL, and Mauk MD. Stimulus generalization of conditioned eyelid responses produced without cerebellar cortex: implications for plasticity in the cerebellar nuclei. *Learn Mem* 10: 346-354, 2003.

Ohyama T, Nores WL, Medina JF, Riusech FA, and Mauk MD. Learning-induced plasticity in deep cerebellar nucleus. *J Neurosci* 26: 12656-12663, 2006.

Okugawa G, Nobuhara K, Takase K, and Kinoshita T. Cerebellar posterior superior vermis and cognitive cluster scores in drug-naive patients with first-episode schizophrenia. *Neuropsychobiology* 56: 216-219, 2007.

Omelchenko N, and Sesack SR. Ultrastructural analysis of local collaterals of rat ventral tegmental area neurons: GABA phenotype and synapses onto dopamine and GABA cells. *Synapse* 63: 895-906, 2009.

Opris I, Santos L, Gerhardt GA, Song D, Berger TW, Hampson RE, et al. Prefrontal cortical microcircuits bind perception to executive control. Scientific reports. 2013;3:2285.

Otani S, Bai J, and Blot K. Dopaminergic modulation of synaptic plasticity in rat prefrontal neurons. *Neurosci Bull* 31: 183-190, 2015.

Ouardouz M, and Sastry BR. Mechanisms underlying LTP of inhibitory synaptic transmission in the deep cerebellar nuclei. *J Neurophysiol* 84: 1414-1421, 2000.

Paine T. A., Slipp L. E., Carlezon W. A., Jr. (2011). Schizophrenia-like attentional deficits following blockade of prefrontal cortex $GABA_A$ receptors. Neuropsychopharmacology 36, 1703–1713.

Palesi F, Tournier JD, Calamante F, Muhlert N, Castellazzi G, Chard D, D'Angelo E, and Wheeler-Kingshott CA. Contralateral cerebello-thalamo-cortical pathways with prominent involvement of associative areas in humans in vivo. *Brain Struct Funct* 220: 3369-3384, 2015.

Palmen SJ, van Engeland H, Hof PR, and Schmitz C. Neuropathological findings in autism. *Brain* 127: 2572-2583, 2004.

Parfitt KD, Gratton A, and Bickford-Wimer PC. Electrophysiological effects of selective D1 and D2 dopamine receptor agonists in the medial prefrontal cortex of young and aged Fischer 344 rats. *J Pharmacol Exp Ther* 254: 539-545, 1990.

Parker KL. Timing tasks synchronize cerebellar and frontal ramping activity and theta oscillations: implications for cerebellar stimulation in diseases of impaired cognition. Front Psychiatry. 2016;6:190.

Parnaudeau S, Bolkan SS, Kellendonk C. The mediodorsal thalamus: an essential partner of the prefrontal cortex for cognition. Biological Psychiatry. 2018;83:648–656.

Pezzulo G. An active inference view of cognitive control. Front Psychol. 2012;3:478.

Pierce K, and Courchesne E. Evidence for a cerebellar role in reduced exploration and stereotyped behavior in autism. *Biol Psychiatry* 49: 655-664, 2001.

Pirot S, Godbout R, Mantz J, Tassin JP, Glowinski J, and Thierry AM. Inhibitory effects of ventral tegmental area stimulation on the activity of prefrontal cortical neurons: evidence for the involvement of both dopaminergic and GABAergic components. *Neuroscience* 49: 857-865, 1992.

Povysheva NV, Gonzalez-Burgos G, Zaitsev AV, Kröner S, Barrionuevo G, Lewis DA, Krimer LS. (2006) Properties of excitatory synaptic responses in fast-spiking interneurons and pyramidal cells from monkey and rat prefrontal cortex. Cereb Cortex 16:541–552.

Prestori F, Bonardi C, Mapelli L, Lombardo P, Goselink R, De Stefano ME, Gandolfi D, Mapelli J, Bertrand D, Schonewille M, De Zeeuw C, and D'Angelo E. Gating of long-term potentiation by nicotinic acetylcholine receptors at the cerebellum input stage. *PLoS One* 8: e64828, 2013.

Pugh JR, and Raman IM. Mechanisms of potentiation of mossy fiber EPSCs in the cerebellar nuclei by coincident synaptic excitation and inhibition. *J Neurosci* 28: 10549-10560, 2008.

Pugh JR, and Raman IM. Nothing can be coincidence: synaptic inhibition and plasticity in the cerebellar nuclei. *Trends Neurosci* 32: 170-177, 2009.

Pugh JR, and Raman IM. Potentiation of mossy fiber EPSCs in the cerebellar nuclei by NMDA receptor activation followed by postinhibitory rebound current. *Neuron* 51: 113-123, 2006.

Pugh J., Raman I. (2006). Potentiation of mossy NMDA receptor activation followed by postinhibitory rebound current. Neuron 51, 113–123.

Racine RJ, Wilson DA, Gingell R, and Sunderland D. Long-term potentiation in the interpositus and vestibular nuclei in the rat. *Exp Brain Res* 63: 158-162, 1986.

Rall W. Electrophysiology of a dendritic neuron model. *Biophys J* 2: 145-167, 1962.

Ramakrishnan KB, Voges K, De Propris L, De Zeeuw CI, and D'Angelo E. Tactile Stimulation Evokes Long-Lasting Potentiation of Purkinje Cell Discharge In Vivo. *Front Cell Neurosci* 10: 36, 2016.

Raman IM, Gustafson AE, and Padgett D. Ionic currents and spontaneous firing in neurons isolated from the cerebellar nuclei. *J Neurosci* 20: 9004-9016, 2000.

Rand S., and Swenson MD. REVIEW OF CLINICAL AND FUNCTIONAL NEUROSCIENCE. 2006.

Rao S.G. Williams, G. V., Goldman-Rakic, P. S. Destruction and creation of spatial tuning by disinhibition: GABA(A) blockade of prefrontal cortical neurons engaged by working memory. *J Neurosci* 20: 485-94, 2000.

Rasmussen A, Jirenhed DA, and Hesslow G. Simple and complex spike firing patterns in Purkinje cells during classical conditioning. *Cerebellum* 7: 563-566, 2008.

Rigas P, Castro-Alamancos MA. Thalamocortical Up states: differential effects of intrinsic and extrinsic cortical inputs on persistent activity. Journal of Neuroscience. 2007;27:4261–4272.

Rogers TD, Dickson PE, Heck DH, Goldowitz D, Mittleman G, and Blaha CD. Connecting the dots of the cerebro-cerebellar role in cognitive function: neuronal pathways for cerebellar modulation of dopamine release in the prefrontal cortex. *Synapse* 65: 1204-1212, 2011.

Roggeri L, Rivieccio B, Rossi P, and D'Angelo E. Tactile stimulation evokes long-term synaptic plasticity in the granular layer of cerebellum. *J Neurosci* 28: 6354-6359, 2008.

Rotaru D. C., Barrionuevo G., Sesack S. R. (2005). Mediodorsal thalamic afferents to layer III of the rat prefrontal cortex: synaptic relationships to subclasses of interneurons. J. Comp. Neurol. 490, 220–238.

Rudy B., Fishell G., Lee S., Hjerling-Leffler J. (2011). Three groups of interneurons account for nearly 100% of neocortical GABAergic neurons. Dev. Neurobiol. 71, 45–61.

Romano V, De Propris L, Bosman LW, Warnaar P, Ten Brinke MM, Lindeman S, Ju C, Velauthapillai A, Spanke JK, Middendorp Guerra E, Hoogland TM, Negrello M, E DA, and De Zeeuw CI. Potentiation of cerebellar Purkinje cells facilitates whisker reflex adaptation through increased simple spike activity. *Elife* 7: 2018.

Rowland NC, and Jaeger D. Coding of tactile response properties in the rat deep cerebellar nuclei. *J Neurophysiol* 94: 1236-1251, 2005.

Rowland NC, and Jaeger D. Responses to tactile stimulation in deep cerebellar nucleus neurons result from recurrent activation in multiple pathways. *J Neurophysiol* 99: 704-717, 2008.

Roy D, Sigala R, Breakspear M, McIntosh AR, Jirsa VK, Deco G, and Ritter P. Using the virtual brain to reveal the role of oscillations and plasticity in shaping brain's dynamical landscape. *Brain Connect* 4: 791-811, 2014.

Sachidhanandam S, Sreenivasan V, Kyriakatos A, Kremer Y, Petersen CC. Membrane potential correlates of sensory perception in mouse barrel cortex. Nature Neuroscience. 2013;16:1671–1677.

Saffari R., Teng Z., Zhang M., Kravchenko M., Hohoff C., Ambrée O., Zhang W. NPY(+)-, but not PV(+)-GABAergic neurons mediated long-range inhibition from infra- to prelimbic cortex. Transl. Psychiatry. 2016;6 e736.

Sanchez-Vives MV, McCormick DA. Cellular and network mechanisms of rhythmic recurrent activity in neocortex. Nature Neuroscience. 2000;3:1027–1034.

Sawaguchi T., Matsumura M., Kubota K. (1989). Delayed response deficits produced by local injection of bicuculline into the dorsolateral prefrontal cortex in Japanese macaque monkeys. Exp. Brain Res. 75, 457–469.

Schmahmann JD. Disorders of the cerebellum: ataxia, dysmetria of thought, and the cerebellar cognitive affective syndrome. J Neuropsychiatry Clin Neurosci. 2004;16(3):367–78.

Schmahmann JD. From movement to thought:anatomic substrates of the cerebellar contribution to cognitive processing. *Hum Brain Mapp* Vol. 4, issue 3: 174-98, 1996.

Schmahmann JD, and Sherman JC. The cerebellar cognitive affective syndrome. *Brain* 121 (Pt 4): 561-579, 1998.

Schmajuck NA, Lam YW, Gray JA. Latent inhibition: a neural network approach. J Exp Phsychol. 22; 321-349; 1996.

Schonewille M, Belmeguenai A, Koekkoek SK, Houtman SH, Boele HJ, van Beugen BJ, Gao Z, Badura A, Ohtsuki G, Amerika WE, Hosy E, Hoebeek FE, Elgersma Y, Hansel C, and De Zeeuw CI. Purkinje cell-specific knockout of the protein phosphatase PP2B impairs potentiation and cerebellar motor learning. *Neuron* 67: 618-628, 2010.

Schweighofer N, Doya K, and Kuroda S. Cerebellar aminergic neuromodulation: towards a functional understanding. *Brain Res Brain Res Rev* 44: 103-116, 2004.

Seamans JK, Gorelova N, Durstewitz D, and Yang CR. Bidirectional dopamine modulation of GABAergic inhibition in prefrontal cortical pyramidal neurons. *J Neurosci* 21: 3628-3638, 2001.

Seamans JK, Lapish CC, Durstewitz D.Comparing the prefrontal cortex of rats and primates:insights for electrophysiology. Neurotox Res. **2008** Oct;14(2-3):249-62.

Sesack SR, and Bunney BS. Pharmacological characterization of the receptor mediating electrophysiological responses to dopamine in the rat medial prefrontal cortex: a microiontophoretic study. *J Pharmacol Exp Ther* 248: 1323-1333, 1989.

Shadmehr R, Krakauer JW. A computational neuroanatomy for motor control. Exp Brain Res. 185(3):359–81; 2008.

Shadmehr R, Smith MA, Krakauer JW Error correction, sensory prediction, and adaptation in motor control. *Annu. Rev. Neurosci.* 33 89–108; 2010.

Shambes GM, Gibson JM, and Welker W. Fractured somatotopy in granule cell tactile areas of rat cerebellar hemispheres revealed by micromapping. *Brain Behav Evol* 15: 94-140, 1978.

Smith MA, Ghazizadeh A, and Shadmehr R. Interacting adaptive processes with different timescales underlie short-term motor learning. *PLoS Biol* 4: e179, 2006.

Snider RS, and Maiti A. Cerebellar contributions to the Papez circuit. *J Neurosci Res* 2: 133-146, 1976.

Snider RS, Maiti A, and Snider SR. Cerebellar pathways to ventral midbrain and nigra. *Exp Neurol* 53: 714-728, 1976.

Solinas S, Forti L, Cesana E, Mapelli J, Schutter ED, and Angelo ED. Fast-reset of pacemaking and theta-frequency resonance patterns in cerebellar Golgi cells : Simulations of their impact in vivo. 1: 1-9, 2007.

Sparta DR, et al. Construction of implantable optical fibers for long-term optogenetic manipulation of neural circuits. Nat Protoc. 2012;7:12–23.

Steriade M, Nuñez A, Amzica F. A novel slow (< 1 Hz) oscillation of neocortical neurons in vivo: depolarizing and hyperpolarizing components. Journal of Neuroscience. 1993a;13:3252–3265.

Sugihara I, Lang EJ, and Llinas R. Serotonin modulation of inferior olivary oscillations and synchronicity: a multiple-electrode study in the rat cerebellum. *Eur J Neurosci* 7: 521-534, 1995.

Suska A., Lee B. R., Huang Y. H., Dong Y., Schlüter O. M. (2013). Selective presynaptic enhancement of the prefrontal cortex to nucleus accumbens pathway by cocaine. Proc. Natl. Acad. Sci. U S A 110, 713–718

Swadlow H. A., Gusev A. G., Bezdudnaya T. (2002). Activation of a cortical column by a thalamocortical impulse. *J. Neurosci.* 22 7766–7773.

Sweeney JE, Lamour Y, and Bassant MH. Arousal-dependent properties of medial septal neurons in the unanesthetized rat. *Neuroscience* 48: 353-362, 1992.

Swenson RS, Kosinski RJ, and Castro AJ. Topography of spinal, dorsal column nuclear, and spinal trigeminal projections to the pontine gray in rats. *J Comp Neurol* 222: 301-311, 1984.

Sánchez-Campusano R, Gruart A, and Delgado-García JM. Dynamic associations in the cerebellar-motoneuron network during motor learning. *J Neurosci* 29: 10750-10763, 2009.

Sánchez-Campusano R, Gruart A, and Delgado-García JM. The cerebellar interpositus nucleus and the dynamic control of learned motor responses. *J Neurosci* 27: 6620-6632, 2007.

Takeda T, and Maekawa K. Transient direct connection of vestibular mossy fibers to the vestibulocerebellar Purkinje cells in early postnatal development of kittens. *Neuroscience* 32: 99-111, 1989.

Thach WT. Discharge of Purkinje and cerebellar nuclear neurons during rapidly alternating arm movements in the monkey. J Neurophysiol. 1968;31:785–797.

Thomson A. M., Bannister A. P., Interlaminar connections in the neocortex. Cereb. Cortex 13, 5–14 (2003)

Timofeev I. Neuronal plasticity and thalamocortical sleep and waking oscillations. *Prog Brain Res* 193: 121-144, 2011.

Trantham-Davidson H, Kröner S, and Seamans JK. Dopamine modulation of prefrontal cortex interneurons occurs independently of DARPP-32. *Cereb Cortex* 18: 951-958, 2008.

J.K. Trevathan, A.J. Asp, E.N. Nicolai, J.M. Trevathan, N.A. Kremer, T.D. Kozai, D. Cheng, M. Schachter, J . J. Nassi, S. L. Otte, J. G. Parker, J. L. Lujan, K. A. Ludwig Calcium imaging in freely-moving mice during electrical stimulation of deep brain structures. bioRxiv 460220

Uylings HB, Groenewegen HJ, Kolb B. Do rats have a prefrontal cortex? Behav Brain Res. **2003** Nov 30;146(1-2):3-17

Uusisaari MY, De Schutter E. The mysterious microcircuitry of the cerebellar nuclei. *J Physiol* 2011 Jul 15;589(Pt 14):3441-57.

Uusisaari MY, Knopfel T. Functional classification of neurons in the mouse lateral cerebellar nuclei. *Cerebellum* 2011 Dec;10(4):637-46.

Uusisaari MY, Knöpfel T. Diversity of neuronal elements and circuitry in the cerebellar nuclei. *Cerebellum* 11: 420-421, 2012.

Valera AM, Binda F, Pawlowski SA, Dupont JL, Casella JF, Rothstein JD, Poulain B, and Isope P. Stereotyped spatial patterns of functional synaptic connectivity in the cerebellar cortex. *Elife* 5: 2016.

Vargas DL, Nascimbene C, Krishnan C, Zimmerman AW, and Pardo CA. Neuroglial activation and neuroinflammation in the brain of patients with autism. *Ann Neurol* 57: 67-81, 2005.

Vertes R. P. (2006). Interactions among the medial prefrontal cortex, hippocampus and midline thalamus in emotional and cognitive processing in the rat. Neuroscience 142, 1–20.

Vyazovskiy VV, Olcese U, Hanlon EC, Nir Y, Cirelli C, Tononi G. Local sleep in awake rats. Nature. 2011;472:443–447.

Vos BP, Volny-Luraghi A, and De Schutter E. Cerebellar Golgi cells in the rat: receptive fields and timing of responses to facial stimulation. *Eur J Neurosci* 11: 2621-2634, 1999.

Wang D, Smith-Bell CA, Burhans LB, O'Dell DE, Bell RW, and Schreurs BG. Changes in membrane properties of rat deep cerebellar nuclear projection neurons during acquisition of eyeblink conditioning. *Proc Natl Acad Sci U S A* 115: E9419-e9428, 2018.

Watson TC, Becker N, Apps R, and Jones MW. Back to front: cerebellar connections and interactions with the prefrontal cortex. *Front Syst Neurosci* 8: 4, 2014.

Watson TC, Jones MW, and Apps R. Electrophysiological mapping of novel prefrontal - cerebellar pathways. *Front Integr Neurosci* 3: 18, 2009.

Watson T. C., Obiang P., Torres-Herraez A., Watilliaux A., Coulon P., Rochefort C., et al. Anatomical and physiological foundations of cerebello-hippocampal interactions. Elife 8:e41896; 2019.

Whitney ER, Kemper TL, Bauman ML, Rosene DL, and Blatt GJ. Cerebellar Purkinje cells are reduced in a subpopulation of autistic brains: a stereological experiment using calbindin-D28k. *Cerebellum* 7: 406-416, 2008.

Witter L, Canto CB, Hoogland TM, de Gruijl JR, and De Zeeuw CI. Strength and timing of motor responses mediated by rebound firing in the cerebellar nuclei after Purkinje cell activation. *Front Neural Circuits* 7: 133, 2013.

Witter L, Rudolph S, Pressler RT, Lahlaf SI, and Regehr WG. Purkinje Cell Collaterals Enable Output Signals from the Cerebellar Cortex to Feed Back to Purkinje Cells and Interneurons. *Neuron* 91: 312-319, 2016.

Yarden-Rabinowitz Y, and Yarom Y. In vivo analysis of synaptic activity in cerebellar nuclei neurons unravels the efficacy of excitatory inputs. *J Physiol* 595: 5945-5963, 2017.

Yizhar O. (2012). Optogenetic insights into social behavior function. Biol. Psychiatry 71, 1075–1080.

Yizhar O, Fenno LE, Davidson TJ, Mogri M, Deisseroth K. Optogenetics in neural systems. Neuron. 2011;71:9–34.

Zhang F., Gradinaru V., Adamantidis A. R., Durand R., Airan R. D., de Lecea L., Deisseroth K., Optogenetic interrogation of neural circuits: Technology for probing mammalian brain structures. Nat. Protoc. 5, 439–456 (2010)

Zhang GJ, Wu MC, Shi JD, Xu YH, Chu CP, Cui SB, and Qiu DL. Ethanol Modulates the Spontaneous Complex Spike Waveform of Cerebellar Purkinje Cells Recorded in vivo in Mice. *Front Cell Neurosci* 11: 43, 2017.

Zhang W, and Linden DJ. Long-term depression at the mossy fiber-deep cerebellar nucleus synapse. *J Neurosci* 26: 6935-6944, 2006.

Zhang W, Shin JH, and Linden DJ. Persistent changes in the intrinsic excitability of rat deep cerebellar nuclear neurones induced by EPSP or IPSP bursts. *J Physiol* 561: 703-719, 2004.

Zheng N, and Raman IM. Synaptic inhibition, excitation, and plasticity in neurons of the cerebellar nuclei. *Cerebellum* 9: 56-66, 2010.